by

Matilde Marchi

for the award of the degree of

DOCTOR OF PHILOSOPHY

"Dynamic imaging of the intracellular trafficking of ERK suggests a novel mechanism at the basis of the functional differences between ERK1 and 2"

SCUOLA NORMALE SUPERIORE

Supervisor: Dr. Gian Michele Ratto

Pisa, February 2009

“As natural selection works solely
by and for the good of each being,
all corporeal and mental endowments
will tend to progress towards perfection.”

C. Darwin *“The origin of species”* , 1859

INDEX

ABSTRACT

In this thesis I studied the localization and trafficking in living cells of the Extracellular Regulated Kinase signaling by making visible ERK1 and ERK2 with a fluorescent tag. This approach allowed to identify different dynamical properties of the two kinases, posing the bases for the understanding of the functional differences between ERK1 and ERK2.

The nucleo-cytoplasmic trafficking of tagged ERK1/2 has been measured by means of FRAP experiments. Surprisingly, I found that ERK1 shuttles at a much slower rate than ERK2. Moreover, I demonstrated that this difference is caused by an unique domain of ERK1 located at its N-terminus, since the progressive deletion of these residues converts the shuttling features of ERK1 into those of ERK2. Conversely, the fusion of this ERK1 sequence at the N-terminus of ERK2 slows down its shuttling to a similar value found for ERK1 and, when fused to small cargos such as a GFP monomer, it is capable of hampering their shuttling too. In addition, I identified some crucial aminoacids at ERK1 N-terminus, responsible in large part of this phenotype. Finally, I have demonstrated that the speed of nucleo-cytoplasmic shuttling critically affects the ERK capability of activating downstream effectors.

In conclusion, I propose a novel biochemical model, in which the regulation of nucleo-cytoplasmic trafficking might provide a sensitive mechanisms through which cells modulate their response to extracellular stimulus. This mechanism significantly contributes to the differential ability of ERK1 and 2 to generate an overall signaling output.

WORKING HYPOTHESIS

This work focused on dissecting protein dynamics inside a molecular pathway of crucial importance: the Extracellular Regulated Kinase (ERK) signaling, which is activated by a wide plethora of stimuli and is involved in almost every cellular process.

Understanding the basic control mechanisms of a biological system like a molecular signaling cascade will help to develop new therapies, drugs and sensitive diagnostics tools.

This work is characterized by a multidisciplinary approach, indispensable to unveil differences between the two kinases ERK1 and 2 which share a high sequence homology and the majority of the regulatory partners. The proteins of interest have been made visible by fusing them with fluorescent proteins. The resulting chimerical proteins were expressed in mammalian cells and were tested by experiments of live imaging. Furthermore, the functional consequences of the slower trafficking of ERK1 have been evaluated by computational models and biochemical assays.

SPECIFIC AIMS

- Characterizing the biochemical-functional properties of GFP-ERK fusion proteins in order to validate them as investigation tools in living cells.
- Deciphering nuclear translocation dynamics of ERK2, investigating the interplay between the activation and deactivation systems.
- Measuring the nucleo-cytoplasmic shuttling of ERK1 and 2, by FRAP experiments.
- Evaluating the effects of ERK trafficking on the signaling to the nucleus. The regulation of nuclear access constitutes a fundamental check point to control downstream effects.
- Studying the capability of ERK1 N-terminus of influencing the trafficking across the nuclear barrier and the functional outputs.
- Identification of specific residues at ERK1 N-terminus, which are responsible of the slower phenotype of nuclear shuttling.

SIGNIFICANCE OF THE WORK

In this thesis the following results have been obtained:

The mechanisms at the basis of ERK regulation have been better elucidated focusing on the spatio-temporal patterns of ERK phosphorylation and trafficking in living cells. In particular, I have found that there is a continuous counterbalance between the activation drive (MEK mediated) and the deactivation reactions (by Phosphatases). This is true also in basal conditions, given that a small percentage of MEK activity is still present. This push-pull mechanism is highly modulated in strength and over time, and is responsible for the on/off switching of the pathway.

Furthermore, it has been measured the nucleo-cytoplasmic shuttling of ERK1 and 2, by FRAP experiments, finding out that ERK1 and 2 drastically differ in their capability of crossing the nuclear envelope. Computational, biochemical and functional evidences proved that this trafficking difference causes ERK1 and 2 to have different signaling capabilities to the nucleus. Indeed, I demonstrated that the rate of nucleo-cytoplasmic shuttling is a crucial regulator of the signaling to the nucleus, representing a novel possible target for the molecular control of this pathway.

Finally, it has been demonstrated that the difference in nuclear shuttling between ERK1 and 2 is caused by a short domain located at the N-terminus of ERK1. This region is necessary and sufficient to cause the differences of permeation and functional properties between ERK1 and 2. By directed mutagenesis some crucial residues have been identified to be responsible of the slow permeation of ERK1.

LIST OF ABBREVIATIONS

CLSM: Confocal Laser Scanning Microscopes
cPLA2: cytosolic PhosphoLipase A2
CREB: Cyclic AMP Response Element-Binding
CRM1: Chromosome Region Maintenance Protein 1
DSP: Dual Specificity Phosphatases
DsRFP: Discosoma Red Fluorescent Protein
EGF R: Epidermal Growth Factor Receptor
ERK: Extracellular Regulated Kinase
EYFP: Enhanced Yellow Fluorescent Protein
FAK: Focal Adhesion Kinase
FGF: Growth Factor for Fibroblast
FRAP: Fluorescence Recovery After Photobleaching
FRET: Fluorescence Resonance Energy Transfer
GAP: GTPase-Activating Proteins
GEF: Guanine nucleotide Exchange Factors
GFP: Green Fluorescent Protein
Grb: Growth factor Receptor-Bound protein
GTP: Guanine Triphosphate
HePTP: Hematopoietic Protein Tyrosine Phosphatase
IF: Immobile Fraction
JNK: c-Jun NH_2-terminal kinase
KD: Kinase Domain
KSR: Kinase Suppressor of Ras
MAP-2: Microtubule Associated Protein 2
MAPK: Mitogen Activated Protein Kinase
MBP: Myelin Binding Protein
MeCP2: Methyl CpG–binding Protein 2
MKP: MAP Kinase Phosphatase
MLCK: Myosin Light Chain Kinase
MP1: MEK Partner 1
MSK: Mitogen- and Stress-activated Protein Kinase
NES: Nuclear Export Signal
NGF: Nerve Growth Factor
NGF: Nerve Growth Factor
NLS: Nuclear Localization Signal
NPC: Nuclear Pore Complex
NUP: Nucleoporin
PDGF: Platelet-Derived Growth Factor
PEA-15: Phosphoprotein Enriched in Astrocytes, 15kDa
PKC: Protein Kinase C
PP2A: Protein Phosphatase 2A
PPAR γ1: Peroxisome Proliferator Activated Receptor γ1
PTB: Phospho-Tyrosine Binding
PTK: Protein Tyrosine Kinase
Rap1: Repressor activator protein 1
RSK: Ribosomal S6 Kinase
SAPK: Stress-Activated Protein Kinase
SH: Src Homology

SMAD: this name is the combination between the *C. elegans* protein SMA and the drosophila protein Mothers Against Decapentaplegic
Sos: Son of Sevenless
SRF: Serum Response Factor
TAD: Transactivation Domain
TCF: Ternary Complex Factor
TKR: Tyrosine Kinase Receptors
TMP: Thrombin-Mimicking Peptide
TRD: Transcription Repression Domain

LIST OF PAPERS DERIVED FROM THIS STUDY

Marchi M, D'Antoni A, Formentini I, Parra R, Brambilla R, Ratto GM, Costa M.
The N-terminal domain of ERK1 accounts for the functional differences with ERK2.
PLoS ONE. 2008;3(12):e3873. Epub 2008 Dec 4.

Marchi M, Guarda A, Bergo A, Landsberger N, Kilstrup-Nielsen C, Ratto GM, Costa M.
Spatio-temporal dynamics and localization of MeCP2 and pathological mutants in living cells.
Epigenetics. 2007 Sep;2(3):187-97. Epub 2007 Sep 18.

Costa M, Marchi M, Cardarelli F, Roy A, Beltram F, Maffei L, Ratto GM.
Dynamic regulation of ERK2 nuclear translocation and mobility in living cells.
J Cell Sci. 2006 Dec 1;119(Pt 23):4952-63. Epub 2006 Nov 14.

INTRODUCTION

Signal transduction: the keystone of living matter

Why and how studying a molecular pathway?

In biology, signal transduction refers to any process by which a cell converts an extra-cellular signal in a series of intracellular events leading to adaptive responses of the cell to the changing environment. This involves ordered sequences of biochemical reactions, carried out by enzymes and linked through second messengers or protein-protein interactions. Such processes are usually rapid, lasting on the order of milliseconds, as in the case of ion fluxes, to minutes for the activation of proteins and lipid-mediated kinase cascades. The main feature of most pathways is the capability of generating a “signal cascade”: indeed the number of proteins and other molecules participating in these events increases as the process goes on from the initial stimulus, providing amplification and the possibility of integrating different signals on common effectors. Each protein is committed to act in a well defined range of activities and it behaves like a fine sensor of the surrounding environment. All these components form highly interactive networks responsible of the first level of complexity in a living organism. The stunning perfection of the molecular orchestration inside a pathway is not only fascinating *per se*, but hides essential clues necessary to understand how a biological system works. Furthermore, understanding basic control mechanisms will help to develop new therapies, drugs and sensitive diagnostics tools.

In this thesis I focused on dissecting protein dynamics inside a molecular pathway of crucial importance: the Extracellular Regulated Kinase (ERK) signaling. ERK pathway is activated by a wide plethora of stimuli, including growth factors, cytokines, integrins and hormones. It is involved in almost every cellular process like cell cycle, motility, differentiation, apoptosis and synaptic plasticity. Indeed, the ERK pathway represents a hot spot of investigation because of its large impact on widespread and serious diseases: for example, it has been reported that ERK1/2 activity is massively upregulated in several human cancers (Hoshino et al., 1999).

The basic assembly of the ERK pathway is a three-component module conserved in all eukaryotes, from yeast to humans. This module includes three serially linked kinases (Raf/MEK/ERK) of which ERK is the last effector.
In mammals there are at least two “isoforms” for each level: Raf1, B-Raf and A-Raf for the upstream form, MEK1 and MEK2 for the intermediate and ERK1 and ERK2 at the lower level. In this work I will investigate the differences between these two last proteins, that, although sharing many known features, they still hold some secrets.
ERK1 and ERK2 have been considered as redundant isoforms for a long time, since they share the same regulatory machinery and targets. In addition, the identification of their individual role is complicated by technical difficulties in separating the action of each kinase. Given that ERK1 and 2 are characterized by a high degree of sequence homology (90% in humans), their existence raises the question of why they have been both conserved to date.

Studying cellular processes in living cells

Although biological processes and structures are dynamic in nature, most investigations into their mechanisms have been carried out in ex-vivo specimens using, for example, immunocytochemistry and biochemical assays. This incongruity has been imposed in large part by a lack of tool to analyze signal transduction in living cells. Recent developments in *in vivo* microscopy techniques and the discovery of the green fluorescent protein (GFP) and its spectral variants (Chalfie et al., 1994) have allowed the non destructive investigation of a wide range of dynamic processes in living cells [reviewed in (Lippincott-Schwartz et al., 2001; Misteli and Spector, 1997)]. In this work I took advantage of these new tools: ERK1 and 2 were made visible by fusion with fluorescent proteins. Then, the resulting chimeras were expressed in living cells to follow the dynamics of their movements between different compartments and their localization after specific stimuli. These experiments offered a different perspective on ERK function compared to the classic biochemical approach, and, as I will show, allowed to evidence differences between the two kinases ERK1 and 2 that were, upon now, unsuspected.

In the following of this introductory chapter two main sections will be developed:

- in the first part I will discuss the biological background of the proteins investigated; I will review the state of art of ERK biology specifically focusing on the molecular aspects concerning ERK targets, the regulatory mechanisms of the pathway and the communication between nucleus and cytoplasm.

- in the second part I will introduce the multidisciplinary approach that characterizes this work, indispensable to unveil differences between the two kinases. I will illustrate potentialities and advantages of the imaging techniques used in tight conjunction with more classical molecular and biochemical methods. This kind of approach has made possible to unveil different kinetic and functional properties of ERK1 and 2.

INTRODUCTION: Part 1

The ERK1/2 cascade

This pathway is one of the primordial signaling systems; it exists in all eukaryotes and controls fundamental cellular processes such as proliferation, differentiation, survival and apoptosis. The ERK cascade was originally discovered as a critical regulator of cell division and differentiation and this is the reason why it was firstly named Mitogen-Activated Protein Kinase (MAPK) cascade. As further details of this molecular signaling were worked out, it became clear that the ERK cascade is in fact a prototype for a family of signaling cascades that shares the motif of three serially linked kinases, which regulate each other by sequential phosphorylation. Thus, a revised nomenclature uses the term MAPK to refer to the entire superfamily of signaling cascades, comprising also SAPK/JNK (Stress-Activated Protein Kinase/c-Jun NH_2-terminal kinase) and p38, and it specifies the prototype MAPK as ERK (Extracellular-Regulated Kinase). SAP/JNK and p38 are principally activated by cellular stresses including osmotic shock, inflammatory cytokines, lipopolysaccharides (LPS) and ultraviolet light. Conversely ERK1/2 are primarily recruited by mitogens (such as polypeptide growth factors as well as insulin) and neurotrophins, but also by cytokines and hormones through Tyrosine Kinase Receptors (TKRs). Here I will focus on the dynamic regulation of the ERK1/2 pathway, activated by growth factors. The basic arrangement in the ERK pathway includes membrane receptors (principally TKRs) and a G-protein (Ras) which sits upstream of a core module consisting of a MAPK Kinase Kinase (Raf), that phosphorylates and activates a MAPK Kinase (MEK), which finally activates ERK1/2 (Fig. 1).

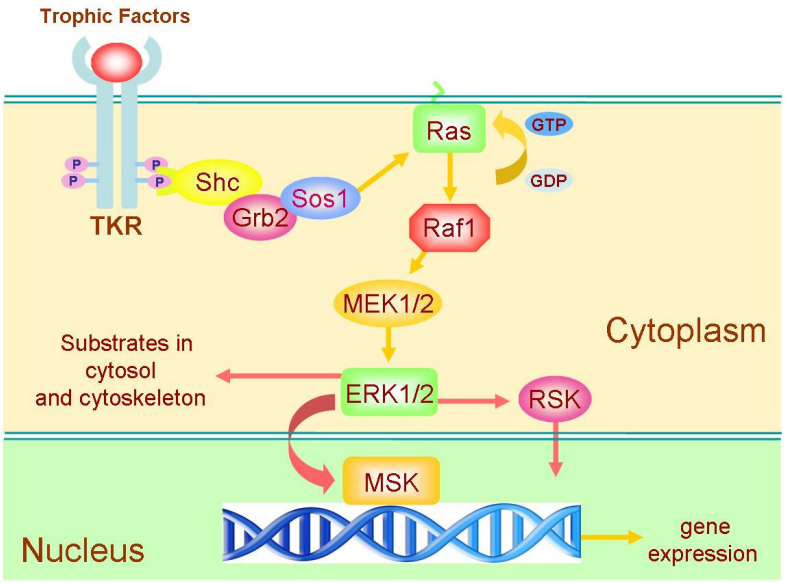

Figure 1
Schematic representation of the major components involved in ERK pathway (activated by trophic factors).

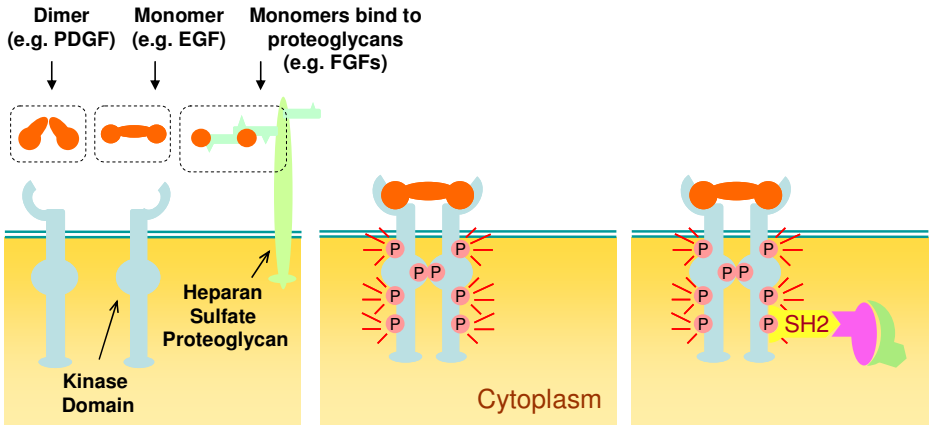

Figure 2
Tyrosine Kinase Receptors and their ligands
The binding of specific extracellular signals with the extracellular domains of Tyrosine Kinase Receptors (TKR) activate the intracellular Tyrosine Kinase Domain (TKD). Before or after ligand binding, the dimerization of TKRs occurs. To activate a TKR the ligand usually has to bind simultaneously to two adjacent receptor chains. PDGF is a dimer and crosslinks two receptors together; EGF is monomeric and FGFs, also monomers, form multimers by binding to heparan sulfate proteoglycans. Once activated, the TKD transfers a phosphate group (autophosphorylation) from ATP to selected tyrosine side chains, both on the receptor protein itself and on intracellular signaling proteins, that subsequently binds to the phosphorylated receptor. Phosphorylation of Tyr within the Kinase Domain (KD) increases the kinase activity of the enzyme. Phosphorylation of Tyr residues outside the KD creates high affinity docking sites for the binding of scaffold proteins (with SH2, PTB and SH3 domains).

Upstream of ERK

Tyrosine Kinase Receptors (TKRs)

Membrane spanning cell surface receptors of the TKR family are endowed with intrinsic tyrosine kinase activity, catalyzing the transfer of the α-phosphate of ATP to the hydroxyl groups of tyrosines on target proteins. All TKRs frequently contain a glycosylated extracellular ligand binding domain, connected to the cytoplasmic domain, which has a conserved Protein Tyrosine Kinase (PTK) core and regulatory regions that are subjected to autophosphorylation and phosphorylation by other kinases (Schlessinger, 2000a). Nearly all TKRs are monomers at the cell membrane, with ligand binding or ectopic overexpression resulting in receptor dimerization and tyrosine autophosphorylation in trans (Fig. 2). As the first TKR to be discovered (Downward et al., 1984), the epidermal growth factor receptor (EGF R, also known as ErbB1 from the v-erb-B transforming protein of an avian retrovirus) has helped to establish many of the principles of TKR functions (Schlessinger, 2002).

Activating mutations and transforming overexpression, mimicking receptor oligomerization of EGFR and its fellow family members, have been implicated in numerous cancers, including mammary carcinomas, squamous carcinomas and glioblastomas (Blume-Jensen and Hunter, 2001).

Scaffold proteins

The EGF receptor contains at least nine tyrosine residues in its cytoplasmic domain capable of being phosphorylated, and seven of these are autophosphorylation sites (Levkowitz et al., 1999). The autophosphorylation of Tyr sites on EGFR and other TKRs provides a mechanism for the recognition of specific scaffold proteins and it represents a platform for the assembly of signaling complexes. Phosphorylated sites of EGFR are recognized and bound by Src Homology 2 (SH2) (Pelicci et al., 1992) and Phospho-Tyrosine Binding (PTB) domains (Schlessinger, 2000b). Shc can assist the binding of an other protein, the Growth factor receptor bound protein 2, Grb2 (Rojas et al., 1996), a cytosolic adaptor, containing a central SH2 domain flanked by two Src Homology 3 (SH3) domains, that allows it to associate constitutively with the proline-rich regions of the nucleotide exchange factor Son of Sevenless (Sos) (Li et al., 1993). The recruitment of Grb2 from the cytoplasm to the plasma membrane brings Sos near the membrane-bound Ras. Through guanine exchange, Sos

enhances GDP release and GTP binding to Ras, converting this GTPase into its active conformation.

In a general view, it can be considered that the mammalian ERK pathway contains a central fifth-tiered module, which is strongly conserved and includes:

- the GTPase protein Ras (H-Ras, K-Ras and N-Ras) and other still unknown kinases;
- Raf (Raf-1, Raf A and Raf B);
- MEK1 and 2;
- ERK1 and 2;
- RSK, MSK and MNK.

In the following, I will describe features and functions of each components, particularly focusing on the isoforms which are principally involved in ERK1 and 2 signaling (Raf1 and Raf-B, MEK1 and MEK2).

Ras

Ras is a notable member of the large family of GTPases, proteins that bind and hydrolyze GTP. First discovered as transforming oncogenes of murine sarcoma viruses (v-ras), three highly related 21 kDa mammalian proteins, Harvey-Ras (H-Ras), Kirsten-Ras (K-Ras) and Neuroblastoma-Ras (N-Ras) have been identified (Bos, 1989). Ras family members are anchored to the cytoplasmic side of the plasma membrane by carboxyl-terminal farnesylation (post-translational modification by the attachment of an isoprenoid to the C-terminal cysteine residue). This localization to the inner leaflet brings Ras into close proximity with Sos, stimulating the exchange of GDP bound to Ras with GTP from the cytosol (Fig. 3). This exchange conformationally activates Ras, allowing it to interact with a number of downstream effectors (Avruch et al., 1994). Within the ERK signaling cascade, active Ras functions as an adaptor that binds to the effectors Raf kinases with high affinity, causing their translocation to the cell membrane, where Raf activation takes place (Jelinek et al., 1996).

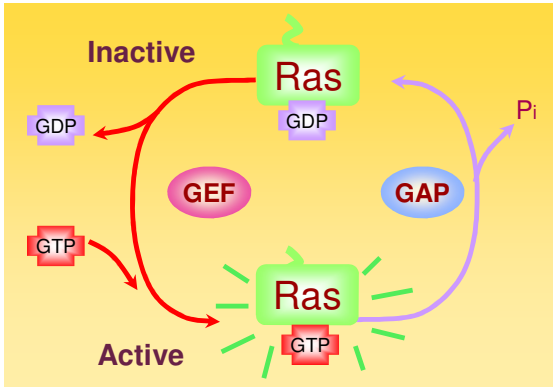

Figure 3
Ras-GDP/GTP cycle
Ras functions as a switch, cycling in two distinctive conformational states: Active, when GTP is bound and Inactive when GDP is bound.
Two classes of signaling proteins regulate Ras activity by influencing its transition: Guanine Nucleotide Exchange Factors (GEF) and GTPase-Activating Proteins (GAP). GEF stimulate the dissociation of GDP and the uptake of GTP, while GAP increase the rate of hydrolysis of bound GTP by Ras, inactivating Ras.

It has been well established that specific alterations in members of the ras gene family can convert them into active oncogenes. These malignant transformations lead to a subversion of cellular pathways that regulate the proliferation, differentiation and survival of cells, resulting in altered cell growth (oncogenic transformation). In Ras family these alterations are either point mutations occurring in either codons 12, 13 or 61 or, alternatively, a 5- to 50-fold amplification of the wild-type gene resulting in Ras overexpression.

Activating mutations of these Ras isoforms, which impair GTPase activity and stabilize the GTP bound state, are found in nearly one-third of all human cancers, making these oncoproteins among the most potent transforming polypeptides known (Seger and Krebs, 1995).

The transformant properties of mutated Ras isoforms have been recently used to show that ERK1 and 2 differently transduce Ras-dependent cell signaling and proliferation (Vantaggiato et al., 2006). Ectopic expression of ERK1 but not of ERK2 in NIH 3T3 cells inhibits oncogenic Ras-mediated proliferation and colony formation.

The linear module Raf-MEK-ERK

This module is actually the central core module. Once activated, it accomplishes for the convergence of different up-stream stimuli, providing for a high degree of signal integration.

Raf

Raf is a Ser/Thr protein kinase, catalyzing the phosphorylation of hydroxyl groups on specific Ser and Thr residues (Chong et al., 2003). Like Ras, Raf was first discovered in the form of a mutant retroviral transforming agent, v-raf (Rapp et al., 1983). Mammals have 3 Raf proteins, ranging from 70 to 100 kDa in size: Raf-1, Raf-A and Raf-B.

Raf-1 is ubiquitously expressed and studies on knockout mice indicated that Raf-1 may serve a general role in tissue formation (Mikula et al., 2001).

B-Raf is present in multiple isoforms and it is strongly expressed in fetal brain and adult cerebrum (Barnier et al., 1995) and it seems to fulfill more specialized duties (Wojnowski et al., 1997).

Recruitment to the plasma membrane by GTP-bound Ras is the initial event in Raf activation. Different Ras isoforms appear to activate Raf with varying ability, despite binding *in vitro* with comparable affinity. For example, K-Ras both recruits Raf-1 to the plasma membrane more efficiently, and activates the recruited Raf-1 more potently than H-Ras (Yan et al., 1998). It has also been suggested that Raf-B is the primary target of oncogenic Ras isoforms (Marais et al., 1997). Activating mutations of raf-B were reported in 66% of malignant melanomas (Davies et al., 2002).

MEK

Phosphorylated Raf activates MEK1 and MEK2 (Zheng and Guan, 1993). These kinases are about 45 kDa each and share 80% sequence identity. It is unclear why two MEKs exist, although conservation of both forms throughout eukaryotic species suggests non-redundant functions. Both MEKs are expressed ubiquitously in mammalian cells at micromolar levels, although some tissue-specific variation has been noted (Brott et al., 1993). Raf family activation of MEK1 and MEK2 occurs through phosphorylation of two Ser found in the activation loop (Alessi et al., 1994). While Raf isoforms are enzymes of relatively low abundance, the high concentration of MEKs allows for amplification of signaling (Huang and Ferrell, 1996). MEK1 or MEK2 may activate ERK1 or

ERK2. At endogenous levels of expression, there is evidence for preferential coupling, which may depend on the upstream kinase or adapter proteins in addition to differences in their direct interactions. Several studies showed that Raf-1 complexes preferentially with MEK1 and ERK2 (Huang et al., 1993; Jelinek et al., 1994).

MEK1 and MEK2 have distinct ways to contribute to the regulation of ERK activity and the mammalian cell cycle progression; MEK1 is required for Golgi fragmentation (Colanzi et al., 2000), whereas MEK2 is thought to be essential for progression through the G2/M checkpoint (Abbott and Holt, 1999). The phenotypes for loss of MEK1 versus loss of MEK2 have been studied in CT116 cells, a colon cancer line with WT p53 (Ussar and Voss, 2004). Depletion of either MEK subtypes by RNA interference generated a unique phenotype. The MEK1 knockdown led to the induction of a senescence-like phenotype and permanent ablation of MEK1 resulted in reduced colony formation potential, indicating the importance of MEK1 for long term proliferation and survival. In contrast, MEK2 deficiency was accompanied by a massive induction of cyclin D expression and the centrosome over-amplification, inducing a delay in mitosis.

Knockout studies have demonstrated that the inactivation of MEK1 gene leads to embryonic lethality, suggesting that MEK1 has a unique role during embryogenesis; while MEK2 is not necessary for the normal development of the embryo and its loss can be compensated by MEK1 (Belanger et al., 2003). All these experiments demonstrated that the two isoforms of MEK are not interchangeable, since interfering with one or the other causes different phenotypes.

ERK

ERK was evidenced for the first time as a kinase protein phosphorylating the microtubule-associated-protein 2 (MAP2) in extracts of 3T3-L1 adipocytes (Sturgill and Ray, 1986). This polypeptide was identified to be the same found phosphorylated by many growth factors (Nakamura, 1983; Cooper, 1984; Cooper 1985; Khono, 1985) and phorbol esters (Gilmore, 1983); these fidings reinforced the possibility that it might be an ubiquitous effector of mitogenic stimuli. This realization prompted the ridesignation of acronym “MAP” from “microtubule-associated-protein” to “mitogen-activated-protein”. ERK genes were purified and cloned the beginning of the nineties’ (Boulton et al., 1991).

ERK1 and ERK2 are 44 and 42 kDa Ser/Thr kinases with 90% sequence identity in mammals. The two kinases are both expressed in most, if not all, mammalian tissues, with ERK2 levels generally higher than ERK1. Knockout studies in mice demonstrated that ERK2 may at least partially compensate for the other's loss, although ERK1 has been found to regulate specifically thymocyte maturation (Pages et al., 1999). Dual Thr and Tyr phosphorylations activate both ERK1 and 2 at Thr202/Tyr204 for human ERK1 and at Thr185/Tyr187 for human ERK2. Unlike MEK, significant ERK activation requires phosphorylation at both sites, with Tyr phosphorylation preceding that of Thr (Ferrell and Bhatt, 1997).

The regulation of ERK localization by activation and inactivation mechanisms

In resting conditions ERK is mostly retained in the cytoplasm bound to MEK, which carries a Nuclear Export Signal, NES (Adachi et al., 1999; Rubinfeld et al., 1999). Indeed, ERK does not display any localization sequence, and theoretically could be homogeneously distributed. MEK prevents basal levels of ERK from entering the nucleus in unstimulated cells. Only upon stimulation, the cascade activation propagates through the different components till ERK phosphorylation by MEK and the subsequent detachment of the two proteins. This event determines the massive translocation of ERK in the nucleus (Chen et al., 1992), as exemplified in figure 4.

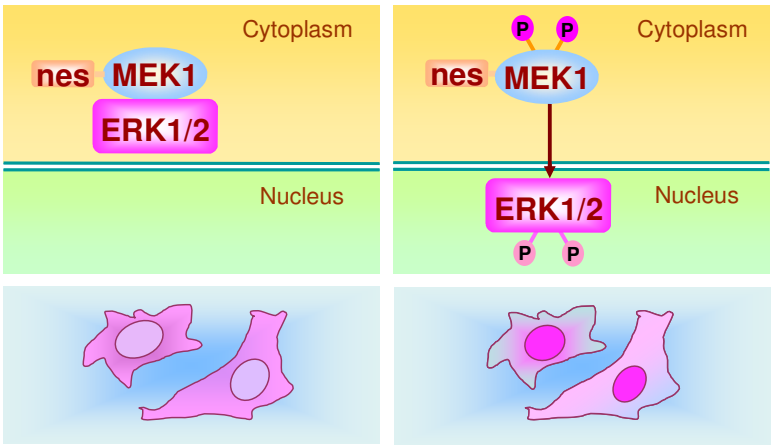

Figure 4
In resting conditions ERK1/2 are mostly retained in the cytoplasm by MEK, which carries a NES (Nuclear Export Signal). Upon stimulation of the pathway MEK doubly phosphorylates ERK1 and 2, which detach from their cytosolic anchor and accumulate in the nucleus. Besides, also MEK has been demonstrated to be able to cross the nuclear barrier, being continuosly exchanged between the cytoplasm and the nucleus (Fukuda et al., 1997; Jaaro et al., 1997; Tolwinski et al., 1999).

Also MEK1 can be continuosly exchanged between the nucleus and the cytoplasm, as demonstrated by several researchers (Fukuda et al., 1997; Jaaro et al., 1997; Tolwinski et al., 1999). However, the presence of the NES and the mantainance of its localization in the cytoplasm also after stimulation suggest that MEK has not any nuclear target. In conclusion, it is plausible that MEK principally acts as ERK1 and 2 activator, retaining them in the cytoplasm ready for sequential cycles of burst activity.

Analyzing the control of ERK localization on multiple levels, it clearly emerges that there is a complex regulation operated by a network made of several components of the pathway. As already described, ERK activation is propelled by the Raf-MEK route and many feedbacks have been elucidated. For example, ERK has demonstrated to be able to phosphorylate Sos on multiple residues following growth factor stimulation (Waters et al., 1996). This phosphorylation destabilizes the Sos-Grb2 complex, eliminating Sos recruitment to the plasma membrane and interfering with Ras activation.

To counterbalance the activation process and to restore the basal conditions, there are at least two major effectors responsible of the switch down of the signaling: phosphatases (either in part up regulated by ERK itself) and sprouty.

Phosphatase action provides ERK dephosphorylation and makes possible to re-localize the kinase in the cytoplasm under MEK control. Because ERKs and other MAPKs require both Thr and Tyr phosphorylation for full activity, Dual Specificity Phosphatases (DSPs, more frequently called MKPs), that dephosphorylate both sites, are uniquely positioned to regulate MAPK signal transduction cascades. At least 9 MKPs have been identified in mammalian cells (Camps et al., 2000), but the MKPs more frequently associated with ERK inactivation include: MKP3, MKP4, and Phosphatase of Activated Cells 1 (PAC1). MKP3 is present in many tissues and is more specific for ERKs versus other MAPKs. MKP4, expressed in kidney, placenta and embryonic liver, strongly dephosphorylates ERKs, but it shows some reactivity with JNK and p38 as well. The hematopoietically expressed PAC1 also shows limited reactivity with JNK and p38 and it is transcriptionally upregulated by p53 (Yin et al., 2003). In addition to MKPs, the phosphatases PP2A and HePTP have been implicated in ERK2 dephosphorylation at Thr185 and Tyr187, respectively (Zhou et al., 2002).

ERKs are also capable to regulate negatively themselves by phosphorylating MKPs, reducing the degradation of these phosphatases through the ubiquitin-directed proteasome complex (Brondello et al., 1999).

Sprouty is an inhibitor of the ERK pathway that is phosphorylated on a tyrosine residue in response to growth factor stimulation and it acts as an inhibitor of ERK activation.

Recently, it has been demonstrated that human Sprouty2 coimmunoprecipitates with protein phosphatase 2A (PP2A) in cells upon FGF receptor activation (Lao et al., 2007). c-Cbl and PP2A compete for binding on Sprouty2 and it can find at least two distinct pools of Sprouty2, one that binds PP2A and another that binds c-Cbl. c-Cbl binding likely targets Spry2 for ubiquitin-linked destruction, whereas the phosphatase binding and activity are necessary to dephosphorylate specific Ser/Thr residues. The resulting change in tertiary structure, following dephosphorylation, enables the binding with Grb2, a necessary step for Sprouty2 to act as a Ras/ERK pathway inhibitor in FGF signaling.

ERK and its targets

ERK1 and ERK2 are proline-directed protein kinases which phosphorylate consensus P-X-S/T-P sequences in a large number of substrates throughout the cell, leading to diverse cellular outcomes. Docking sites present on physiological substrates confer additional specificity (Tanoue et al., 2000).

To date, about 160 ERK substrates have been identified, including several transcription factors and immediate early gene products that facilitate the dramatic effects of ERK activation on gene expression and cell functions.

The wide variety of incoming signals which conveys on the module Raf-MEK-ERK is converted to a variety of actions owing to the phosphorylation of downstream effectors both in the cytoplasm and in the nucleus. This spatial segregation provides for diverse temporal profile of the following downstream effects. Indeed, the activation of cytoplasmic targets is responsible of acute effects: the major targets are represented by cytoskeleton proteins and other cofactors, which cooperatively act in migratory processes and outgrowth. Conversely, the translocation of activated ERK1/2 in the nucleus (Lenormand et al., 1993) is a necessary step for the long-term actions of the pathway on gene expression (Brunet et al., 1999), for morphological transformation of fibroblasts (Cowley et al., 1994) and for neurite extension in PC12 (Robinson et al., 1998). In

the following, I will explore some of the most significant targets for each category, in more details.

Cytoplasmic Targets

Ribosomal protein S6 Kinases (RSKs)

ERK1 and ERK2 indirectly regulate transcription by phosphorylating RSKs, a family of broadly expressed Ser/Thr kinases activated in response to mitogenic stimuli, including growth factors and tumor-promoting phorbol esters (Chen et al., 1991). RSK is phosphorylated in the cytoplasm and it shortly enters into the nucleus where it actually explicates its action on transcription factors. A highly conserved feature common to all RSK family members is the presence of tandem non-identical catalytic domains, involved in both exogenous phosphorylation and auto-activation (Dalby et al., 1998). These domains are activated in a sequential manner by a series of phosphorylation following the binding of active ERK1 or ERK2 to cytoplasmic RSK (Gavin and Nebreda, 1999). Active RSK plays a major role in transcriptional regulation, translocating to the nucleus and phosphorylating factors such as the product of proto-oncogene c-fos, serum response factor (SRF) and cyclic AMP response element-binding protein (CREB) (Chen et al., 1993b; Xing et al., 1996). Although RSK1 was initially purified and named on the base of its ability to phosphorylate the ribosomal protein S6 *in vitro*, this translational component is apparently the physiological substrate for the p70 S6 kinase, and not the RSKs (Chung et al., 1992).

ERK-mediated cell migration

I cannot get tired to outline the importance of spatial segregation; indeed, the intracellular and extracellular surface organization reflects a high degree of compartmentalization providing for precise and coordinated actions in response to exogenous signals. The targets herein discussed represent the major ERK-mediated effectors involved in cellular response to migratory signals. These are typical examples of asymmetric stimuli, given that they are often characterized by a spatial gradients in the extracellular environment. Cells are able to sense well defined spatial oriented stimuli, that can cause migration of the cell towards or away from the active substance. This local activation on restricted areas of the cell surface is transduced intracellularly with the recruitment of specific proteins, which coordinate opposite actions in different region of the cell (e.g., elongation of phylopodia towards the direction of the migratory stimulus versus retraction in

the diametrically opposite region). This fine regulation provides for an efficient machinery able to respond to external agents with great flexibility and a short time lag. Molecules involved in this process and that are regulated by ERK are the following:

Myosin light chain kinase (MLCK) phosphorylates myosin's regulatory light chain (and thus activates myosin) during nonmuscle cell contraction, cytokinesis, stress fiber formation and motility. Inhibition of the ERK pathway impairs MLCK and MLC phosphorylation and cell migration; expression of active MEK1 promotes phosphorylation of MLCK and MLC and enhanced cell migration in COS-7, MCF-7 human breast cancer and HT1080 fibrosarcoma cells (Klemke et al., 1997). Moreover, ERK phosphorylates MLCK and causes some increase in MLCK activity (Klemke et al., 1997).

Calpains are a family of Ca2+-activated proteolytic enzymes that are involved in cell migration (Dourdin et al., 2001; Huttenlocher et al., 1997). ERK phosphorylates m-calpain Ser50 both *in vitro* and *in vivo* (Glading et al., 2004) and this is required for adhesion turnover and cell migration because Ser50 mutation inhibits cell migration (Glading et al., 2004). m-calpain also associates with the N-terminus of FAK upon Src activation (Carragher et al., 2003); the FAK–m-calpain interaction is involved in targeting m-calpain to focal adhesions, where calpain degrades cytoskeletal proteins and causes adhesion disassembly (Cuevas et al., 2003).

Focal Adhesion Kinase (FAK) is a non-receptor protein tyrosine kinase that localizes at focal adhesions or focal contacts (Schaller, 2001). ERK phosphorylates FAK both *in vitro* and *in vivo* (Hunger-Glaser et al., 2003).

Paxillin is constitutively associated with MEK and extracellular stimuli induce the subsequent binding of active Raf and inactive ERK to paxillin, thus mediating ERK activation at focal complexes (Ishibe et al., 2003). The paxillin-FAK interaction is also involved in ERK activation (Subauste et al., 2004). Liu et al. have shown that ERK phosphorylates paxillin both *in vitro* and in hepatocyte-growth-factor-stimulated epithelial cells, and that paxillin phosphorylation in turn enhances paxillin-FAK association (Liu et al., 2002). However, Hunger-Glaser et al. have reported that ERK-mediated phosphorylation of FAK blocks the interaction of FAK with paxillin (Hunger-Glaser et al., 2003). These observations suggest that there might be a fine and complicated regulation of the FAK-paxillin complex, in which ERK might initially promote complex-assembly by

phosphorylation of paxillin and then promote disassembly by subsequent phosphorylation of FAK.

Integrins: ERK might also participate in cell migration by suppressing the ability of integrins to bind to their extracellular matrix ligands. It is well known that dynamic integrin activation is required for cell migration (Huttenlocher et al., 1996; Palecek et al., 1997) and that the Ras-Raf-MEK-ERK pathway regulates the affinity of integrins for their substrates (Chou et al., 2003; Hughes et al., 1997), although the molecular mechanism remains to be elucidated.

Cytoskeleton regulation

Microtubule associated protein 2 (MAP-2) was one of the first known substrates of ERK (Ray and Sturgill, 1987), this is the reason why it was also originally named Microtubule-Associated Protein-2 Kinase. MAPs are a group of proteins that stabilize microtubules, organize them into bundles, and connect them to membranes and intermediate filaments (Maccioni and Cambiazo, 1995). They are phosphorylated in response to cell stimulation and this inhibits their capacity to stabilize the microtubules (Jameson and Caplow, 1981).

In proliferating cells evidences suggests that MAPK is involved in cytoskeletal regulation (Reszka et al., 1995).

There is still no clear idea about the role of ERK in neurons; however several evidences pointed out to a regulational control of microtubule remodeling in axons. For example, Campenot chamber studies have shown that the ERK pathway is required for neurotrophin-induced axon assembly (Atwal et al., 2000), thus, application of pharmacological inhibitors of ERK to the side compartment blocks axon extension into the side chamber. Recent studies have also identified a potential downstream target of ERK, MAP-1b, reinforcing the idea of a link between ERK and axonal microtubule dynamics (Goold and Gordon-Weeks, 2005). Furthermore, ERK inhibition in growing axons has been shown to induce actin depolymerization and growth cone collapse (Atwal et al., 2000).

ERK signaling likely regulates actin filaments in the growth cone by using local protein translation, a mechanism that could ensure an efficient control of axon growth and guidance (Campbell and Holt, 2003). In support of this idea, increasing evidence shows that the synthesis of many cytoskeletal related proteins involved in axon growth and guidance is locally regulated in the axons;

e.g. mRNAs of b-actin (Bassell et al., 1998), the actin binding protein cofilin (Willis et al., 2005) and GAP43 (Smith et al., 2004).

ERK has been also demonstrated to be capable of phosphorylating Ser-Pro and Thr-Pro motifs in tau proteins, a specific class of microtubule-associated proteins that are abundant in neurons in the central nervous system (Weingarten et al., 1975), that have been found pathogenically hyperphosphorylated in Alzheimer disease (Anderton et al., 2001).

Nuclear Targets

ERK nuclear accumulation upon MEK-mediated phosphorylation is the crucial event to nuclear targeting: this provides a direct link between an extracellular signal, an internal signaling pathway and the genetic response. Even if ERK1/2 do not directly interact with the final effectors responsible of the transcriptional regulation, they control many nuclear targets, influencing and coordinating their activity. These effects are responsible of long term actions, leading to functional changes on wider time scales and inducing deep transformations of the cellular morphology. Herein, I will present the most important targets localized in the nuclear compartment.

The ETS transcription factor family

Cumulative data have revealed that this family of transcription factors are down-stream effectors of the Ras-MAPK signaling cascades (Wasylyk et al., 1998). The Ets family is defined by a conserved winged helix-turn-helix DNA binding domain (Papas et al., 1989; Wasylyk et al., 1998; Werner et al., 1995). Specific phosphorylation of Ets proteins greatly enhances their ability to activate transcription and regulate specific genes; this is achieved through interactions with other transcription factors on DNA.

Two major groups within this family have been extensively studied, the Ets group, including Ets1, Ets2 and Pointed, and the ternary complex factors (TCFs) which includes Elk1, Sap1a, Sap1b, Fli1 and Net (Fig. 5). The first group of Ets family members has a single MAPK phosphorylation site located near the pointed domain (Brunner et al., 1994; Wasylyk et al., 1997). TCFs, on the other hand, contain a transactivation domain that can be phosphorylated on multiple serine and threonine residues (Hipskind et al., 1994; Treisman, 1994). Phosphorylation generally enhances their ability to activate transcription by binding to specific sequences termed Ras-Responsive Elements (RREs) and Serum Response

Elements (SREs) present in the promoters of many immediate early response genes (Fig. 5).

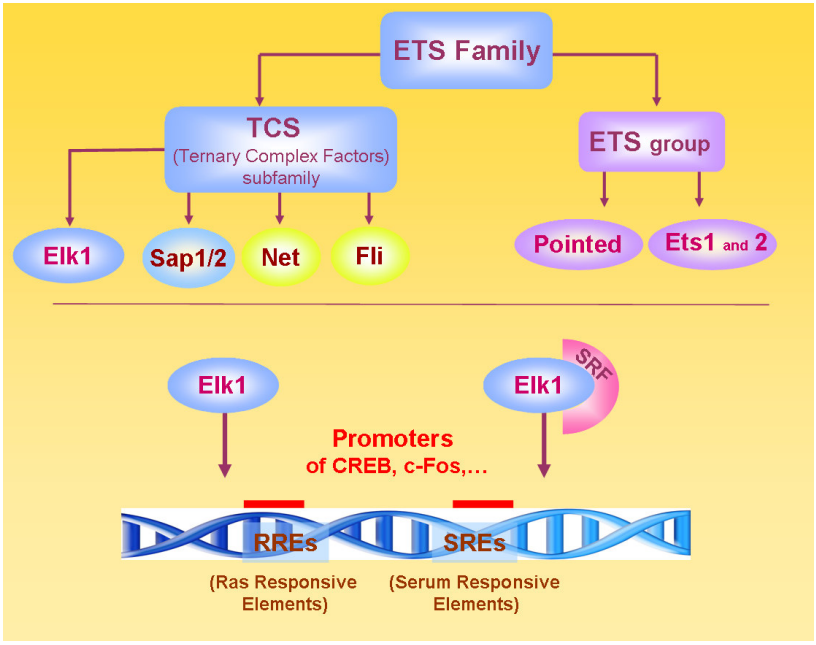

Figure 5
The major members of ETS family.
These transcription factors are characterized by the presence of the ETS DNA-binding domain and sequence conservation, within this domain alone is sufficient to classify ETS-domain proteins into subfamilies. Elk-1 is recruited to the SRE (Serum Response Factor) by a combination of protein-DNA and protein-protein interactions.

Elk1 represents the founding member of the TCF subfamily; it is directly phosphorylated by ERK1 and ERK2 at multiple sites (Marais et al., 1993), presenting two different domains acting as MAP kinase docking sites, the D-domain (Jacobs et al., 1999; Yang et al., 1998) and the FxF motif (Jacobs et al., 1999). Elk1 forms a complex with the Serum-Response Factor (SRF) and it recognizes the regulatory sequence SREs. Elk1 phosphorylation both enhances Elk1 recruitment to DNA (either in ternary complexes or autonomously) and potentiates its transcriptional activation activity. ERK-mediated Elk1 phosphorylation is also thought to promote the formation of quaternary complexes containing two Elk1 molecules (Gille et al., 1996).

There are several indications that Elk1 might have a role in neurons, indeed, Elk1 is expressed in neuronal cell types in the rat brain, and becomes phosphorylated in response to the activation of glutamate receptors (Sgambato et al., 1998).
Upon activation, Elk1 binds to the promoters of many immediate early genes, e.g. c-*fos*, *egr-1*, *egr-2*, *nur77*, *pip92*, b-*actin*, *vinculin* and *jun-B* (Wasylyk et al., 1997), however, the full spectrum of TCF target genes it is still not known.
Elk1 is not the unique ERK target belonging to the TCF family, Sap1 and Sap2 have been shown to be phosphorylated by ERKs (Price et al., 1995).
The TCFs are direct targets also of other MAP kinases, like JNK (c-Jun N-terminal kinase) and p38 cascades (Cohen, 1997; Robinson and Cobb, 1997). In contrast with the ERK cascade, which is activated by growth factors and mitogens, the JNK and p38 cascades respond to cytokines and stress stimuli.

The AP-1 (activating protein-1) transcription factor family

The activation of AP-1 family of transcription factors is one of the earliest nuclear event induced by growth factors that stimulates extracellular signal-regulated kinases (Karin, 1996). The AP-1 family consists of several bZIP (basic region leucine zipper) domain proteins, like Jun, Fos, ATF1 (Activating Transcription Factor 1), which all have to dimerize before they can bind to AP-1 DNA sequences, in order to regulate the gene expression of their DNA target sites (Fig. 6). Indeed, structural and functional analysis of c-Fos have revealed that it heterodimerizes with c-Jun and binds DNA through its bZIP DNA binding domain (Halazonetis et al., 1988; Kouzarides and Ziff, 1988; Nakabeppu et al., 1988; Sassone-Corsi et al., 1988).

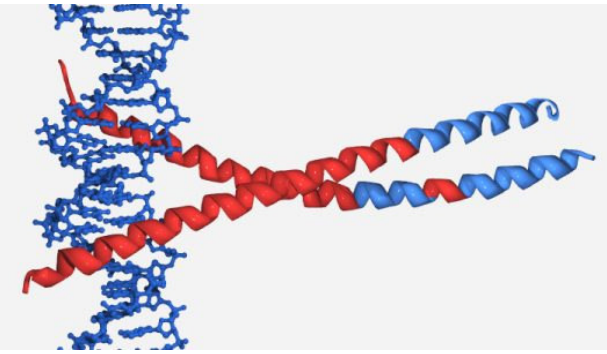

Figure 6
Structure of the c-fos/c-jun/DNA complex
PONDR® predicted disorder and order are represented respectively by the red and the blue ribbons.
(Molecular Kinetics, Inc., Washington State University)

The levels of expression and activities of these proteins are regulated by a variety of extracellular stimuli. They are thought to function in nuclear signal transduction

processes in many different cell types. The role of Fos and Jun in gene transcription is complex and may be regulated in several ways including association with different dimerization partners, interactions with other transcription factors, effects on DNA topology, phosphorylation and finally, reduction/oxidation of a conserved cysteine residue in the DNA-binding domain. In the case of c-Fos, activation of ERKs leads to the coordinated stimulation of c-*fos* expression by acting on transcription factors bound at the c-*fos* promoter (Treisman, 1994; Whitmarsh et al., 1995); ERK also induces the post-translational modification of c-Fos by the direct phosphorylation of the c-Fos Carboxy-terminal Transactivation Domain (TAD) (Chen et al., 1993a; Murphy et al., 2002), thereby enhancing c-Fos transcriptional activity (Monje et al., 2003).
However, the precise mechanism by which phosphorylation by ERKs alters the function of these transcription factors remains not fully understood. For example, reversible phosphorylation may result in changes in the stability, the nuclear localization, the rate of binding to target DNA sequences, and/or the positive or negative modulation of the transactivating activity of these transcription factors (Hill and Treisman, 1995). In the latter case, it is possible that the phosphorylation of specific residues may favor the interaction with other transcription factors or with the transcriptional initiation complex, either directly or through the recruitment of co-activators. In this regard, it has been shown that c-Fos interacts with the TATA box binding protein (Metz et al., 1994) and the transcriptional activator cAMP-responsive element binding protein (Bannister and Kouzarides, 1995).

Mitogen and Stress-activated Kinase (MSK)

MSK1 is localized in the nucleus and, as RSK, it catalyzes the phosphorylation of CREB at Ser133, indirectly linking ERK activity to the control of gene expression (Deak et al., 1998). MSK1 and the closely related MSK2 can mediate the stress-induced phosphorylation of CREB, because they are also activated in cells by SAPK2/p38 (Deak et al., 1998). In addition, the overexpression of MSK2 stimulates CREB-dependent reporter gene transcription in transfected cells (Pierrat et al., 1998). Finally, using knockout mice, MSKs were also found to phosphorylate histone H3 and the high-mobility-group protein HMG-14, facilitating the rapid induction of immediate early genes following mitogenic stimulation (Soloaga et al., 2003).

Duration, magnitude and compartmentalization of ERK response

The serially linked members of the ERK pathway provide not only for signal amplification, but, even more importantly, for additional regulatory interfaces that allow the specificity, duration and amplitude of activity to be precisely tuned. Despite having enjoyed a decade in the limelight of scientific investigation, which led to reveal a plethora of new insights into the circuitry of signaling pathways in general, this cascade still holds many secrets. These pertain mainly to how specific biological responses are encoded by spatial and temporal changes in the activity and sub-cellular distribution of the pathway components and how these fluctuations are orchestrated at the molecular level. The complexity of ERK signaling does not lie only in the enormous number of partners involved or in the variety of stimuli by which ERK can be activated; there are also other sophisticated levels of control represented by the duration, the magnitude and the subcellular compartmentalization of ERK activation/inactivation mechanisms.

Accumulating evidences have demonstrated that differences in the duration, magnitude and subcellular compartmentalization of ERK activity determine signaling specificity. For example, ERK activation can elicit opposite outcomes depending on the situation: cell proliferation versus cell-cycle arrest, cell survival versus cell death, and so on. This cannot be fully explained by cell type specificity, because ERK activation has distinct outcomes even in the same cell type (Schaeffer and Weber, 1999; Tan and Kim, 1999).

In the following, I will separately present the most important determinants of the temporal pattern of ERK activation (paragraph "*Duration*") and of the spatial segregation and amplification of ERK signaling (paragraph "*Magnitude and compartmentalization*").

Duration

Treatment of PC12 cells with nerve growth factor (NGF) induces sustained activation of ERK and causes their differentiation into sympathetic-like neurons, which is characterized by neurite outgrowth. By contrast, epidermal growth factor (EGF) stimulates transient ERK activation and causes cell proliferation (Gotoh et al., 1990; Marshall, 1995); furthermore, when the EGF receptor (EGF-R) is overexpressed in PC12 cells, ERK activity becomes sustained and the cells undergo differentiation in response to EGF (Traverse et al., 1994). The duration of ERK activity therefore appears to determine PC12 cell fate.

The ERK-signal-duration affects different cellular responses also in other cell types. Sustained, but not transient, activation of ERK is required for quiescent fibroblasts to begin to proliferate (Balmanno and Cook, 1999; Dobrowolski et al., 1994). When quiescent fibroblasts are treated with thrombin or platelet-derived growth factor (PDGF), they display sustained ERK activation and enter S phase. By contrast, thrombin-mimicking peptide (TMP) or EGF stimulate transient ERK activation and cannot induce the onset of S phase (Murphy et al., 2002; Vouret-Craviari et al., 1993). Indeed, blocking ERK activity with a specific MEK inhibitor, even several hours after growth factor stimulation, effectively blocks S phase entry (Weber et al., 1997). Murphy et al. have provided clues for understanding how sustained ERK activation causes fibroblast proliferation (Murphy et al., 2004). Whereas both transient and sustained activation of ERK induce transcription of immediate early genes (e.i. Fos, Jun, Myc, Egr1), only sustained ERK activation causes phosphorylation and stabilization of the proteins they encode. Because most immediate early genes encode transcriptional factors, they should in turn change expression levels of other genes crucial for cell proliferation. In fact, the mRNA and protein levels of cyclin D1 (a transcriptional target of the Fos-Jun complex and important for S-phase entry) are both elevated and maintained by sustained ERK activation (Weber et al., 1997).

What causes the difference in the duration of the ERK signal? Several determinant have been evidenced, herein I will discuss the principal positive regulators.

Ras and Rap1. In PC12 both EGF and NGF induce transient Ras activation but NGF stimulation also leads to sustained Rap1 activation (York et al., 1998). Recently, a combination of computational simulations and experimental validation has provided a more detailed analysis of Ras and Rap1 dynamics (Sasagawa et al., 2005).

PKC. It stimulates ERK activation through activation of Raf. ERKs activate cytosolic phospholipase A2 (cPLA2), and the arachidonic acid produced by cPLA2 activates PKC. Inhibition of PKC signaling has no effect on initial ERK activation, but blocks sustained ERK activation.

Growth factor receptor. The dynamics of the activation of TRK receptors might contribute to the different effects on the duration of ERK activity (Di Fiore and Gill, 1999). Upon EGF stimulation, the EGF-R undergoes rapid internalization

followed by degradation, which terminates ERK activation and thus makes it transient.

I can conclude that the duration and extent of ERK activation is the results of the balance between activating processes, as described before, and inactivating reactions directly carried out by phosphatases (ERK dephosphorylation) or indirectly by sprouty, which sequesters Grb2, impairing full activation of Ras cascade and, consequentially, ERK recruitment (as described in the paragraph "*The regulation of ERK intracellular localization by activation and inactivation mechanisms")*.

Magnitude and compartmentalization

In addition to the simple linear Ras–Raf–MEK–ERK module, all of these core signaling proteins have additional means of regulation. The enormous potential for convergence and divergence of signals onto and from the Ras–Raf–MEK–ERK pathway raises the question of how specificity is achieved, and the answer lies partially in scaffold proteins, molecules that tether signaling proteins in the vicinity of one another.

Recent studies have revealed scaffolding as a mechanism that helps the ERK cascade to transduce signals with both high efficiency and specificity. Scaffold proteins could play an important role in the regulation of the magnitude of ERK activity and they physically segregate ERK in specific loci of the intra-cellular environment. Experiments in mammals have focused on two scaffolding proteins: Kinase Suppressor of Ras (KSR) and MEK Partner 1 (MP1). KSR1 translocates to the plasma membrane on receptor activation, localizing MEK and activated Raf at the plasma membrane and providing a docking platform for ERK. This facilitates the sequential phosphorylation events needed for ERK activation, after which ERK dissociates from the complex to bind substrates in the cytoplasm and/or nucleus (Kolch, 2005; Nguyen et al., 2002). Experiments with KSR-deficient mice indicate that KSR is not absolutely required, but it enhances signaling from Ras (Nguyen et al., 2002).

The specialized adapter protein MP1 tethers MEK with ERK and seems to favor the activation of ERK1 over ERK2, linking exclusively MEK1 with ERK1 (Schaeffer et al., 1998). The physiological significance of this differential activation is not understood, but reduction of MP1 using RNA interference results

in defective ERK signal transduction with a decreased ERK activation in response to growth factor stimulation (Teis et al., 2002).

Modeling: a bridge between biochemistry and computation

In silico modeling represents an important tool of investigation and I firmly believe that, in order to maximize its efficacy, there should be a tight integration between models and experimental data. This approach can provide not only the validation or refusal of the hypothesis formulated to explain the observed phenomena, but it also helps to guide the design of new experiments. In this perspective, data coming from experiments must be quantitatively analyzed, in order to get specific parameters that can be used as input data for the computational model. This method allows to reduce the number of freedom degrees assumed for a certain model and it might represent a far more powerful tool, compared to only computational simulations.

ERK signaling has been object of investigation of several scientists, particularly concerning the dynamics controlling the signaling network at the basis of ERK-dependent functional outputs.

Bhalla et al. have conducted computational simulations and they reported that sustained ERK activation in fibroblasts is brought by a positive feedback loop between ERK and protein kinase C (PKC) signaling (Bhalla and Iyengar, 1999; Bhalla et al., 2002).

Sasagawa and coworkers have developed a simulation model of ERK signaling by constraining *in silico* dynamics on experimental data from living cells. In particular, they correlated the temporal pattern of ERK activation of two stimuli (EGF and NGF) with different outputs, and they demonstrated the involvement of Ras and Rap1 dynamics in the specification of PC12 fate. In particular, Ras and Rap1 capture the temporal rate of the stimuli presentation and the concentration of growth factors and then, they encode these physical properties into transient and sustained ERK activation (Sasagawa et al., 2005).

In this work, I took advantage of this integrated approach by modeling our experimental data in order to quantitatively estimate the effects of ERK nuclear inactivation and trafficking speed on the nuclear ERK phosphorylation. I tested the hypothesis that the relevant differences observed between the two kinases could be explained with a basic assumption of an equilibrium between the different states in which ERKs can exist.

In conclusion, ERK activity is the result of the synergy of several control mechanisms and regulatory feedbacks that are continuously modulated and that can operate differently in different cellular compartments. The resulting “average” state of ERK activity, that is seen by the nuclear targets and that is crucial for determining cell fate, is due to the integration of these processes.

Nucleo-cytoplasmic shuttling of ERK

A hallmark of eukaryotic cells is their separation into compartments, which are surrounded by membranes, impermeable to macromolecules, so specific transport systems have evolved to allow protein to be exchanged between different compartments.

For specific molecular components it is essential to move towards a particular compartment (e.i., RNAs once translated in the nucleus must move to the cytoplasm, chromatin remodeling proteins have to localize in the nucleus, etc…). The directionality of this process is provided by the presence of specific tags, which specifies the compartment of destination. The transport of the cargo presenting such special signals is mediated by specific transporters energy-dependent, like the importins and karyopherins (see later).

Nevertheless, there are proteins that are able to continuously move back and forth between the nucleus and the cytoplasm without the help of any carrier and in an independent-energy manner; these proteins are key factors in conveying information on nuclear and cytoplasmic activities within the cell. One of these is ERK; it notifies the nucleus of biochemical events upstream its activation which occurs in the cytoplasm. Then, the biochemical information coded in the ERK activation state is transduced in the regulation of gene expression.

In this work I investigated the exchange of ERK1 and 2 across the nuclear membrane in different conditions of pathway activation. In the following chapter, I will present the main features of the trafficking through the nuclear barrier. In particular, I will describe the complex structure which characterizes nucleoporins and the main routes followed by most cargos, paying particular attention to the anomalous transport system (not completely elucidated yet) which is responsible of ERK delivery.

Nuclear Pore Complexes: the gatekeepers of the nuclear entry

The spatial separation of transcription and translation provides eukaryotes a powerful mechanisms for controlling gene expression, but also necessitates

selective transport between the nuclear and cytoplasmic compartments to maintain the distinctive composition of each.

There are several nuclear transport pathways, each of which delivers a specific range of macromolecules either into or out of the nucleus (Moore, 1998; Peters, 2005; Wente, 2000). Most pathways use a homologous family of carrier molecules collectively called β-karyopherins, with import carriers called importins and export carriers called exportins. Many proteins are imported using importin-β (often using importin-α as an adaptor), although some are imported using other importins, such as transportin; many proteins are exported using the export carrier CRM1, whereas pre-microRNA and tRNA are exported by exportin-5 and exportin-t (all of which are importin-β homologues). In each pathway, cargo proteins (macromolecules that are greater than ~40 kD) usually present short Nuclear Localization Signal (NLS) sequence motifs or Nuclear Export Signals (NES), being actively transported, respectively, in or out of the nucleus, using soluble transport factors or carrier molecules that cycle between the cytoplasm and nucleus (Sorokin et al., 2007).

Trafficking across the nucleus occurs by transiting through the NPCs, huge macromolecular assemblies that perforate the nuclear envelope and form the conduit for the bidirectional exchange of molecules between the cytoplasm and nucleus through a central channel that has a limiting diameter of ~25–30 nm (Beck et al., 2004). NPCs are constructed from multiple copies of ~30 different proteins collectively called nucleoporins; these frequently contain FG sequence repeats, large regions consisting of tandem repeats based on highly conserved cores, containing one or two phenylalanines linked by hydrophilic spacers of variable sequence, but rich in charged and polar residues (Doye and Hurt, 1997; Rout et al., 2000; Ryan and Wente, 2000).

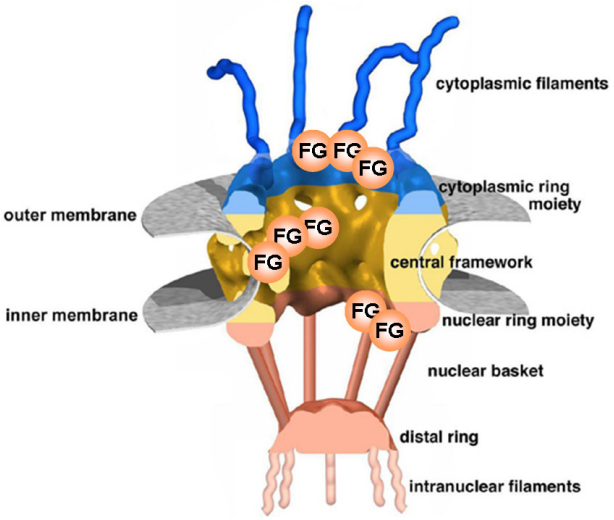

Figure 7
Schematic representation of the nuclear pore complex.
FG repeat regions have been found on the inner and outer surface and inside the pore channel.

The two most common cores are GLFG or FxFG (where x is usually serine, glycine or alanine), and some nucleoporins contain over 20 copies of these repeats. FG repeat regions of nucleoporins may not have a large amount of regular structure in solution and so may be very flexible (Bayliss, R 2000 Cell). Nucleoporin FG repeats appear to be directly involved in nuclear trafficking (Bayliss et al., 2000). Complementary postembedding studies, by using antibodies that label FxFG repeats indicate that FG nucleoporins, are found in the central channel as well as on both faces of NPCs (Grote et al., 1995) (Fig. 7).

Recently, quantitative measurements, by using cell-free nuclei reconstituted in *Xenopus* egg extract, showed that nuclear accumulation follows first-order kinetics and reaches steady state with a Michaelis–Menten function (Kopito and Elbaum, 2007). This saturation suggests that receptor-mediated translocation across the nuclear pore occurs bidirectionally. A far-reaching consequence is that the nuclear localization signal dictates the fate of a protein population rather than that of the individual molecules that bear it, which remain free to shuttle back and forth. This implies an open communication between the nucleus and cytoplasm and an ubiquitous mechanism for signaling in both directions.

Concerning ERKs shuttling across the nuclear barrier, it has to be considered that ERK does not display any obvious sequence corresponding to known NLS or NES sequences (Whitehurst et al., 2002). It seems to enter the nucleus by a carrier-independent mechanism (Adachi et al., 1999) and might therefore be ferried across the nuclear membrane (Whitehurst et al., 2004) by virtue of binding to other proteins such as the phosphatases MKP-3 (Camps et al., 1998), MEK

(Adachi et al., 2000; Burack and Shaw, 2005; Fukuda et al., 1997) or the phosphoprotein enriched in astrocytes, PEA-15 (Formstecher et al., 2001). Nevertheless, PEA-15, in contrast to MEK and MKP-3, would retain ERK2 in the cytoplasm in the active state, so it not only impairs nuclear signaling, but it also favors ERK signaling to cytoplasmic targets (Formstecher et al., 2001; Whitehurst et al., 2004). Recently, it has been identified a 3 aminoacid region (SPS), which when phosphorylated allows the interaction with importin7 (Chuderland et al., 2008). Interestingly, this site has been found also in other proteins which were thought to cross the nuclear envelope without the help of any carriers (Xu et al., 2003; Xu et al., 2000), like SMAD 3 (Chuderland et al., 2008). Furthermore it has been demonstrated that ERK can directly interact with NUP214/CAN and NUP153 (Matsubayashi et al., 2001; Whitehurst et al., 2002). Again, the interaction interface was mapped to the FG-repeats of NUP214/CAN and NUP153, although the exact ERK2 domain that is involved in such interaction remains undefined (Matsubayashi et al., 2001; Whitehurst et al., 2002). Only recently, using import reconstitution assays, Yazicioglu et al. have examined a group of ERK2 mutants defective in known protein interactions to determine structural properties of ERK2 that contribute to its nuclear entry. Several ERK2 mutants defective in interactions with FxF motifs displayed slowed rates of nuclear import and also showed reduced binding to a recombinant C-terminal fragment of nucleoporin 153 which is rich in FxF motifs (Yazicioglu et al., 2007). These results further support the idea that direct interactions with nucleoporins are involved in ERK2 nuclear entry and that multiple events contribute to the ligand dependent relocalization of this protein kinase.

ERK1 and ERK2: the "different twins"

ERK1 and 2 share approximately 90% of aminoacid identity; they are activated by the same stimuli and are believed to bear similar substrate recognition properties and subcellular localization (Boulton et al., 1991; Seger and Krebs, 1995). Although it has been assumed that ERK1 and 2 were functionally equivalent, recent studies have shown critical functional differences between these two proteins. While the genetic ablation of ERK2 in mice results in embryonic lethality, loss of ERK1 only causes deficits in tymocyte maturation and, surprisingly, leads to a dramatic enhancement of striatum-dependent long-term memory (Mazzucchelli et al., 2002; Pages et al., 1999). Significant

differences between the two kinases also appear in the control of cell growth, at least in cultured fibroblasts (Vantaggiato et al., 2006). Only very recently knockdown mice have been generated in which ERK2 expression was partially (20-40%) reduced; these mutants showed a deficit in long-term memory in classical fear conditioning, whereas short-term memory was normal (Satoh et al., 2007).

Combining together all these data, it is getting clear that the two kinases have only partially overlapping roles, and that they might undergo differential regulation. However, it has not yet emerged a clear molecular mechanism at the basis of these differences.

Since the long term effects of ERK action depends on the biochemical communication to the nucleus, I wondered whether some of the differences between ERK1 and 2 might originate in different trafficking properties. To this effect I resorted to imaging-based techniques to study trafficking across the nuclear envelope of the two kinases. I corroborated the imaging data with the help of classical biochemistry methods and *in silico* models. By using “dynamics techniques” it has been possible to unmask “dynamic properties” of fundamental importance to understand ERK functions and differences.

INTRODUCTION: Part 2

Dissecting a pathway: techniques to investigate molecular mechanisms

Every biological system is well described using a fundamental keyword: “dynamics”; communication is strictly and “dynamically” controlled at each level (molecule, cell, tissue and finally the entire body) and the regulation of each component is “dynamic” so that the system can answer quickly to different external agents.

I developed my study at the cellular level, investigating kinetics and relationship between cardinal proteins acting in several primary processes. There is no doubt that the best way to study a living system is to investigate the internal mechanisms without perturbing their homeostasis. This approach is nowadays possible and reliable, because of great improvements in molecular biology techniques and in the latest sophisticated technologies of living cell imaging.

The behavior of a molecule can be followed along time and space: the temporal scale plays a pivotal role in the hierarchy of molecular events and, on the other side, cells are strictly structured in ordered compartments that efficiently communicate together. Many processes take place in specific areas and only recruitment of critical proteins in specific loci are successful in determining a cascade activation.

I adopted fluorescence-based imaging techniques that allow to collect data with high spatial and temporal resolution in a living system. This would be impossible to achieve by using classical methods of investigation only (western blot, immunocytochemistry, etc…), that, although providing precious information about the state of chemical modifications or about the selective discrimination of molecules, cannot follow in real time and in physiological conditions what it is happening inside a cell. All the experiments in the present study have been conducted in living cells transfected with a plasmid carrying the cDNA of the protein of interest, tagged with a gene encoding a fluorescent protein belonging to the GFP family (Green Fluorescent Protein). This approach permits to visualize the fluorescent probes localization in real time.

In the following, I will discuss features and potentialities of imaging techniques in more detail, specifically, I will address:

- the generation of fluorescent fusion proteins and their validation;

- the tracking of protein movements and their relationship with the protein biochemistry;
- the measure of Fluorescence Recovery After Photobleaching (FRAP) to study protein trafficking inside or between different intracellular compartments.

Generation of fusion proteins and their validation

The fine tuning of geography, movement and chemistry gives proteins their extraordinary capability of virtually regulating all dynamic process in living cells. It is required making the proteins visible, in order to unveil how they move. The discovery and development of Green Fluorescent Protein (GFP) from the jellyfish *Aequorea victoria* (Fig. 8) have revolutionized our ability to study protein localization, dynamics and interactions in living cells (Tsien, 1998).

The chromophore (Fig. 9) is composed by an amino-acid triplet, Ser-Tyr-Gly, that undergoes a chemical rearrangement to form a fluorophore (Heim et al., 1994) in two steps reaction (cyclization and oxidation).

Advances in GFP biology, most notably the molecular engineering of the GFP-coding sequence, have resulted in optimized expression of GFP in different cell types, as well as the generation of GFP variants, with more favorable spectral properties including increased brightness and relative resistance to the effects of pH variation on fluorescence and photo-stability (Fig. 10). In addition, new fluorescent proteins have been discovered that are excited at longer wavelengths, like the Red Fluorescent Protein (DsRed), derived from the sea anemone *Discosoma striata,* increasing the current availability of fluorescent protein variants (Fig. 10).

Any fragment of cDNA, codifying for a specific protein or small parts of it, can be cloned in frame with the cDNA of a fluorescent protein and introduced into a suitable vector. Once created, the recombinant plasmid is transfected into cells, so they can produce by themselves the fusion protein that accumulates in different compartments according to the specification of functional domains. GFP fusion proteins have been used to address a wide range of questions in individual cells, as well as in tissues of a particular organism.

The resulting chimera often retains parent-protein targeting and functions when expressed in cells (Tsien, 1998) and therefore it can be used as a fluorescent reporter to study protein dynamics.

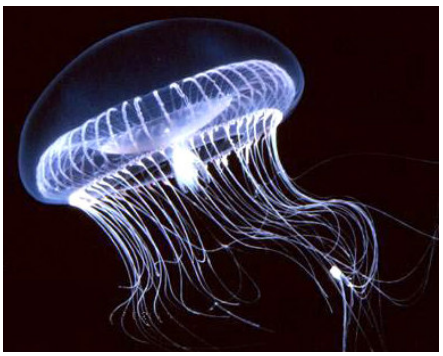

Figure 8
The jellyfish Aequorea victoria.

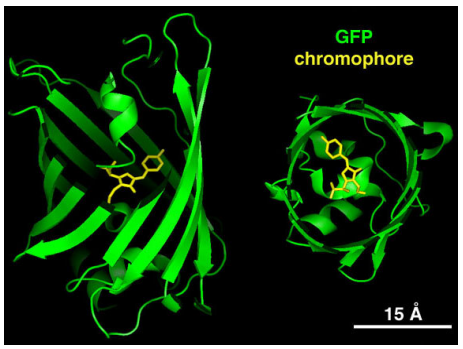

Figure 9
Tridimentional structure of the GFP.
The chromophore is protected inside the beta-barrel.

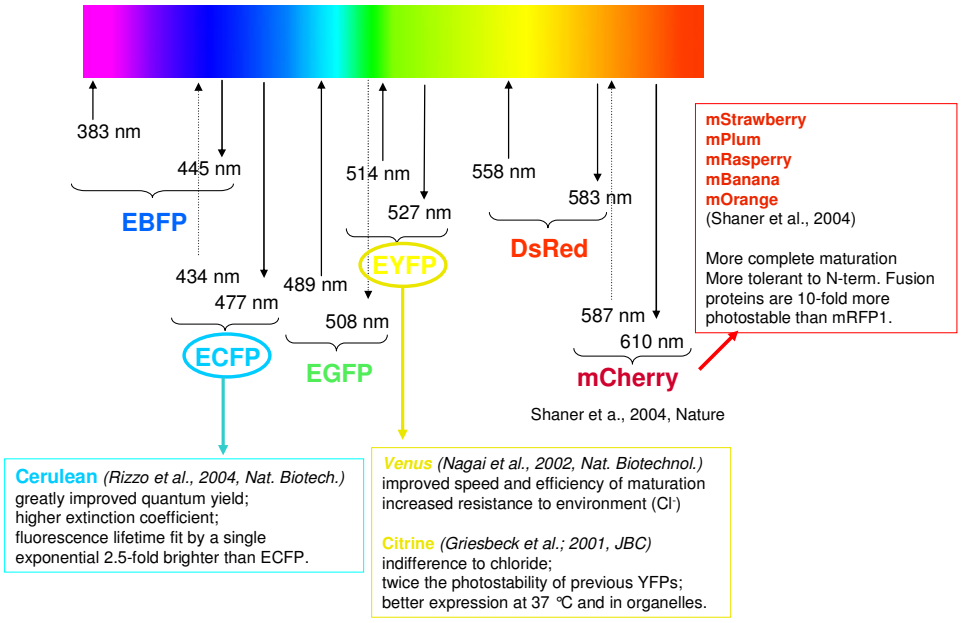

Figure 10
Representation of the most common fluorescent proteins
The reported proteins emitting from blue to yellow (EBFP, CFP, YFP and their optimized variants) have been obtained by mutagenesis of the GFP codifying gene (from the jellyfish *Aequorea victoria*); the red-shifted variants have been obtained from DsRed (from the Reef coral *Discosoma striata*). Numerous other variants have been identified and optimized also from other species of sea animals.

Of course, every new fusion protein has to be validated in order to demonstrate that it behaves like the corresponding endogenous protein. The following fundamental aspects have to be taken into account:

1. The fluorescent tag must not interfeare with the protein operations. It is important to make sure that fusion proteins correctly undergo to the same post-traduction modifications of the corresponding endogenous forms. Furthermore, in case of tagged enzymes, control experiments are required to test that the addiction of an exogenous protein (GFP) does not interfere with their catalytic activity. Virtually GFP can be tagged to any protein either N- or C-terminally. This is due to the fact that both termini of GFP are rather flexible on the surface of the beta-barrel, so that both the structure of GFP and of the protein of interest are not significantly distorted. Notwithstanding this, it is of crucial importance controlling by specific biochemical tests, whether proper post-translation modifications can occur once the chimera is expressed in a cellular system.

2. It is essential that the concentration of the chimera is as low as possible in order to preserve the physiological conditions and the endogenous homeostatic mechanisms. As I will show in the following, it is impossible to underevaluate the importance of this condition, since excessive overexpression of the fusion protein can cause an unbalancing of the pathway, leading to pathological or artificial conditions. For example, the localization of the fusion protein MP1 (MEK binding Partner1), GFP-tagged, reveals a strong dependency on over-expression, as shown in further details in Box 2.

To overcome the problem of overexpression there are at least two other methods. In the following, related benefits and drawbacks are reported:

Co-expression of the main regulatory components of the protein of interest.

This approach has been applied by Burack et al. in a live cell imaging study; ERK-YFP and MEK-CFP were coexpressed (Burack and Shaw, 2005) (Fig. 11).

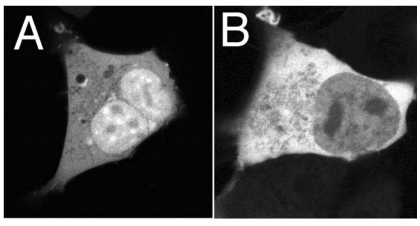

Figure 11
A) A cell overexpressing only ERK-YFP: the protein is mostly localized in the nucleus, despite that the cell has been starved.
B) The cotransfection of MEK-CFP and ERK2-YFP rescues the ectopic localization of ERK, causing its exclusion from the nucleus. Both images were collected in the YFP channel, so only the signal of ERK localization is visualized.
From Burack and Shaw, J. Biol. Chem., 2005.

Cotransfecting both the binding partners it is possible to restore the stoichiometric balance between MEK and ERK, and now the correct localization is achieved. However, this approach causes the overexpression of both proteins and this condition can influence other molecular equilibria through the pathway.

Silencing of the endogenous form and replacing it with the fusion protein. This can be achieved in culture cells, by siRNA technology, while in primary cells (derived from a fresh tissue) the generation of transgenic animals is required.

Tracking protein movements

Protein localization following exogenous stimuli or modifications of cellular shape, can be recorded with time lapse imaging techniques, which consist in collecting a long series of images of cells, at predetermined time intervals, while a certain process is occurring.

There is a great variability in the duration of cellular processes (milliseconds, minutes, hours to days); for example cell division occurs every 24 hr, while changes in ions concentration can occur as rapidly as few seconds. For these reasons, it is very important to know the right time scale of a certain process, in order to collect pictures of all the fundamental phases (see Box 3).

Initially, imaging recordings were done using photographic films and these movies were instrumental in demonstrating the dramatic behavior of cell motility. Over the last 25 years, cell biology has benefited from improvements in electronic imaging technologies that have largely replaced film recordings. Computer-based digital image-capture systems have revolutionized the study of the dynamic events of cell biology with their high quantum efficiency, low-noise characteristics and ease of use.

Working with imaging techniques, many technical requirements and strategies for maintaining cell viability during imaging have to be considered. Tight control of the culture environment is one of the most critical factors in successful live-cell imaging experiments. Aspects of the environment that are readily manipulated include the physical parameters of the chamber in which the cells (especially from mammals) are grown and imaged: temperature (cellular functions are exquisitely sensitive to temperature), atmospheric conditions (gas mixture and humidity), nutritional supplements, growth medium buffering (pH) and osmolarity of the culture medium. Specific chambers providing the control of the main environmental parameters are now available. Furthermore, time-lapse imaging

can be compromised by several artifacts that can affect the focus, like minute changes in temperature of the microscope (avoided by using thermostatic chambers) or cell motility and bulging.

Finally, an other important parameter to take into account is the illumination-caused photobleaching and phototoxicity, which can constrain time-lapse imaging because of cell damage. Indeed, repeated illumination, even at low intensity, induces the production of reactive oxygen compounds, derived from the excitation of the fluorescent probes imaged; so economizing light exposure would be preferable to reduce the photo-damage. The resultant image sequence portrays the true nature of cellular processes and makes it much easier to grasp the dynamics of these events. But the sequences produced are not just pretty pictures; they provide a wealth of analytical informations that can be readily used to conduct image analysis. The acquired images return a wide variety of informations about motility, morphology or distribution of intracellular components, unmasking how the system reacts. In a fluorescence-based system, the change of the chimera localization in response to stimuli or drugs is the final read out about what it is going on, that can be quantified by using image analysis software.

"Sliding molecules": measuring protein movements with FRAP

Fluorescence Recovery After Photobleaching (FRAP) was developed over 30 years ago (Peters et al., 1974) as a tool to study the molecular mobility in several media, including aqueous solutions, gels and living cells. In cell biology, FRAP was originally used to study membrane diffusion of lipids and proteins coupled to fluorophores (Axelrod et al., 1976; Edidin et al., 1976). In conjunction with GFP tagging of intracellular proteins, the development of confocal laser scanning microscopes (CLSMs) provided scientists with an excellent standard tool to perform FRAP experiments. GFP fusion proteins are ideal to use in FRAP studies because they can be bleached with low degree of damage to the cell (Lippincott et al., 1999). This is presumably because the compact barrel-like structure of GFP shields the external environment from the damaging effects that are caused by reactive intermediates generated by photobleaching (Prendergast, 1999; Yang et al., 1996).

In a typical FRAP experiment a region of the cell is briefly illuminated with a laser beam at high-intensity, with a wavelength near the excitation peak of the expressed fluorescent protein. Consequently, most of the fluorophores inside this

region irreversibly loose their fluorescence, a phenomenon known as photobleaching. As fluorescent proteins are attached to molecules that move in and out of the bleached region, fluorescence inside this zone increases and eventually equilibrium is reached (Fig. 12).

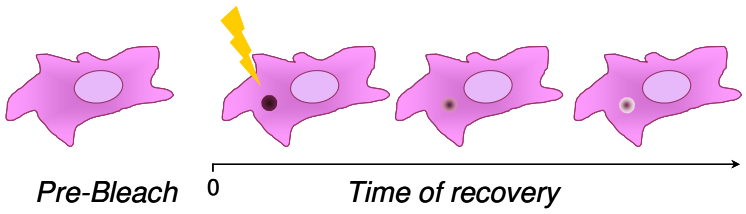

Figure 12
Cell photobleached in a small region of the cytoplasm; the fluorescence recovers from not photobleached nearby regions.

The analysis of the temporal sequence returs a plot of the recovery kinetics displaying fluorescence changes in the bleached regions of the cell over time (Fig. 13). From this plot a number of parameters can be directly extracted, that describe the kinetics of fluorescence equilibration. They
can be extrapolated "descriptive" parameters, not directly linked to a model, but useful to compare the behavior of different proteins.

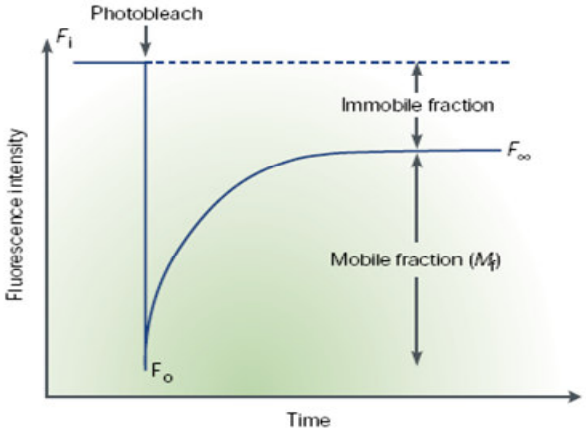

Figure 13
Profile of the fluorescence recovery after photobleaching
Schematic representation of the typical fluorescence recovery of the region that has been photobleached. By fitting with an exponential curve it is possible to estimate the immobile fraction and the time constant.

A typical FRAP curve provides useful informations about molecular mobility, codified by the Mobile Fraction, M_f, and the Diffusion coefficient, D. The Mobile

fraction is the fraction of the total amount of protein that can be exchanged between the bleached area and the nearby regions. It is determined by calculating the ratio of the final to the initial fluorescence intensity in the bleached region, corrected for the amount of fluorescence lost during photobleaching (Swaminathan et al., 1997) (Eqn. 1).

Eqn. 1 $$Mf = \frac{(F\infty - FO)}{(Fi - FO)}$$

A M_f less than 100% indicates that some fluorescent molecules might form immobile aggregates, or the protein is confined to a compartment and cannot contribute to fluorescence recovery in a separate disconnected compartment (Edidin, 1992; Edidin et al., 1994; Feder et al., 1996). In other words, there is a fraction of the entire pool of the protein of interest (Immobile Fraction= 1-M_f) which is partially or permanently immobilized, along the time window explored or that it interacts with other components and has a very high dissociation constant. Alternatively, non-diffusion factors, such as diffusion barriers or discontinuities within the structure where a protein localizes, might be responsible for the reduced mobility (Ellenberg et al., 1997; Feder et al., 1996), this latter condition is common for proteins localized in internal compartments that are disconnected from other structures (for example, endosomes and lysosomes).

The diffusion constant, D, provides a measure of the rate of protein movement in absence of flow or active transport (Lippincott–Schwartz et al., 1999; Axelrod et al., 1976; White et al., 1999). The theoretical D for a protein principally depends on its size and cellular environment, and reflects the mean squared displacement that a protein explores through a random walk over time. D has units of area per time ($\mu m^2\ s^{-1}$). The “effective” diffusion constant for a particle in a free volume is described by the Stokes–Einstein formula (Eqn. 2):

Eqn. 2 $$D = \frac{kT}{6\pi\eta R}$$

where D is the diffusion constant, T is the absolute temperature, η is the viscosity of the solution, k is the Boltzmann constant and R is the hydrodynamic radius of the particle.

Because absolute temperature is usually constant within cells, the most important factors underlying D are the size of a protein (or radius) and the viscosity of the medium within which it is diffusing. For a soluble spherical protein, an eight-fold increase in molecular weight will lead to a two-fold decrease in D. The recovery of relative fluorescence intensity within the bleached region is plotted as a function of time and fitted with various equations from which it is possible to estimate a time constant value (τ), which is indirectly related with the effective D. For example, when a small spot or narrow strip is bleached, simple equations can be used to estimate *D*, such as the equation by Axelrod and colleagues (Axelrod et al., 1976; Ellenberg et al., 1997; Sciaky et al., 1997) (Eqn. 3):

Eqn. 3 $$\tau_D = \frac{\omega^2 \gamma}{4D}$$

where ω is the width of the bleach, γ is a correction factor for the amount of bleaching (a weak function of the beam shape and of the bleach depth) and τ_D is the diffusion time. This formula assumes unrestricted two-dimensional diffusion into a circular bleached area without recovery from above and below the focal plane, so it is valid only for diffusion in membranes. Formulas based on unrestricted diffusion in a free volume are used for characterizing protein diffusion in the cytoplasm.

Even though viscosity and size are key factors underlying the diffusion rate of a protein, other factors also have a role in determining protein diffusion rates inside cells. Deviations from the theoretical value can provide useful information about the environment of the protein. For example, a D significantly lower than a predicted value (indicating slower diffusion) suggests that a fluorescent protein could be incorporated into an aggregate or a large complex, because D is inversely proportional to protein size. Alternatively, the environment of a protein could be notably more viscous than expected, or the protein could be interacting transiently with large or fixed molecules. By contrast, if D is significantly higher than predicted (indicating faster diffusion), the protein might be showing non-diffusive behavior such as flow or directed movement by motor proteins, or the viscosity of the environment might be decreased.

Soluble GFP in the cytoplasm, the mitochondrial matrix and nucleus diffuse three to four times more slowly than GFP in water, indicating that these environments

are more viscous than water (Partikian et al., 1998; Swaminathan et al., 1997); despite this, inert molecules such as GFP can cross the nuclear pores rapidly (Swaminathan et al., 1997). The high mobility of small solute molecules in the cytoplasm and nucleus is likely to be important for coordinating the complex regulatory pathways that operate in these environments. Diffusion of GFP within the ER lumen revealed it to diffuse three- to six-fold slower than GFP in the cytoplasm, so the ER lumen seems more viscous than the cytoplasm (Dayel et al., 1999). The abundance of protein-folding machinery and branched carbohydrate side-chains on proteins in the ER lumen could explain why its viscosity is greater than that of the cytoplasm. The apparent mobility of several nucleoplasmic GFP fusion proteins is surprisingly low. For example, the diffusion coefficients of GFP fused to the high mobility group SF2/ASF (Partikian et al., 1998) or fibrillarin, that have been measured by FRAP experiments, were extremely low, D= 0.24–0.53 $\mu m^2\ s^{-1}$ (Kruhlak et al., 2000; Phair and Misteli, 2000). As these proteins have been shown to associate rapidly with larger steady-state structures in the nucleus (splicing factor complexes and the nucleolus), one explanation for their low D is that recovery reflects two processes: diffusion and binding/release from an immobile substrate (Kruhlak et al., 2000; Phair and Misteli, 2000).

Differences between theoretical and effective D values for a protein can also arise from unusual cellular geometry. Equations of D for a protein in a membrane or a free volume usually assume that the spatial distribution of fluorescence in the cell is uniform (Axelrod et al., 1976). However, GFP fusion proteins are not often distributed homogeneously within the cell, as occurs when complex three-dimensional structures, like the endoplasmic reticulum (ER) and Golgi, are labeled (Cole et al., 1996; Edidin, 1992). Relating the diffusive spread of fluorescence through such structures to an idealized planar membrane or volume has required the development of theoretical models and simulation programs that take topology into account. More sophisticated equations and modeling are also required for analyzing FRAP experiments in which there are several diffusing species or when recovery occurs by more than one process (for example, when diffusion and binding/release from a substrate occur). Anomalous diffusion and flow-based processes can also contribute to recovery in FRAP experiments; the shape of the recovery curve is no longer characteristic of simple diffusion under these conditions.

Changes in the mobility of GFP fusion proteins observed under different conditions can provide insight into how a protein changes its association with other proteins.

Given that there are many ways to interpret different D and M_f or I_f values, it is important to combine FRAP measures with biochemistry and cell biology data to choose the correct interpretation of the observed phenomenon.

BOX 1: ERK variants

ERK1b It is an alternatively spliced form of ERK1 with a 26 aminoacids insertion between residues 340 and 341 of ERK1a (MW 46 kDa), whose kinetics of activation was similar to that of ERK1 and ERK2 in most cell lines and conditions, but showed higher fold activation in response to osmotic shock and epidermal growth factor treatments of Ras-transformed cells. Despite the uniform pattern of expression of ERK1 and ERK2, ERK1b seem to be present only in certain tissues, especially abundant in the rat and human heart. ERK1b seems to not interact with MEK1 and to be the major ERK isoform that responds to exogenous stimulation in Ras-transformed cells probably due to its differential regulation by MEK (Yung et al., 2000).

ERK1c It is an other alternatively spliced form of ERK1 playing a role in Golgi functions (Shaul and Seger, 2006). There are evidences pointing out at ERK1c involvement in cell cycle regulation via modulation of Golgi fragmentation. Although ERK1 was activated in mitosis as well, it could not replace ERK1c in regulating Golgi fragmentation. Thus, ERK1c extends the specificity of the Ras-MEK cascade by activating ERK1/2-independent processes.

ERK3 It is a protein of 62 kDa in size with a C-terminal domain that extends 180 amino acids beyond the conserved core of ERK family protein kinases and it is ubiquitously expressed in a variety of cell lines and tissues (Zhu et al., 1994). ERK3 does not phosphorylate typical MAP kinase substrates, indicating that it has distinct functions. It has been shown that ERK3 specifically interacts with the MAPK-activated protein kinase 5 (MK5 or PRAK) *in vitro* and *in vivo* (Schumacher et al., 2004). Complex formation between ERK3 and MK5 results in phosphorylation and activation of MK5, concomitant stabilization of ERK3, and the nuclear exclusion of both proteins.

ERK4 It is most closely related to ERK3 displaying 62% overall aminoacid sequence identity and 73% within the predicted kinase domain. Both kinases do not contain the highly conserved activation loop motif TXY, substituted by a single phospho-acceptor site within an S-E-G motif; they both carry long C-terminal extensions (Kant et al., 2006). MK5 has been evidenced to interact also with ERK4 (Aberg et al., 2006) however unlike ERK3, ERK4 is a stable protein, and its half-life is not modified by the presence or absence of MK5.

ERK5 It is twice the size of other MAPKs (Lee et al., 1995; Zhou et al., 1995). The amino-terminal half contains the kinase domain (TEY activation motif), whereas the carboxy-terminal half is unique. ERK5 has nuclear localizing activity in its C-terminal region (Yan et al., 2001), owing to a bipartite nuclear localization signal (Kondoh et al., 2006). In addition, ERK5 has nuclear export activity (Buschbeck and Ullrich, 2005; Raviv et al., 2004), even if a NES in ERK5 has not been identified so far. ERK5 is activated by several extracellular stimuli, such as stress stimuli and growth factors, and it has an important role in several cellular responses including cell proliferation and differentiation. Upon stimulation, MEK5 phosphorylates and activates ERK5, and then the activated ERK5 phosphorylates substrates including myocyte enhancer factor 2 (Kato et al., 1997). ERK5, as well as ERK1/2, can also induce immediate early genes, such as c-Fos and c-Jun (Kamakura et al., 1999; Kato et al., 1997). Recent genetic studies have demonstrated that ERK5 is essential for cardiovascular development and neural differentiation. The C-terminal region of ERK5 has transcriptional activation activity (Akaike et al., 2004; Kasler et al., 2000; Terasawa et al., 2003); this region is required for the maximum activation of MEF2, peroxisome proliferator activated receptor γ1 (PPAR γ1) and members of the AP1 family, like c-fos and Fra1.

ERK6 It is a 45 kDa protein which is highly expressed in human skeletal muscle and appears to function as a signal transducer during differentiation of myoblasts to myotubes (Lechner et al., 1996). In addition it has been observed that levels of mRNA transcript and protein abundance for ERK6 are increased during the differentiation of 2 rodent myoblast cell lines in culture, in contrast to the expression of ERK1 and ERK2 whose expression does not change during myogenesis. These results delineate a distinct pattern of ERK6 expression in mature skeletal muscle cells and suggest a specific role for ERK6 in muscle development or muscle function (Tortorella et al., 2003).

ERK7 It is a 61 kDa protein that shares approximately 40% homology with ERK1 and ERK2, but nether MEK1 nor MEK2 phosphorylate ERK7. Kinase phosphorylating ERK7 have not been identified to date. Instead, ERK7 seems to be constitutively active due to autophosphorylation. It is known ERK7 phosphorylates the transcription factor c-Fos and c-Myc and there are some evidences it also phosphorylates the oestrogen receptor-α (Bogoyevitch and Court, 2004; Henrich et al., 2003).

ERK8 It presents 69% overall homology with ERK7. Serum is the only stimulus identified that seems to activate ERK8, through the Src-dependent cascade [reviewed in (Bogoyevitch and Court, 2004)].

BOX 2*:* MEK binding Partner 1

MP1 is a scaffold protein of about 13 kDa (Schaeffer et al., 1998), that has been identified specifically to bind MEK1 and ERK1, but not ERK2, presumably facilitating their activation. Signaling pathways in eukaryotic cells are often controlled by the formation of specific signaling complexes, which are coordinated by scaffold and adaptor proteins.
I fused MP1 either at the N- than at the C-terminal of EYFP; then I transfected the resultant fusion proteins in replicating cells (Fig. Box 2.1).

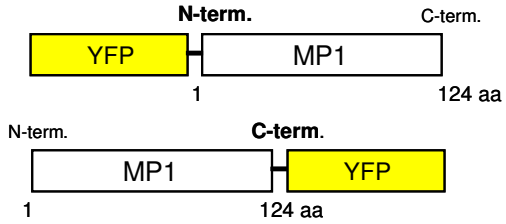

Figure Box 2.1
Schematic representation of the fusion of MP1 at both the C- and N- terminus of YFP.

I noticed that the localization of MP1-YFP was strictly dependent on the concentration of the fusion protein. Indeed, only at very low levels of expression I could detect MP1 on the surface of small round shaped organelles, which actually reflects its putative involvement in endosome signaling. But, as MP1-YFP concentration increases, I can detect the protein diffused all over the cellular compartments, resulting in an impairment of the correct localization (see Fig. Box 2.2).

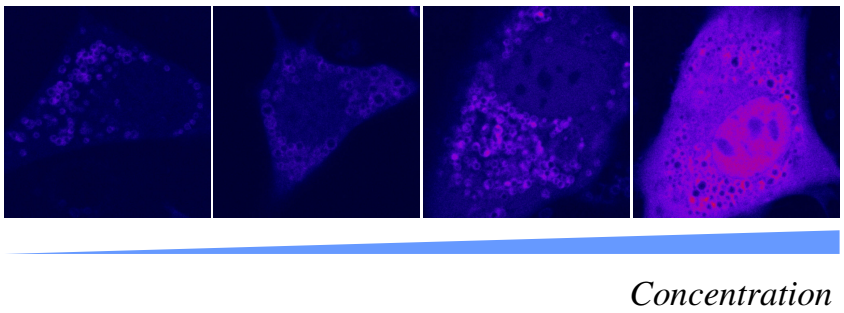

Figure Box 2.2
NIH 3T3 cells transfected with MP1-EYFP. The first image has been acquired at a 4-fold laser intensity; the fluorescent signal results very dim and with a low signal to noise ratio. These acquisition parameters are required for the detection of cells with the correct MP1 localization, but they are inappropriate to conduct prolonged live imaging.

This phenomenon probably reflects the fact that there is a limited number of binding sites on the membrane of the endosome structures, that once saturated cannot retain anymore the protein in place, thus leading to its ectopic delocalization.

BOX 3: Long Term Time Lapse

Visualizing chromatin rearrangement in living cells

Time lapse recording can be used to visualize many kind of cellular and molecular processes: here, as an example, I show a recording covering a time window of 12 hrs. Specifically, fibroblast were transfected with a fluorescent probe for MeCP2 (Methyl CpG–binding protein), a protein involved in the transcriptional regulation and epigenetic mechanisms.
Epigenetics refers to changes in gene expression (e.g. methylation) that are stable between cell divisions, and sometimes between generations, but do not involve changes in the underlying DNA sequence of the organism.
MeCP2 is a X-linked gene coding for a protein functioning as a transcriptional repressor. It is an abundant component of pericentric heterochromatin and its mutations or duplications are present in around 80% of patients with a neurological disorder known as Rett Syndrome. MeCP2 can recognize with high affinity methylated sites on the chromatin, because of the presence of a specific recognition domain, the Methyl Binding Site. MeCP2 action depends critically on its binding to chromatin, indeed the crucial event at the basis of its action is represented by its binding to CpG methylated chromatin.
To study the chromatin rearrangement mediated by MeCP2, the cDNA sequence of MeCP2 wt was fused in frame to GFP (Fig. Box 3.1) and then the resulting fusion protein was expressed in living cells.

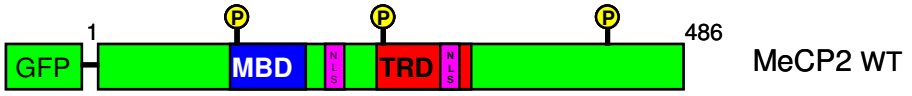

Figure Box 3.1
Wild type MeCP2 fused with GFP
WT: Wild Type, MBD: Methyl Binding Domain; TRD: Transcription Repression Domain; NLS: Nuclear Localization Signal.

By using long term time lapse, it has been obtained for the first time a direct demonstration of the dynamics of chromatin clustering caused by the expression of MeCP2, in living transfected cells. This experimental approach (Fig. Box 3.2) allows to demonstrate that chromocenters clustering proceeded in parallel with the increase of protein concentration and that this process invariably involved nearby chromocenters connected by chromatin filaments enriched with MeCP2 (Marchi et al., 2007).

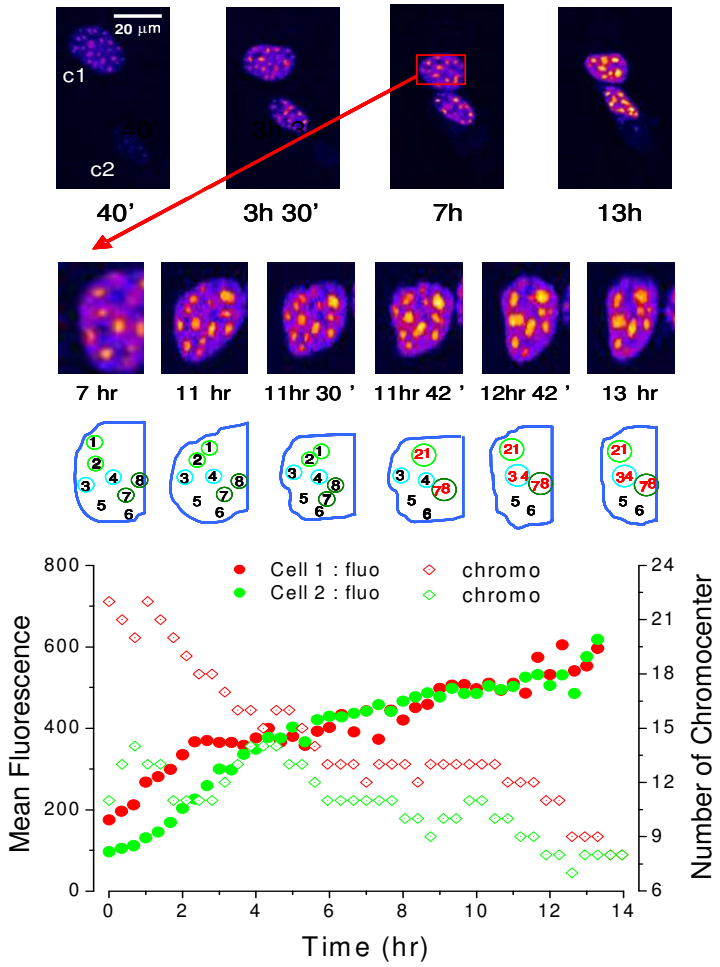

(Marchi et al., Epigentics, 2007)

Figure Box 3.2

Time-lapse imaging of the effects of GFP-MeCP2 expression on chromatin structure.

On the top, time lapse sequence of the nucleus of two NIH3T3 cells transfected with GFP-MeCP2. Imaging begun 7 hours after transfection and the cells were followed for 13 hours. At the beginning of the imaging session cell 2 is barely visible in the first frame of the sequence. As time passes by, the expression of GFP-MeCP2 increased in both cells. At the bottom it is represented a magnification of half nucleus of cell 1, enumerating the different chromocenters present and their successively clustering. The graph shows the relationship between the increasing concentration of MeCP2 in the nucleus (the concentration increases as time passes by after transfection) and the number of chromocenters and the nuclear size as functions of time. During the interval covered by the time-lapse imaging the clustering of chromocenters was paralleled by the decrease of the nucleus area.

RESULTS

All the experiments in the present study have been conducted in living cells minimally perturbed by employing very low level of fusion protein expression; the concentration was estimated by comparing the fluorescence of the cells with artificial micelles loaded with known concentrations of EGFP (see Methods). This approach avoids altering the relative abundance of the chimera compared with the endogenous forms and the upstream and downstream elements.

I generated both the N- and C-terminals fusion proteins for every ERK fusion protein tested. The most important experiments were repeated with both the configurations with similar results.

Herein, I will present data concerning the dynamical regulation and functional-structural differences between the two kinases ERK1 and ERK2.

The ERK1/2 Cascade

The ERK pathway is very complex and includes many components that integrate an enormous variety of stimuli at different levels; I principally focused on:

- Characterizing biochemical-functional properties of ERK fused to a fluorescent protein.
- Deciphering nuclear translocation dynamics of ERK2, investigating the interplay between the activation and deactivation systems;
- Studying the trafficking rate of the kinases ERK1 and ERK2 through the nuclear membrane;
- Evaluating the effects of ERK trafficking on the signaling to the nucleus;
- Studying the capability of ERK1 N-terminus of influencing the trafficking across the nuclear barrier and the functional outputs.

Fluorescent probe validation

Checking for correct post-translational modifications

I fused ERK1 and ERK2 with a fluorescent tag (EGFP) and I transfected the plasmid carrying the resultant cDNA in NIH-3T3 cells; then I tested the chimeras with a western blot assay to check if they retained the correct size and whether they can be correctly phosphorylated (Fig. 14).

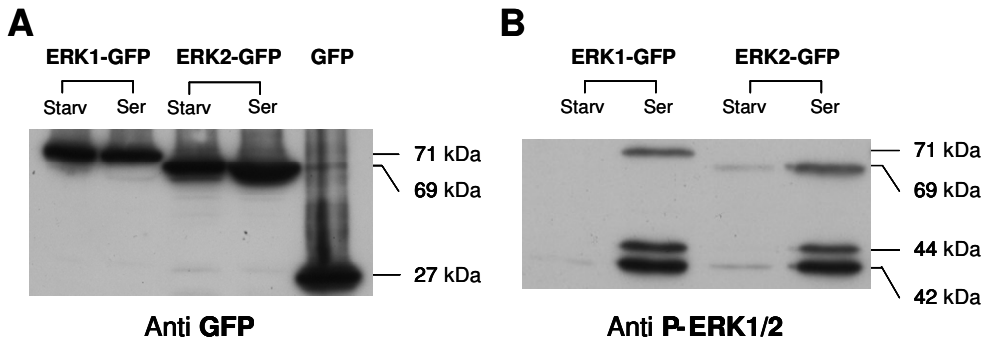

Figure 14
A) Immunoblotting with antibody against GFP displays a band at about 71 kDa in cells transfected with an ERK1-GFP vector, a band of 69 kDa in cells transfected with an ERK2-GFP vector and a band at 27 kDa in cells transfected with GFP only.
B) Immunoblotting with an antibody against phosphorylated ERK demonstrates that the phospho-specific antibody recognized both the wild type ERK1/2 doublet, respectively 44 and 42 kDa, and the fusion proteins after stimulation with 10% serum. Experimental conditions: Starv: starved, cells kept for 24 hr in 1% serum; Ser: serum, starved cells were stimulated for 15 min with 10% serum.

Immunoblotting demonstrates that the pERK antibody recognized both the wild type ERK1/2 doublet and the fusion proteins after stimulation with 10% serum at the expected molecular weight, so the two chimeras can undergo to the same post-translational modification as the endogenous forms do, once expressed in a cellular system.

Testing the catalytic activity

Another important issue to be considered is whether the fusion proteins retain their catalytic activity on specific substrates. I performed a second *in vitro* biochemical assay to verify the capability of phosphorylating downstream targets. I did not address this issue directly on cells, otherwise the test would be influenced by the endogenous form, making impossible to reveal the contribution coming only from the chimera. For this reason, I have isolated the fusion proteins by immunoprecipitation from transfected cells, previously stimulated with serum, in order to select a high percentage of activated protein; then I assayed the capacity of phosphorylating the purified substrate Myelin Binding Protein (MBP), a well known ERK target. Finally, I detected the signal coming from phosphorylated MBP, by staining with an anti-pMBP antibody, as shown in figure 15.

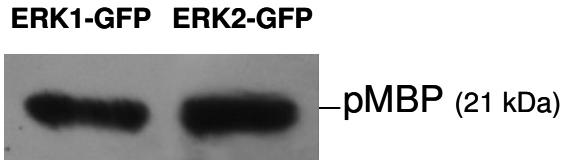

Figure 15
Cells were transfected with a vector carrying respectively ERK1-GFP and ERK2-GFP; then they were stimulated with 10% of serum for 10 min and afterward immunoprecipitated with an anti-GFP antibody. Samples were therefore let to react *in vitro* with the substrate MBP. Finally, they were immunoblotted with an anti-phoshoMBP. Both lanes display a strong signal at 21 kDa, corresponding to the MBP molecular weight.

The presence of the band at 21 kDa, corresponding to the phosphorylated form of MBP, demonstrated that the two chimeras were able to catalyze the phosphorylation of the MBP. These results show that the two fusion proteins are catalytically active, notwithstanding the presence of GFP.

Chimera localization and expression level

In resting conditions ERK predominantly localized in the cytoplasm, since it is retained by MEK which carries a NES (Adachi et.al., J Cell Biol. 2000). The presence of a stimulus (e.g. FGF, serum…) in the external environment induces receptor activation and it starts the signaling of Ras, finally switching on ERK phosphorylation. The next fundamental step is ERK translocation in the nucleus where the two kinases activate specific targets committed to regulate gene transcription.

Immunocytochemistry staining revealed that stimulation for 15 min with FGF caused an increase in the phospho-ERK signal and the nuclear localization of the fusion protein (respectively, in red and green in Fig. 16), this means that the chimera can be activated by the signal transduction elicited in cells by external agents and that it can cross the nuclear barrier and accumulate in the nucleus.

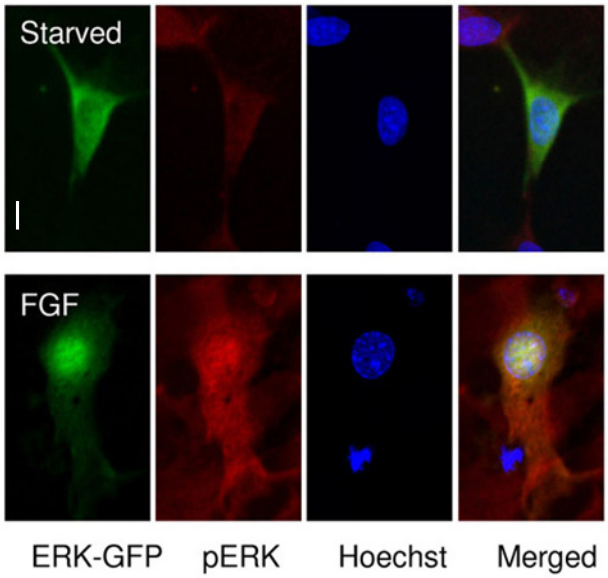

Figure 16
Subcellular localization of ERK2-GFP
In starved cells ERK2-GFP (green) was mostly excluded from the nucleus and the pERK signal (red) was very low. Conversely, upon stimulation with FGF, ERK2-GFP mainly accumulated in the nucleus, colocalizing with a strong pERK signal, which indicates that ERKs have been phosphorylated. I stained the nuclei with the DNA stain Hoechst 33342 (blue; 10 min in 1 µg/ml solution). Cells were imaged by combining 1- and 2-photon excitation: ERK2-GFP and pERK fluorescences were excited at visible wavelengths (respectively, 488 and 543 nm), whereas Hoechst was excited at 870 nm at 2-photons. Similar results were hold for ERK1-GFP. Calibration bar, 20 µm.

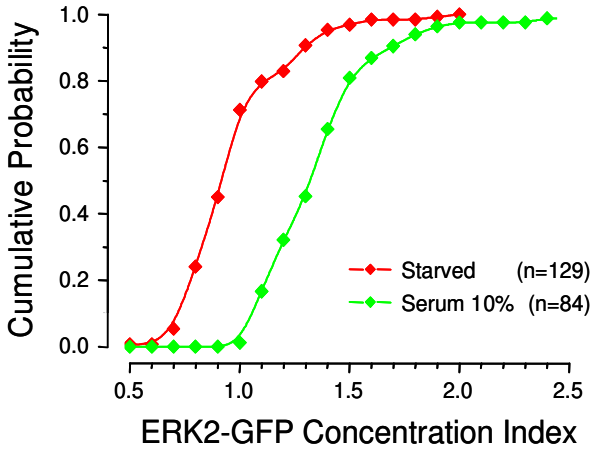

Figure 17
Cumulative probability of ERK2-GFP CI
Distribution of the cumulative probability of the Concentration Index measured in cells transfected with ERK2-GFP and imaged after starvation (red curve) or after stimulation with 10% serum ($P \leq 0.001$, Kolmogorov-Smirnov test). Similar results were hold for ERK1.

In figure 17 I presented a quantification of ERK nuclear accumulation in terms of cumulative probability (the integral to the probability distribution); this method is very effective in displaying the differences between two populations, regardless of their normality (Fig. 17). On the horizontal axis it is reported the value of the Concentration Index (CI), which is a measure of the level of nuclear accumulation of the protein, defined as the ratio between the mean fluorescence of nucleus and cytoplasm (see Methods).

As I have already reported in the introductory chapter, it is essential to work with a low concentration of exogenous protein in order to minimize the perturbation of the endogenous homeostatic mechanisms. Indeed, high amount of expressed ERK-GFP could result in an anomalous accumulation into the nucleus, even in absence of any stimulus. This effect is saturable and it is due to the disruption of the relative ratios between MEK and ERK (Fukuda et al., 1997; Lenormand et al., 1993; Rubinfeld et al., 1999). In previous studies this problem was either ignored (Ando et al., 2004) or overcome by co-expressing MEK1 to rescue this unbalancing (Burack and Shaw, 2005; Horgan and Stork, 2003). Rather than ignoring the problem or introducing a second exogenous protein, I opted for a different strategy. I chose to determine an upper limit for the concentration of ERK-GFP that is low enough to be compatible with the normal cell physiology, but that it is sufficient to allow confocal imaging.

To estimate ERK-GFP concentration I compared the fluorescence of the cells with the fluorescence of artificial cells loaded with known concentrations of EGFP. In this way I can verify whether the abundance of expressed chimera influences its relative distribution between the nucleus and the cytoplasm. I quantified ERK localization by means of the Concentration Index. Figure 18 shows that cells with higher concentrations of ERK-GFP exhibited a pronounced nuclear localization of the chimera. This distribution is not due to ERK activation since cells have been starved for 24 hr before imaging, but it depends only from the threshold saturation of the cytosolic anchor. This plot allows to estimate the upper limit of ERK-GFP expression which is compatible with a physiological localization of ERK (Fig. 18).

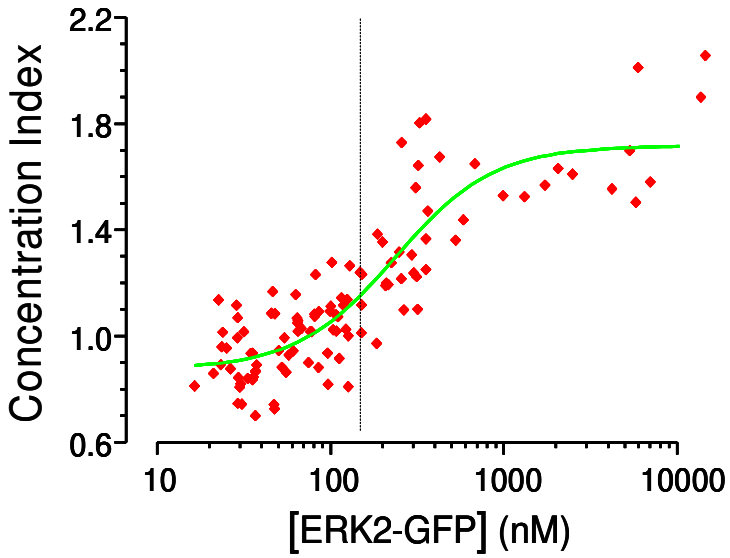

Figure 18
The graph shows the relationship between the transfection level in terms of [ERK2-GFP] (fluorescence averaged on the entire cell) and the nuclear localization of starved cells, measured by the Concentration Index. The dotted line indicates the upper level of expression that I accepted in my experiments (150 nM). To extend the measures on two decades I used varying laser power according to the best imaging conditions for each cell: data were pooled together after normalization to reference imaging conditions. The graph displays only ERK2 concentration values, analogous results were obtained for ERK1.

These data demonstrate that ERK-GFP localization was normal up to about 150 nM and that nuclear accumulation saturated at concentration larger than 1.5 μM (Fig. 18). In about 80% of the cells included in this study the concentration of ERK-GFP was ≤100 nM. Additionally, I have excluded cells that, notwithstanding the low fluorescence, exhibited visible nuclear accumulation in the starved state.

Resolving spatiotemporal dynamics of the ERK activation/inactivation

Notwithstanding the centrality of the process of ERK translocation, most of the dynamical details of this event are still unknown. I focused on the kinase ERK2 and I tried to elucidate various aspects of the translocation event analyzing the contribution of the different counterparts in a living system with the application of specific inhibitors.

ERK2 in action: the nuclear translocation

I evaluated nuclear translocation properties recording several groups of cells transfected with ERK2-GFP and following their distribution after stimulation, provided by adding to the medium the specific growth factor for fibroblast, FGF4 (Fig. 19).

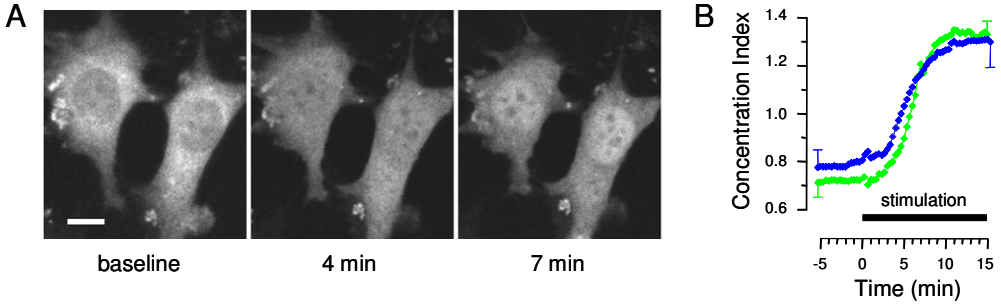

Figure 19
ERK2-GFP translocates in living cells after stimulation.
A) In cells stimulated with 20% serum translocation can be discerned as early as about 4 min from stimulation; the process reached the maximum peak in about 10 min.
Bar 20 µm.
B) Cumulative time courses of the translocation index of cells stimulated with FGF4 (80 ng/ml, blue, n=9) or with serum (10%, green, n=15). The vertical bars are representative of the standard error before stimulation and at the end of the imaging period.

After an initial latency, ERK2-GFP rapidly concentrated into the nucleus reaching 90% of response within about 9 minutes from the onset of stimulation. I presented these data plotting the normalized CI in function of time. The translocation of the N- and C-terminal fusion proteins followed a similar time course excluding a dependency from allosteric influence of the GFP on specific ERK domains. I confirmed the generality of the result presented before finding similar translocation behaviors in other cellular types. In particular I tested NIH L1 pre-adipocytes and mouse primary fibroblasts (Fig. 20).

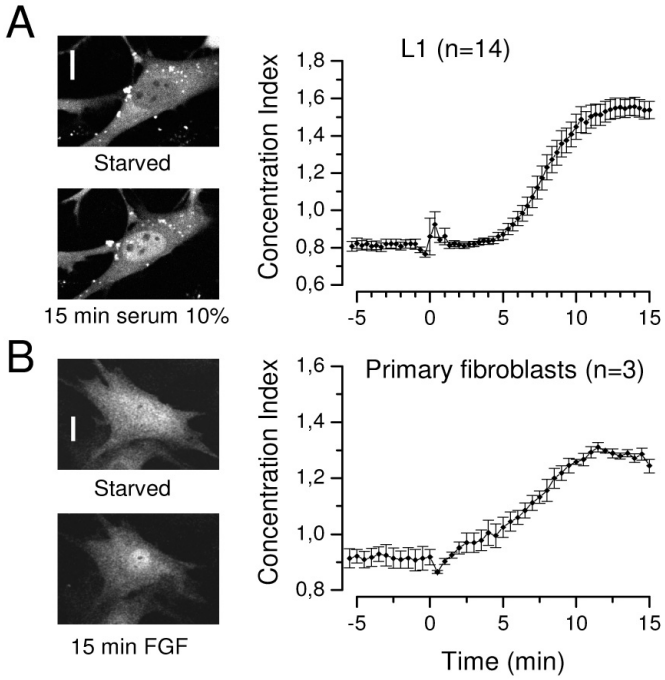

Figure 20
Demonstration of the nuclear accumulation of ERK2-GFP in two additional cell types.
A) NIH L1 preadipocytes were starved for 24 hr in 1% serum before stimulation with 10% serum. Bar, 20 μm. NIH-L1 preadipocytes were cultured according to ATCC protocols. In both panels time 0 indicates the beginning of stimulation.
B) Primary fibroblasts were starved 24 hr prior to the experiment and stimulation with FGF4. Primary fibroblasts were dissociated from the tail of an adult mouse and transfected at passage 3. Both cell types were transfected and imaged as described for NIH-3T3.

Then I compared the responses induced by FGF and different concentrations of serum in NIH 3T3: initially, serum and FGF4 produced similar responses activating a monotonically increasing translocation; after 20 min from the stimulus, the serum-induced response declined gradually, while FGF4 caused constant accumulation during the imaging period, up to 2 hr (Fig. 21).

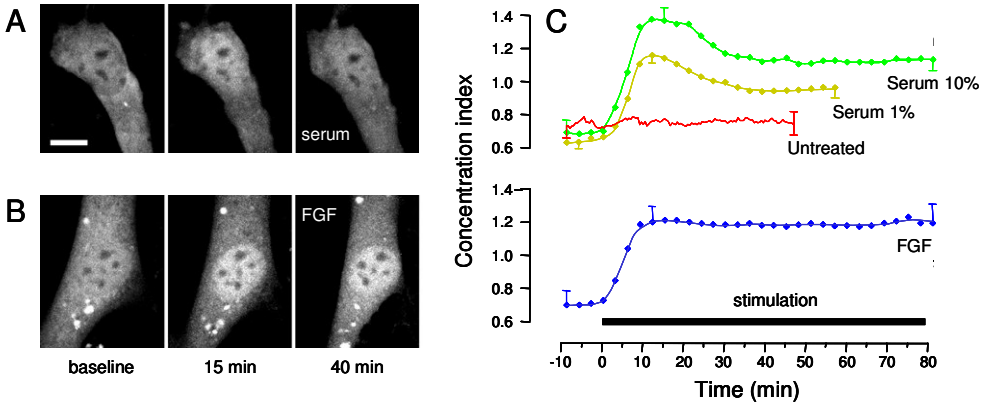

Figure 21
A)-B) Series of images representing cells at three different times during the experiment, respectively with serum (A) and FGF stimulation (B). Bar, 20 µm.
C) Cumulative time courses of ERK2-GFP nuclear accumulation, in terms of CI, after stimulation with two different doses of serum (green, 10%, *n*=7; yellow, 1%, *n*=8) and FGF (blue, *n*=8). Red trace represents untreated control cells (*n*=9).

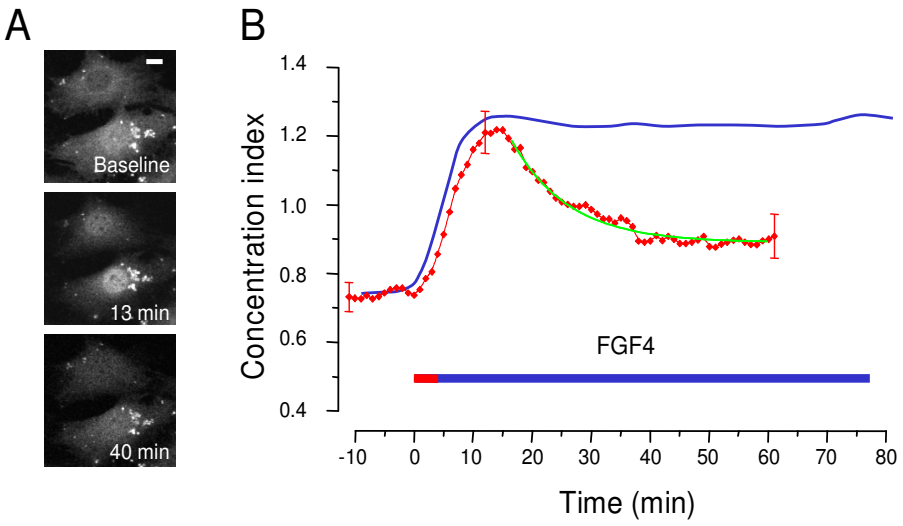

Figure 22
A) Cells have been stimulated with FGF4 (80 ng/ml) for only 4 min. The fusion protein exhibited a transient translocation. Bar 10 µm.
B) Cumulative time course after 4 min of stimulation (red trace, n=15) compared with the kinetic of the response to a stationary stimulus (blue trace). The vertical bars are representative of the standard error during imaging.

Interestingly, 1% serum gave a response of smaller amplitude respect to the maximum stimulation obtained with 10% serum; this might reflect the smaller amount of ERK which is recruited for translocation. I have also looked into the temporal fidelity of ERK nuclear accumulation following the stimulus temporal profile, by treating the cells with a brief presentation of FGF4. Cells were stimulated with FGF for only 4 minutes, washing away the stimulus from the recording chamber afterwards (Fig. 22).

Initially, ERK2-GFP concentration in the nucleus increased like it happened with the response to a stationary stimulus; however soon after peak the CI declined exponentially, almost to baseline level. Notice that the presence of the stimulus is not simultaneous to the response, suggesting that the delay observed is required to start up the pathway machinery and to transduce the activation signal in the ERK-specific output. Besides, this experiment demonstrated that a continuous stimulation is a necessary condition to sustain ERK translocation.

MEK and Phosphatases: the hero and the villain?

Activators and deactivators rigorously play their roles in the plot of ERK life; they simultaneously and continuously act to settle ERK fate. During time lapse recordings I applied selective drugs that selectively affect either the activation or the inactivation pathway. This approach represents a powerful method of investigation: it makes possible to dissect the underneath dynamics between these regulatory proteins (Fig. 23) and to measure separately their activities.

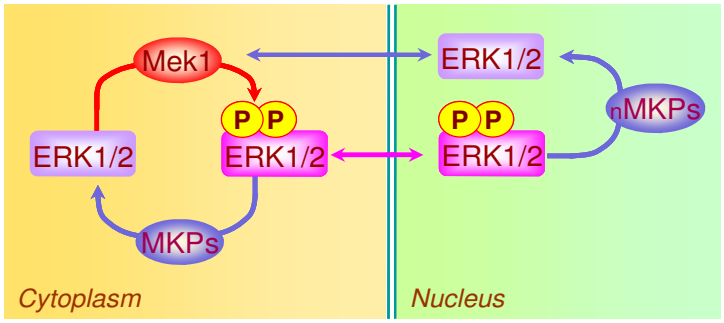

Figure 23
In resting condition ERKs are retained by MEK in the cytoplasm; once the pathway is activated, MEK doubly phosphorylates ERK1 in Thr203/Tyr205 and ERK2 in Thr183/Tyr185 (*Mus musculus*). ERKs translocate into the nucleus where they can act on their substrates. In the nucleus ERKs can only be dephosphorylated by nuclear phosphatases. As I will show later on, ERKs can bidirectionally pass the nuclear barrier in both states: phosphorylated or dephosphorylated.

In starved cells the upstream pathway would not necessarily be totally deactivated: ERK might be regulated by the dynamic equilibrium of a moderate basal activity of the Ras-MEK1-ERK1/2 module with competing phosphatases. The rational of this basal under-threshold activity of MEK is the maintenance of the pathway in a state ready to quickly answer to changes coming from the extracellular environment.

This putative basal activity should be revealed by the blockage of dephosphorylation. Indeed, in resting conditions the majority of ERK molecules are bound to MEK in the cytoplasm, so whether MEK basal activation was present, I should observe a progressive accumulation of ERK in the nucleus upon administration of the phosphatase inhibitor. Indeed, upon perfusion of starved cells with 1 mM of sodium-orthovanadate, ERK2-GFP began to accumulate in the nucleus within few minutes (Fig. 24).

The accumulation of ERK2-GFP in the nucleus gradually increased throughout the duration of the imaging period (up to 1 hour). This demonstrates that even after 24 hours of serum deprivation, the ERK1/2 pathway is undergoing some basal activation that in normal conditions is equilibrated by a corresponding level of phosphatase activity.

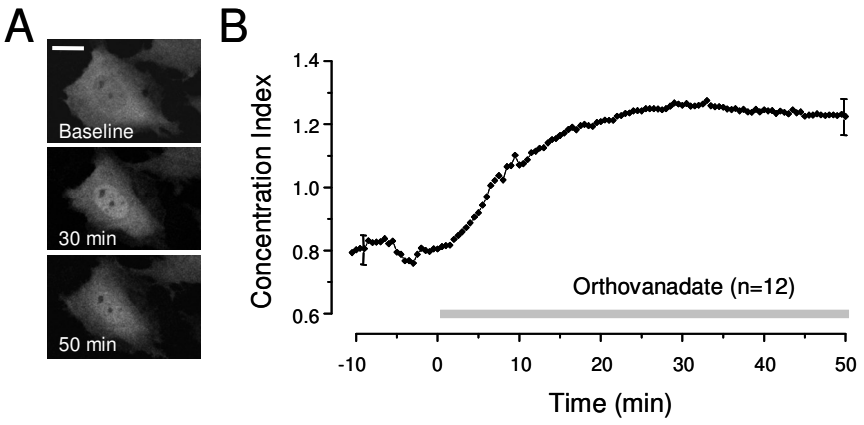

Figure 24
Treatment with the phosphatase inhibitor Sodium Orthovanadate caused gradual nuclear translocation.
A) Cells expressing ERK2-GFP before orthovanadate treatment (1 mM), 30 and 50 min afterwards. Calibration bar 20 µm.
B) Starved cells were treated with the phosphatase inhibitor at time 0.

This nuclear accumulation occurs in parallel with ERK activation, as demonstrated by immunocytochemistry with the pERK antibody (Fig. 25).

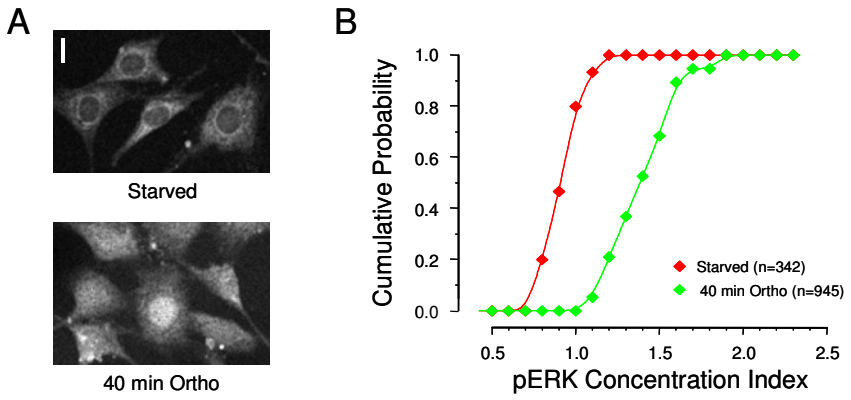

Figure 25
Inhibition of phosphatase causes ERK phosphorylation and translocation.
A) Immunocytochemistry with the pERK antibody conducted on starved cells treated with sodium orthovanadate (1 mM) for 40 min before fixation. Representative images of pERK distribution in starved cells and during treatment with phosphatase inhibitor are shown. Bar 20 μm.
B) Cumulative probability of the Concentration Index of the pERK signal.

Interestingly, the nuclear accumulation caused by the phosphatase inhibitor (Fig. 24) is much slower than the change observed after stimulation, as indicated by the time constants of the two processes (τ= 26 min, after phosphatase inhibitor treatment, and τ= 3.3 min after FGF stimulation). This slow kinetics is likely to reflect the fact that MEK basal activity is much smaller than after activation. However, it is not possible to overstretch this interpretation because the speed of permeation of the inhibitor in living cells is unknown.

The experiment upon presented outlines an essential feature of the MEK-ERK system: the push-pull regulation by activating and inactivating mechanisms operating also at a basal level of activity. If a similar dynamical equilibrium between phosphorylation and dephosphorylation holds also after activation by extracellular stimuli, it would be expected that the sustained nuclear accumulation caused by FGF4 would require continuous activation of the MEK1-ERK pathway. To shed light on this issue, I treated the cells expressing ERK2-GFP with U0126, after 15 min of stimulation with FGF4 (Fig. 26): this caused the immediate

decrease of ERK-GFP concentration in the nucleus. The speed of this process (τ=3 min, see Fig. 27) showed that U0126 diffused rapidly in the intracellular medium and that its effect was very fast. It appears evident that the drug permeation is not a rate limiting factor: U0126 seems to be able to cross the membrane barrier without any difficulty and to promptly act on its target.

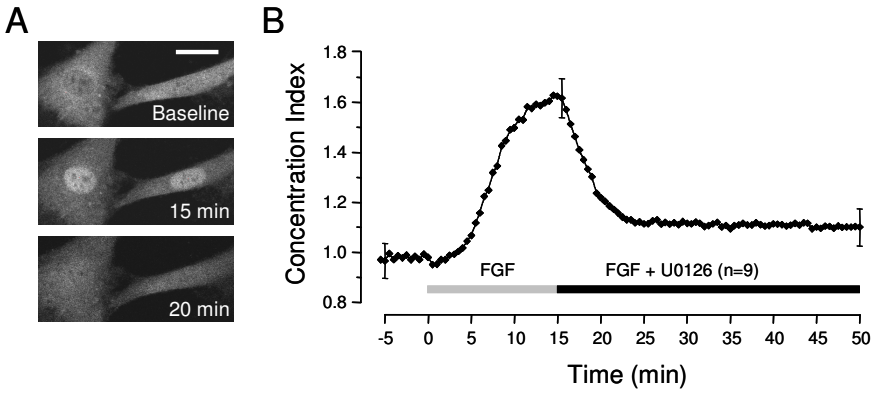

Figure 26
ERK2 activation and consequent translocation required continuous activation of the MEK-ERK pathway.
A) Cells were treated initially with FGF and 15 min later, with 20 μM U0126. Blockage of MEK caused the rapid loss of nuclear fluorescence. Bar 20 μm.
B) Averaged time course.

ERK activation and localization are determined by the balance between two competitive reactions: phosphorylation and de-phosphorylation. Phosphatase activity converts ERK in an inactivated state by dephosphorylation and during the steady-state phase of ERK response, this process is balanced by the phosphorylation operated by MEK. In the experiment shown in figure 26 the addition of the MEK inhibitor, U0126, impairs the steady state equilibrium causing ERK2-GFP outflux from the nucleus.

To allow a better comparison of the time course of all the processes that have been described so far, the change of CI in response to the different treatments has been normalized between 0 and 1 and it is displayed in figure 27. Time 0 corresponds to the beginning of treatment of naïve cells with FGF4 or orthovanadate and of FGF-treated cells with U0126. The continuous lines are exponential fits to the experimental data: the time constant of the loss of ERK concentration from the nucleus is 3.0±0.13 min (R^2=0.99, blue curve), similar to

the FGF-induced response (τ=3.3±0.12 min, R^2=0.99, green curve). In comparison, the rate of nuclear accumulation induced by the block of phosphatases in starved cells is much lower (τ=26±0.48 min, R^2=0.98, red curve), suggesting that upon stimulation the rate of ERK2 phosphorylation increased by almost a factor of ten. The latency of the effect of U0126 is virtually zero, demonstrating that imported ERK2 is rapidly dephosphorylated and exported from the nucleus. In normal conditions the response to FGF4 is seen as ERK2 sustained translocation because of the influx of phosphorylated ERK2; the ihibition of MEK1 bloks this continuous influx and unveils the inactivation process, especially in the nucleus.

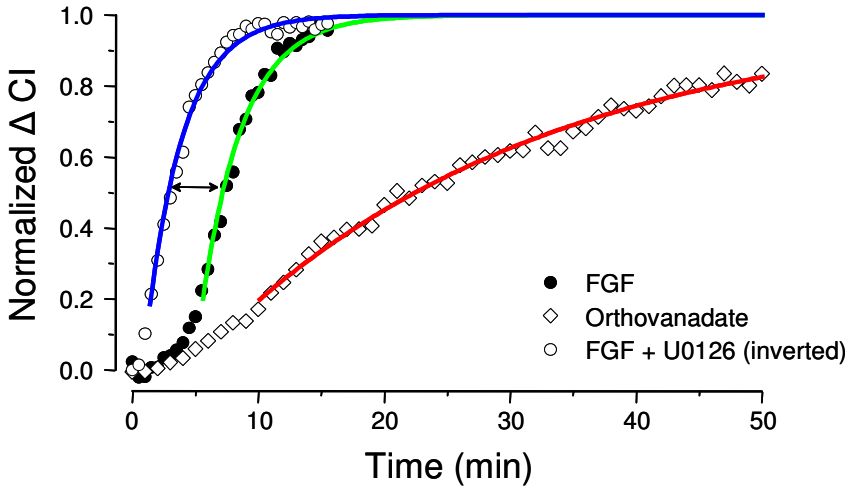

Figure 27
Comparison of the time course of ERK2-GFP translocation in response to FGF, FGF4+U0126 and orthovanadate.
Traces have been normalized from 0 to 1, with 0 indicating the CI at the time of administration of the specific compound and 1 indicating the asymptotic value of the exponential fits. The decline of Concentration Index caused by U0126 (empty circles) has been inverted for a better comparison with the other data. The continuous lines are exponential fits to the top 80% of the data points.

Summarizing these last experiments, I have shown that by disrupting the steady-state balance between the activator MEK and the inactivators Phosphatases, I obtained the following results:

- MEK inhibition caused a net ERK outflux from the nucleus originated by phosphatase activity, that was balanced no more, demonstrating that phosphatases continuously counteract ERK activation;
- Phosphatase inhibition caused ERK accumulation into the nucleus; this demonstrates that in starved conditions phosphatase activity is required to counteract basal activation of the Ras-ERK module.

Whether these considerations were true, I would expect that even at the maximum of ERK translocation, a fraction of dephosphorylated ERK is still present, due to the continuous activity of phosphatases. The continuous operation of phosphatases implies that, after stimulation, nuclear ERK is only partially phosphorylated and the residual inactive ERK should be revealed by blocking phosphatase activity, after having strongly stimulated the pathway. Cells expressing ERK2-GFP were treated with FGF and, within about ten minutes, ERK accumulated in the nucleus; at this time I added the phosphatase inhibitor and in response nuclear ERK2 equilibrated at a higher steady-state level (Fig. 15). This treatment unmasked a small but significative fraction of ERK not previously activated.

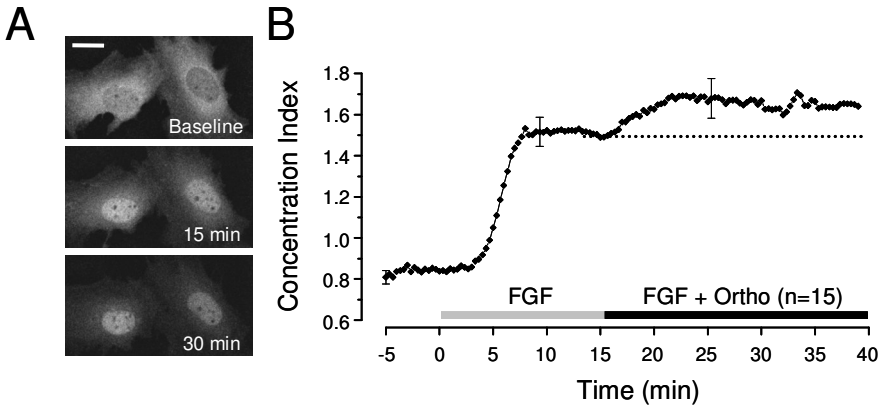

Figure 28
FGF4 alone was not sufficient to cause maximal translocation.
A) ERK2-GFP distribution before in starved condition (baseline), after 15 min from the FGF administration and in co-presence of orthovanadate and FGF (30 min). Bar 20 µm
B) Cells were treated initially with FGF4 and with orthovanadate 15 min later, which caused a 23% increase in the CI.

This experiment demonstrates that nuclear ERK is only partially phosphorylated during steady stimulation with FGF. Comparing the results shown in figure 24 and 28, it is interesting to notice that ERK nuclear accumulation following orthovanadate addition in resting cells (Fig. 24) is slower respect to what I obtained in activated cells (Fig. 28). Exponential fit gave respectively the following time constants: 26 min versus 4 min. This striking difference permits to exclude the hypothesis that the slow rate of ERK nuclear accumulation in starved cells is due to an intrinsic difficulty of the drug to penetrate cells, but it rather seems to reflect a real kinetic property of the occurring process.

ERK1 and ERK2: focus on nucleo-cytoplasmic shuttling properties

Do ERK1 and ERK2 display different temporal patterns of localization?

It is well established that ERK1 and ERK2 are activated by the same upstream kinase MEK and, in accordance, they share the putative recognition regions. Indeed ERK2-GFP and ERK1-GFP translocated to the nucleus with the same kinetics upon stimulation with FGF4 (Fig. 29 A,B). Specific residues at the C-terminal segment of ERK have been proposed to play a key role in the docking to substrates and phosphatases, as well as to MEK1/2 (Rubinfeld et al., 1999; Tanoue et al., 2000; Xu and Goldfarb, 2001). Furthermore, phosphatases seem to interact with both ERK1 and ERK2 (Pulido et al., 1998; Tanoue and Nishida, 2002); so I can suppose that phosphatases react with the two kinases with the same affinity.

Even if these considerations suggest an identical regulation for ERK1 and 2, I was curious to see whether I might detect some difference in the dynamics of the activation/inactivation processes. To this effect, I repeated the FGF-U0126 experiment shown above (Fig. 26) with ERK1-GFP. Surprisingly, this experiment revealed a dramatic difference between ERK1 and 2.

As it can be noticed from figure 29, upon FGF administration both kinases translocated with identical kinetics (Fig. 29 A,B), reaching the peak within 15 minutes. After blockage of MEK activity with the U0126, the behaviuor of ERK1 and 2 drastically diverged: the loss of ERK1 from the nucleus was much slower than ERK2 (τ = 9.3±1.3 min for ERK1-GFP versus τ = 3.0±0.1 min for ERK2-GFP; Fig. 29 C,D).

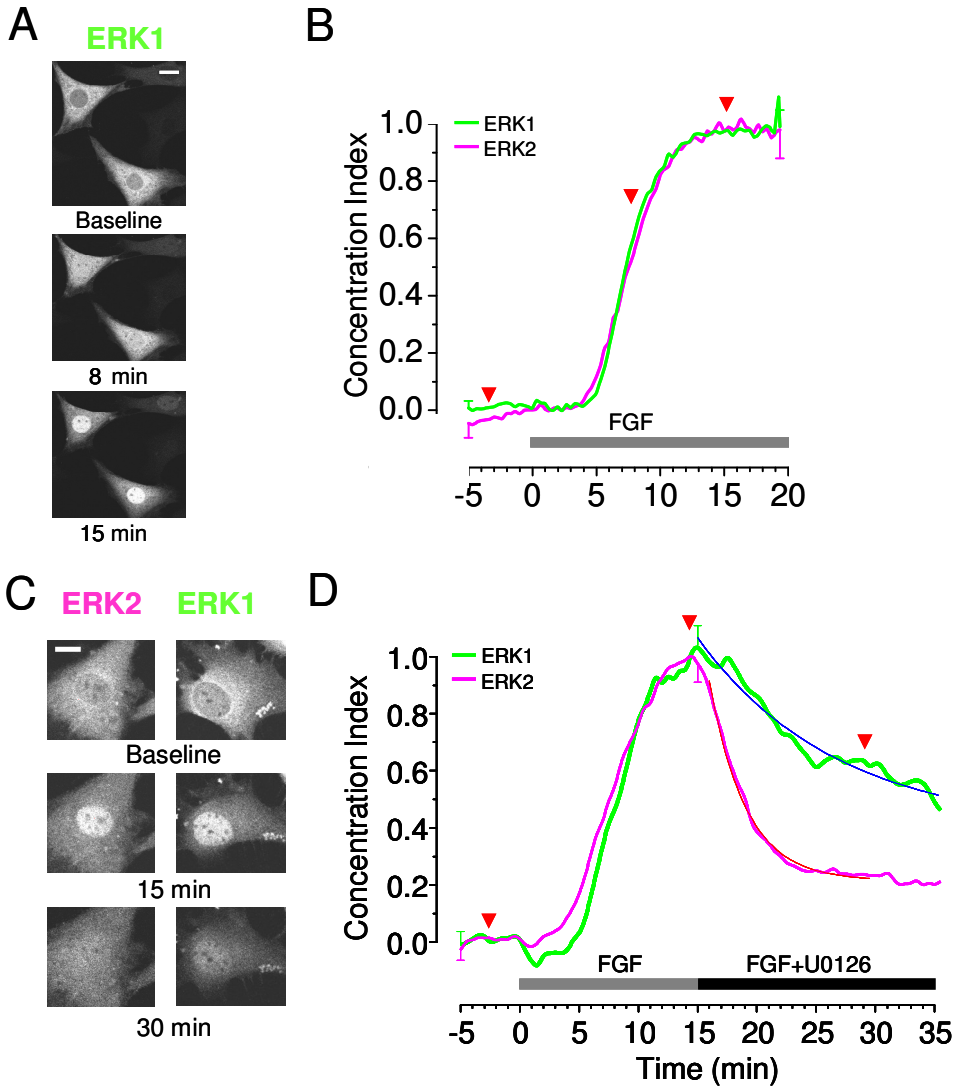

Figure 29

ERK activation required continuous activation of MEK-ERK pathway.

A-C) Selected frames displaying ERK1 and 2 localization at the time points indicated by the red arrow heads in panel B-D Bars 20 µm in all panels.

B) Cumulative nuclear translocations of ERK1 (green, n=18) and ERK2 (magenta, n=12).

D) Cells were treated initially with FGF and 15 min later with 20 µM U0126. Blockage of MEK caused nuclear fluorescence loss with different kinetics for ERK1 (pink, n=9) and ERK2 (green, n=10); the averaged time courses are displayed. The blue and the red traces are first order exponential fits.

This phenomenon underlines again the dynamic regulation of ERK localization and, more interestingly, it suggests that, although the two kinases share common partners and undergo to the same regulatory mechanisms, there might be crucial differences in the true nature of these proteins that have been overlooked until now.

Looking in more details at the particular experimental conditions, I can draw some considerations in order to clarify the real meaning of these results. ERK activation is continuously counteracted by phosphatases, which operate both in the nucleus and in the cytoplasm. In the condition of maximal stimulation (at the peak of the nuclear accumulation after FGF addition), phosphatases dispose of a high abundance of substrate (p-ERK) in the nucleus, so they begin to dephosphorylate ERK immediately. After MEK blockage, the predominant contribution to the net ERK efflux across the nucleoporins is likely to be constituted by dephosphorylated ERK. A simple explanation of the differences observed between ERK1 and ERK2 might be due to a different capability of crossing the nuclear membrane. Following this idea, figure 29 C,D would suggest that in the dephosphorylated state ERK1 crosses the nuclear membrane more slowly than ERK2. In order to clarify this aspect I designed specific experiments of photobleaching to study the trafficking across the nuclear barrier of ERK1 and 2.

Nucleo-cytoplasm exchange of ERK1 and ERK2

To study ERK trafficking across the nuclear barrier, I measured the recovery of ERK-GFP fluorescence after photobleaching of the nucleus. Given that photo-bleaching is irreversible, any recovery of nuclear fluorescence must be due to the influx of unbleached ERK-GFP from the cytoplasm. Since the protein concentration in the nucleus is left unaffected by photobleaching, this influx is in equilibrium with an equal efflux of bleached chimera and the time constant of the recovery is inversely proportional to the permeability through the nuclear membrane.

The shuttling must be fast enough to replenish a pool of nuclear pERK that is dephosphorylated and exchanged with the cytosol through a process with $\tau \approx 3$ min. I can compute two important parameters from nuclear FRAP experiments: the speed of protein exchange between the two compartments and the fraction of immobilized protein inside the nucleus. Cells transfected with ERK1-GFP or ERK2-GFP have been photobleached for few seconds in the nucleus, then the

recovery of fluorescence has been imaged until equilibrium is re-established. The traces of the recovery were fitted with remarkable accuracy by a single exponential in all measured cells; therefore, the process can be described by its time constant τ and asymptotic value. τ is related to the speed of protein shuttling across the membrane, and the asymptotic value can be used to calculate the immobile fraction (see Methods). I measured the shuttling time constant of ERK1 and 2 in two fundamental conditions: starved and after stimulation with FGF.

Figure 30 shows that ERK2-GFP is continuously exchanged between nucleus and cytoplasm and that the turnover accelerated after activation, as demonstrated by the time course of the fluorescence recovery before and after stimulation.

I repeated the FRAP measure on ERK1-GFP expressing cells. The fluorescence recovery of the two kinases exhibited strikingly different values of τ (Fig. 31), in particular ERK1 was remarkably slower respect to ERK2, both in starved conditions and after stimulation.

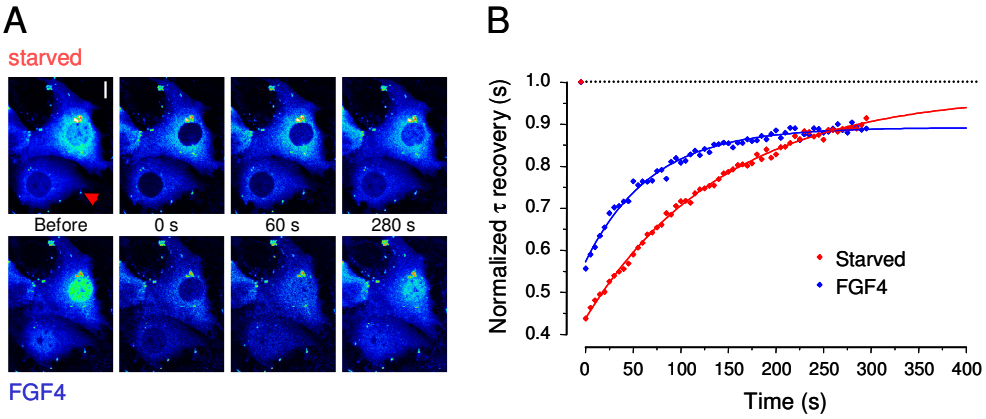

Figure 30
ERK2-GFP continuously shuttles through the nuclear membrane.
A) Images of two cells recorded during a nuclear FRAP experiment in starved conditions (upper sequence) and 30 min after stimulation with FGF4 (80 ng/ml). Bar 10 µm.
B) Time course of the recovery of the nuclear fluorescence in the cell indicated by the red arrow in A. Stimulation caused a faster turnover of ERK2-GFP through the nuclear membrane since the time constant of the fluorescence recovery decreased from 144 s down to 69 s. A similar effect occurred to the upper cell in A (starved τ=236 s; FGF4 τ=84 s). The exponential fit of the fluorescence recovery (continuous lines) is used to compute time constants.

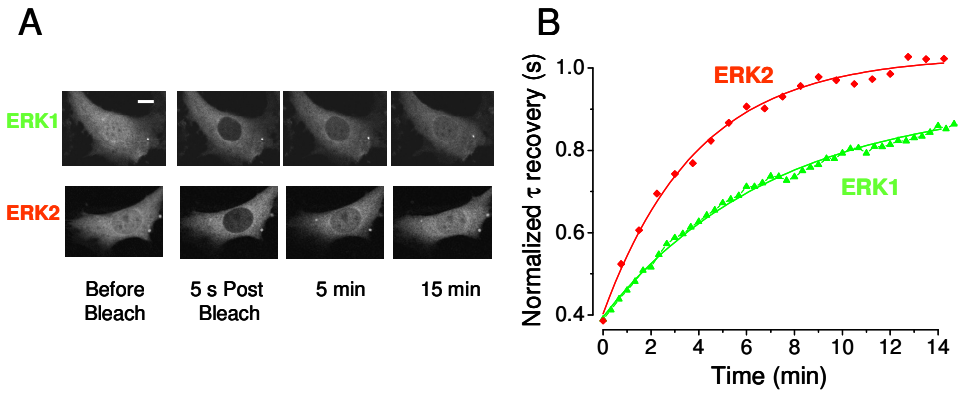

Figure 31
Comparison of the nucleo-cytoplasmic shuttling of ERK1 and 2 in starved conditions.
A) Series of images collected during the nuclear fluorescence recovery of a cell transfected with ERK1-GFP (at the top) and ERK2-GFP (at the bottom). ERK1 fluorescence recovered more slowly than ERK2, indicating a slower turnover of ERK1 across the nuclear membrane.
Calibration bar 10 µm.
B) Time course of the fluorescence recovery of the cells showed in A. Data points were well fitted by single exponentials with respectively the following time constants (τ) of 430 s (ERK1) and 235 s (ERK2).

Since ERK1 is heavier than ERK2 I felt necessary to wonder whether the difference in shuttling speed might be simply due to their different size, which obviously affects permeation though the nuclear pore. For this reason, I studied the trafficking of two molecules of different molecular weight undergoing passive diffusion: a GFP monomer and a dimer GFP-GFP (54 kDa), which serve as control of size-limit. The monomer shuttled very rapidly with a rate slightly faster than activated ERK2-GFP (respectively 58 s ± 5 s versus 84 s ± 5 s; Fig 32), in spite of the fact that ERK2-GFP is far heavier (69 kDa ERK2-GFP *vs.* 27 kDa GFP). Interestingly, the dimer GFP-GFP was much slower if compared with all the other proteins (1360 s ± 171 s *vs.* 654 s ± 43 s of ERK1-GFP and 267 s ± 26 s of ERK2-GFP, both in in starved cells; Fig. 32), even if it is sensibly smaller that both ERK1-GFP and ERK2-GFP. This demonstrates that ERKs-GFP must diffuse across the nuclear pore by mean of a facilitated mechanism.

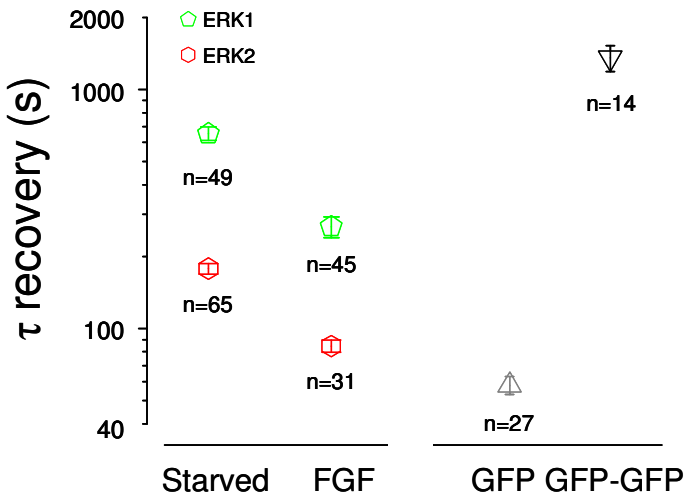

Figure 32
Mean time constants of ERK1 and 2 GFP-tagged, GFP alone and double GFP nucleo-cytoplasmic shuttling.
The time constant is not proportional to the increasing molecular weight as demonstrated by the τ obtained with the double GFP (in black, 54 kDa against 69 kDa of ERK2, in red, and 71 kDa of ERK1, in green). Although GFP-GFP has a slightly smaller molecular weight than both ERK1/2-GFP, it showed an unquestionable higher turnover.

Since the time course of the fluorescence recovery was rather variable between different cells, I thought necessary to perform the FRAP experiments in the same cell before and after stimulation to confirm our results (Fig. 33).

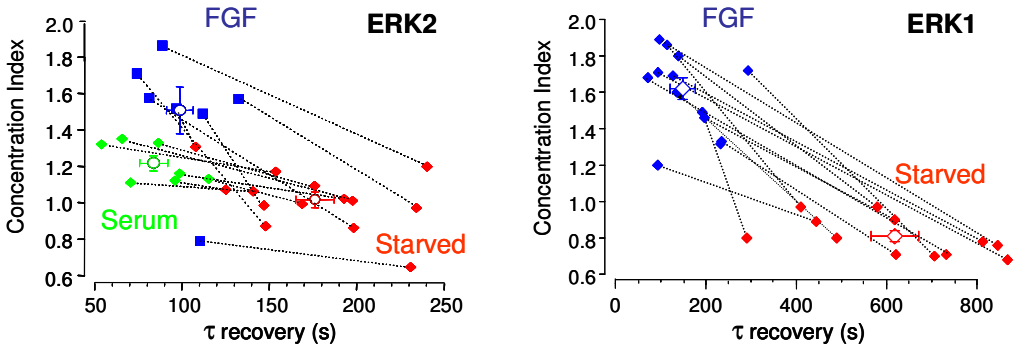

Figure 33
Scatter diagram correlating the time constant of the recovery and Concentration Index
The two panels show the measures performed for ERK1-GFP and ERK2-GFP. A similar accelerating trend clearly emerged in all of the paired cells considered.

I wondered about the possible cause of the striking difference between the nucleo-cytoplasmic exchange of ERK1 and ERK2. Since they share all the major regulatory components (see Box 7), I hypothesized that the secret should be hold somewhere in the protein structure. For this reason I compared the primary aligned sequences (Fig. 34) in order to identify some crucial region or single residues which could be responsible of such behavior.

ERK1 N-terminus: a key domain for understanding functional differences between ERK1 and ERK2?

Comparison of the sequences of ERK1 and ERK2

The two kinases have been considered for a long time simply as isoforms, which undergo to the same regulatory mechanisms and that are responsible for the same biological outputs. Nevertheless, the high degree of evolutionary conservation through a widespread phylogenic scale rises some doubts about their interchangeability: why evolutionary driving force should have maintained two almost indistinguishable isoforms? Which would be the real advantage of that? Actually several evidences have recently come to light that pointed out to relevant differences between the two kinases (see introductory chapter). Suffice to say that, while the ERK2 knockout is lethal at very early stages of the development, the ERK1 knockout is perfectly vital, exhibiting only some deficits in tymocyte maturation and, surprisingly, small but striking differences at the level of the nervous system (Mazzucchelli et al., 2002; Pages et al., 1999). In the previous pages I have reported a surprising difference between ERK1 and ERK2 at a completely different level. I decided next to investigate which domains of ERK1 and ERK2 might be responsible for the trafficking differences that I have just described. Comparing the aligned amino acidic sequences (Fig. 34), it can be noticed that there are several isolated differences (darker colored characters in figure 34) distributed all over the two proteins. None of these residues are located in mapped functional domains (Box 7). The major difference resides in the N-terminus of ERK1, which contains a region completely absent in ERK2. I sought a way to ascertain whether this region holds a key for the understanding of the functional differences between ERK1 and 2.

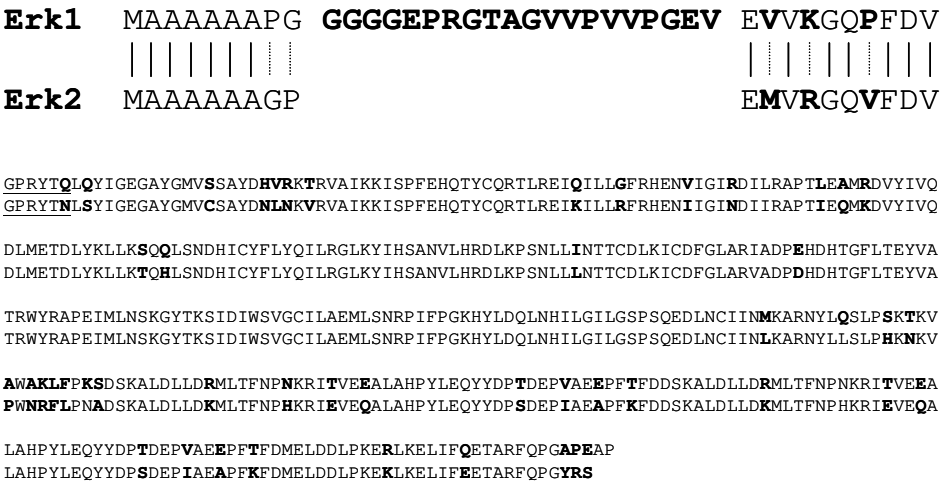

Figure 34
Aligned primary amino acidic sequences of the two kinases (Mus musculus).
Bold represent different residues. Underlined residues have been demonstrated for ERK2 to contribute to the kinase *activity (Eblen et al., 2001).*

I chose the strategy of deleting portions of ERK1 N-terminus and consequently verifying whether these changes alter the trafficking properties of the modified ERK1-GFP. To implement this idea, I have analyzed the N-terminus of ERK1 in more details identifying three regions (Fig. 35):

1. aa 1-9, an alanine enriched cap in common with ERK2 (region 1, blue box);
2. aa 10-29, an unique sequence present only in ERK1 (region 2, red box);
3. aa 30-39, a homologous, but not exactly identical, domain respect to ERK2 (region 3, green box).

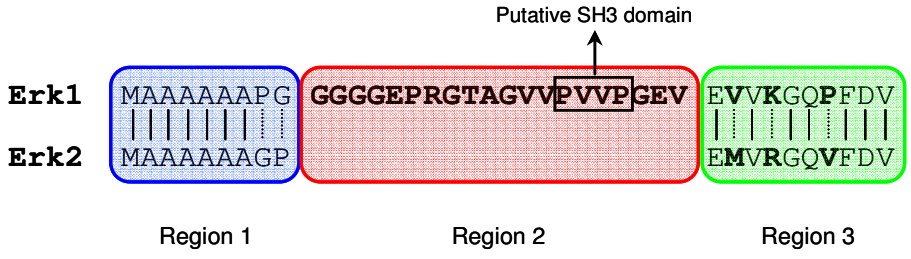

Figure 35
Comparison between the N-terminal of ERK1 and ERK2 (Mus musculus).
Dotted lines indicate different aminoacids. The domain PVVP in region 2 has been identified as a putative SH3 domain interaction sites with the SH3-Hunter web server (Ferraro et al., 2007).

Such organization does not pretend to formally classify functional domains, but it only represents a simple way to dissect ERK1 N-terminus in distinct compartments to clarify the involvement of each one in ERK1 shuttling.

I opportunely designed, different transgenes selectively deleting one or more of the domains displayed in figure 35; then I tested the resulting truncated derivative by measuring the shuttling rate through the nuclear envelope, both in starved condition and upon stimulation with FGF4 (Fig. 36).

Surprisingly, the deletion of the entire N-terminus of ERK1 (in the deleted proteins E1Δ^{7-39} or E1Δ^{39}) converts the characteristic slow phenotype in a faster one (very similar to ERK2), suggesting that the N-terminus is able, *per se*, to slow down the permeation through the nuclear envelope. This observation suggests that the difference in shuttling is due to the N-terminus, so, in the following experiments, I focused only on this region.

Interestingly, the partial deletion in E1Δ^{26} showed an intermediate result. In contrast, the deletion of the poly-A sequence (aa 1-7) did not alter trafficking (not shown); this is in accordance with previously results which showed that the deletion of ERK2 N-terminal from Ala_3 to Ala_7 did not impair the interaction with MEK, the protein localization and the kinase activity (Eblen et al., 2001). These data encouraged us to attempt the opposite approach: would it be possible to transform the shuttling properties of ERK2 to ERK1 by fusing the N-terminus of ERK1 to ERK2? To answer to this question I opportunely fused the N-terminus of ERK1 on ERK2 (Δ^{39}E2) and therefore, I tested the new chimera with FRAP (Fig 37).

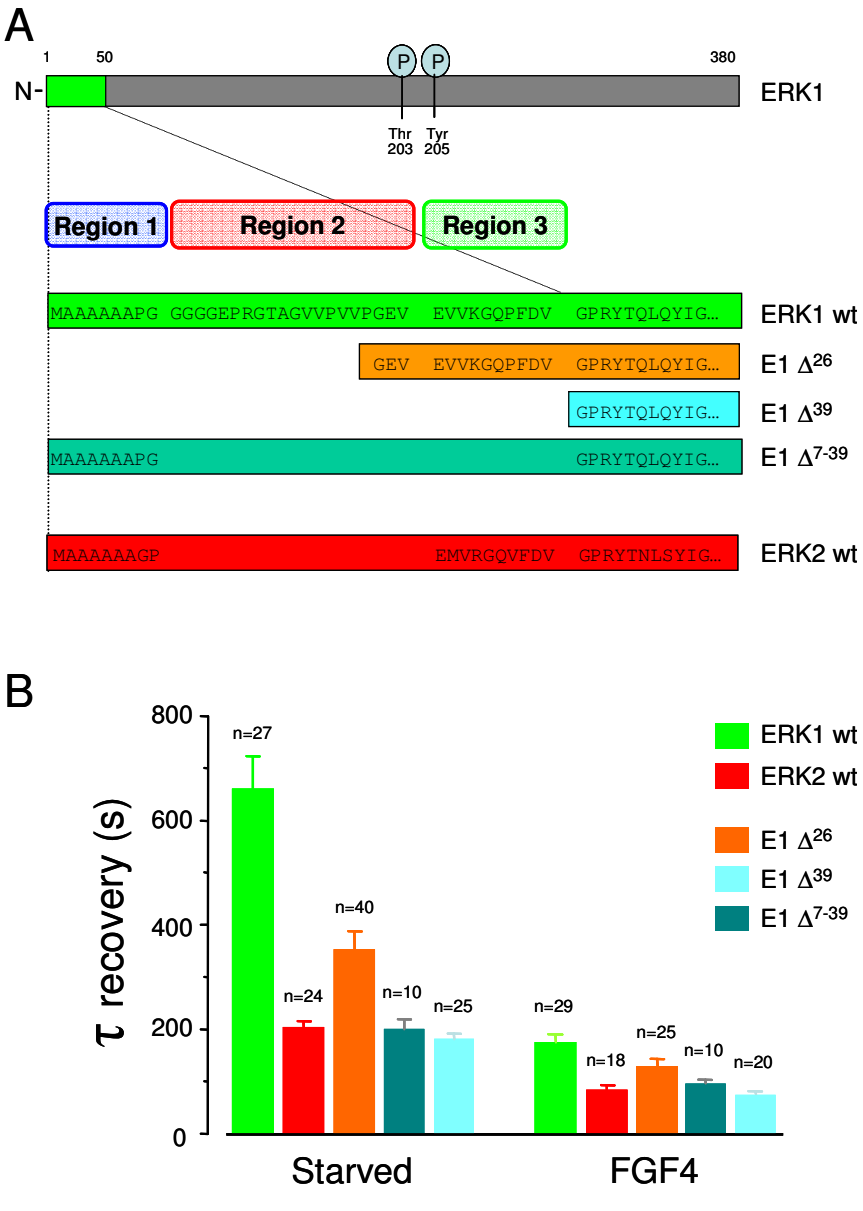

Figure 36
ERK1 N-terminus is responsible for slowing down the nucleo-cytoplasmic shuttling.
A) ERK1 wild type (from *Mus musculus*) contains a series of aminoacids at its N-terminus which are not present in ERK2. I produced fusions with GFP of three different deletions of ERK1, as indicated in the diagram.
B) The time constant of the nucleo-cytoplasmic shuttling of ERK1 mutants is strongly affected by the N-terminus portion.

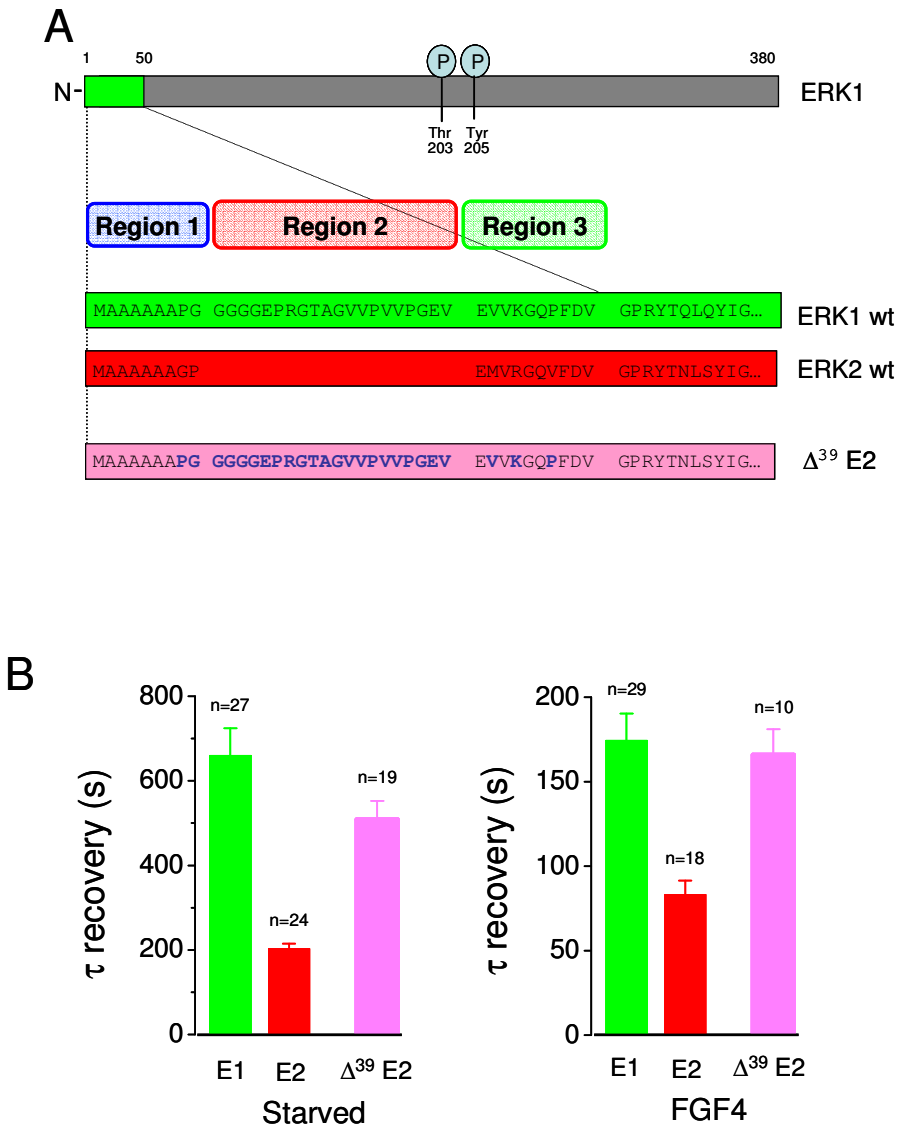

Figure 37
Fusion of ERK2-GFP with the N-terminal of ERK1 (Δ^{39}E2).
A) Alignment of the N-terminus of ERK1, ERK2 and Δ^{39} E2.
B) The domain added at the ERK2 N-terminus considerably decreases the speed of nucleo-cytoplasmic turnover both in the starved (*t*-test E1 *vs.* Δ^{39}E2, p= 0.134) and stimulated state (*t*-test, 0.911).

As predicted, the shuttling rate across the nuclear membrane of the new fusion protein changed accordingly: the trafficking of Δ^{39}E2 was much slower than ERK2 wt (Fig. 37 B).

In conclusion, I can propose some considerations about the specific role of each of the three regions of ERK1 N-terminus:

- The alanine rich cap (1-9 aa) does not seem to play any role in controlling the shuttling rate given that its absence did not change the trafficking (E1Δ^{7-39} and E1Δ^{39} showed indistinguishable results). This suggest that the region 1 (in particular aa 1-7) is not involved in the passage across the nuclear barrier.
- Conversely, the protein lacking aa 1-26 (E1Δ^{26}) gave an intermediate results between ERK1 wt and ERK2 wt. This deleted protein completely lacks the region 1 (that I demonstrated not being involved in the shuttling) and almost the entire region 2 (aa 10-26 respect to 10-29); consequently I can conclude that region 2 seems to be heavily involved in this phenomenon, although not uniquely responsible.
- E1Δ^{39} lacks the entire N-terminus (all the regions: 1, 2 and 3) and only in this condition the slow phenotype of ERK1 shuttling can be completely reverted into the ERK2. I can conclude that also region n.3 (aa 30-39) contributes to slow down the rate of trafficking.

In the following I will investigate in more details the involvement of each region, by directly fusing fragments of the ERK1 N-terminus to GFP and studying their behavior in terms of nuclear shuttling.

ERK1 N-terminus: specific functional domain or steric hyndrance for nuclear access?

I demonstrated that ERK1 N-terminus influences the kinetics of nuclear shuttling as a sufficient and necessary condition; but I did not provide any possible explanation concerning the involved mechanisms.

The slowing down of ERK1 shuttling rate could be explained by hypothesizing that the folding of the N-terminus masks the sites on ERK structure which are responsible of the interaction with nucleoporins, thus impairing ERK1 capability of passing through the pores. In other words, the slower trafficking would be not caused by specific interactions of the N-terminus, but it would simply be an indirect effect caused by its steric hindrance. To test this hypothesis I decided to

directly fuse GFP with ERK1 N-terminus (Fig. 25) and to measure the velocity of nucleo-cytoplasm exchange by FRAP experiments.

First of all I produced a series of N-terminus fragment fused to GFP, including different regions of the entire domain (Fig. 38 A).

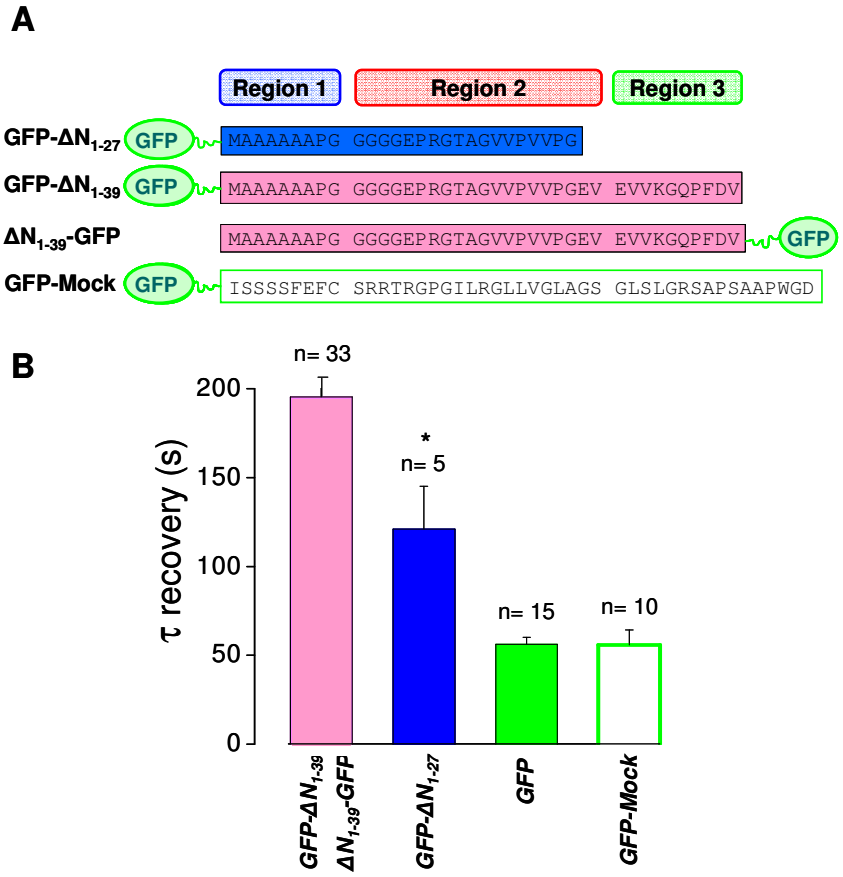

Figure 38

A) Alignment of ERK1 N-terminus of different lengths fused to the GFP, the GFP alone and a random sequence of comparable length, fused to GFP, in order to exclude that results would simply be affected by the heavier molecular weight.

B) All the ERK1 N-terminal proteins showed an unquestionable slower behavior compared to the controls.

GFP-ΔN_{1-39} and ΔN_{1-39}-GFP were not significantly different, so I pooled together all the relative data. GFP-ΔN_{1-27} showed an intermediate time constant, significantly different from the GFP-ΔN_{1-39} (*p=0.01 *t*-test).

These data clearly show that ERK1 N-terminus is able *per se* to slow down the speed of exchange across the nuclear envelope (Fig. 38 B) and this property is not related with its size, since a protein obtained by fusing GFP with a random sequence of similar lengt to the N-terminus (GFP-Mock) behaves exactly like GFP. In addition, I can exclude that this terminal region would mask some critical sites on the ERK ternary structure responsible of the interaction with nucleoporins, indeed, this peptide succeeded in slowing down also the GFP.

A second interesting aspect clearly emerges from these results: the two truncated domains fused to GFP (GFP-ΔN_{1-39} and GFP-ΔN_{1-27}) decreased the shuttling rates to a different extent. Specifically, GFP-ΔN_{1-27} was faster than GFP-ΔN_{1-39}, but it resulted significantly different from the GFP and the random sequence. These data confirm that the "slow" phenotype is due to the combination of at least two factors, one connected with the region 2 (aa 9-29) and the other one related to region 3 (aa 30-39). I believe that the slow rate of trafficking could be due to protein-protein interactions mediated by specific domains of ERK1 N-terminus. I decided to investigate which aminoacids confer such phenotype, generating a series of mutagenized derivatives of region 2 and 3 of ERK1 N-terminus. I tested the following two non exclusive hypothesis:

1. In region 2, the sequence presents a putative SH3 domain recognition site. It can be supposed that the PVVP site might interact specifically with a SH3 binding partner and that this interaction might be somehow responsible for the slower permeation. To verify the importance of this particular site, I generated a series of mutations targeted to one or both the prolines (the SH3 recognition site is a proline-rich sequence with the basic motif PxxP) and a deletion of the whole region PVVP (Fig. 39).
2. In region 3 of ERK1 there are only three different aminoacids respect to the homologous region of ERK2 (Fig. 39). I mutated V_{31} and K_{33} converting them in alanine (aminoacid with a very small lateral chain and characterized by low reactivity) in order to neutralize their potential influence on the shuttling process.

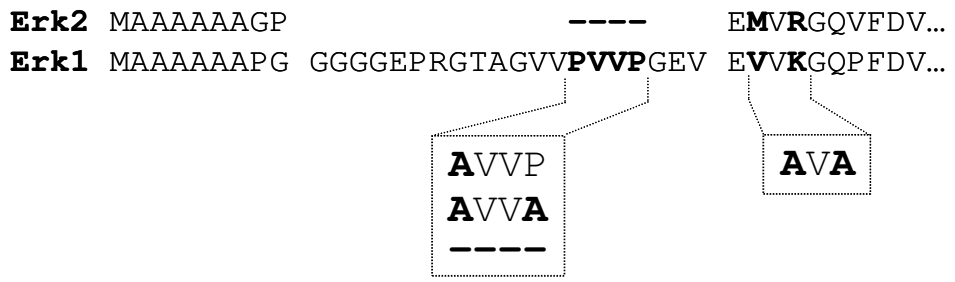

Figure 39
Mutagenized ERK1 N-terminus
Figure displays the wild type N-terminus of ERK1 and ERK2 evidencing the putative SH3 interactor site and the two different aminoacids: V_{31} and K_{33}.
Mutagenized sites are reported in the magnification under the sequences; aminoacids under test have been neutralized in alanine.

The same design of mutagenesis was applied both to the N-terminus of ERK1 fused to the GFP (GFP-$\Delta N_{1\text{-}39}$) and to the entire wild type ERK1 fused to GFP.
In order to verify and/or exclude some of the upon presented hypothesis I tested all the new mutants by measuring the time constant of shuttling trough the nuclear envelop (Fig. 40). In the following, I will first present the data from GFP-$\Delta N_{1\text{-}39}$ mutants and afterwards the data obtained from the entire mutagenized ERK1.

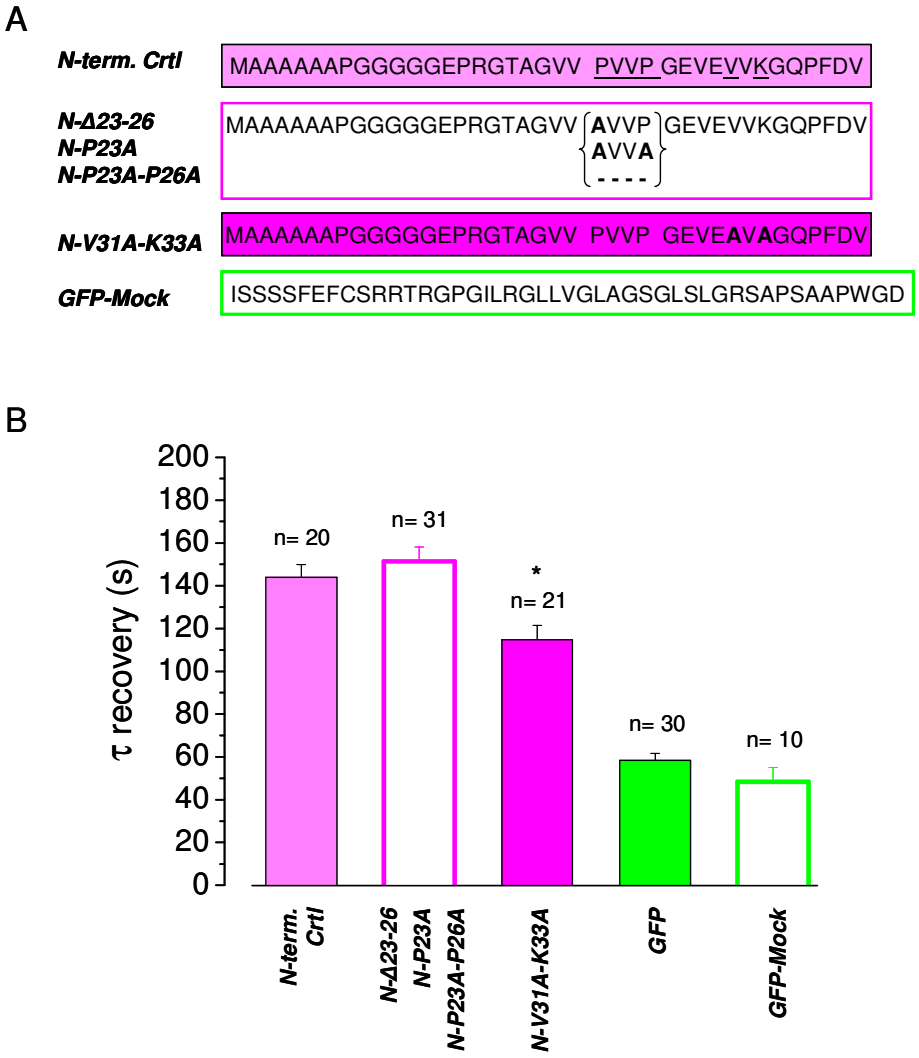

Figure 40
A) Aminoacidic composition of the mutagenized ERK1 N-terminus. All the mutants have been fused either to the N- or C- terminus of GFP, obtaining identical results.
B) Cumulative data of nucleo-cytoplasm shuttling of mutants.
All the cells have been measured in starved conditions. Only the mutant N-V31A-K33A showed a faster shuttling respect to the control (p=0.02). There were not significative difference between all the modified N-terminus at the PVVP, so we pooled all the relative data together.

The modification of the putative SH3 interacting site did not give any different result compared to the control, in any kind of rearrangement of the target sequence. This suggests that, even if some interacting sequence might exist, it does not interfere with the nuclear trafficking. Conversely, the neutralization of V_{31} and K_{33} conferred a strikingly faster rate of exchange. This is quite surprising given that, although ERK1 and ERK2 show different aminoacids in position 31 and 33 these residues can be classified as belonging to the same chemical category. Indeed, ERK1 has a valine instead of a methionine in position 31, both non polar aminoacids, and a lysine instead of an arginine in 33, both positively charged. I converted the valine and the lysine in alanine, a very small non polar aminoacid, because alanine has not a large lateral chain so its insertion presumably does not overstretch or distort the entire structure. In addition, its low reactivity should not influence neighboring residues.

The conversion of V_{31} and K_{33} in alanine sensibly affects the nuclear turnover of ERK1 N-terminus leading to a faster rate of exchange across the nucleus respect to the control (Fig. 40; $p=0.02$), even if this modification is not sufficient to obtain a GFP-like behavior. This probably means that V_{31} and K_{33} are determinant for slowing down the passage though the nuclear pores, but not uniquely responsible. This is consistent with the data shown before (Fig. 36), thus confirming the presence of some kind of cooperation with the upstream residues of the region 2.

I can hypothesize that the entire N-terminal peptide undergoes to a specific folding, which takes in proximity the aminoacids V_{31} and K_{33} (region 3) with the residues of region 2, creating a ternary complex which is responsible for the effect I observed. As a further control, I mutagenized also the entire ERK1, in the same way as it has be done for the isolated N-terminus (Fig. 41). As all the manipulation on PVVP site gave identical results and they did not differ from the control. In contrast, the neutralization of V_{31} and K_{33} confirmed the result of a sensible acceleration of the shuttling respect to ERK1.

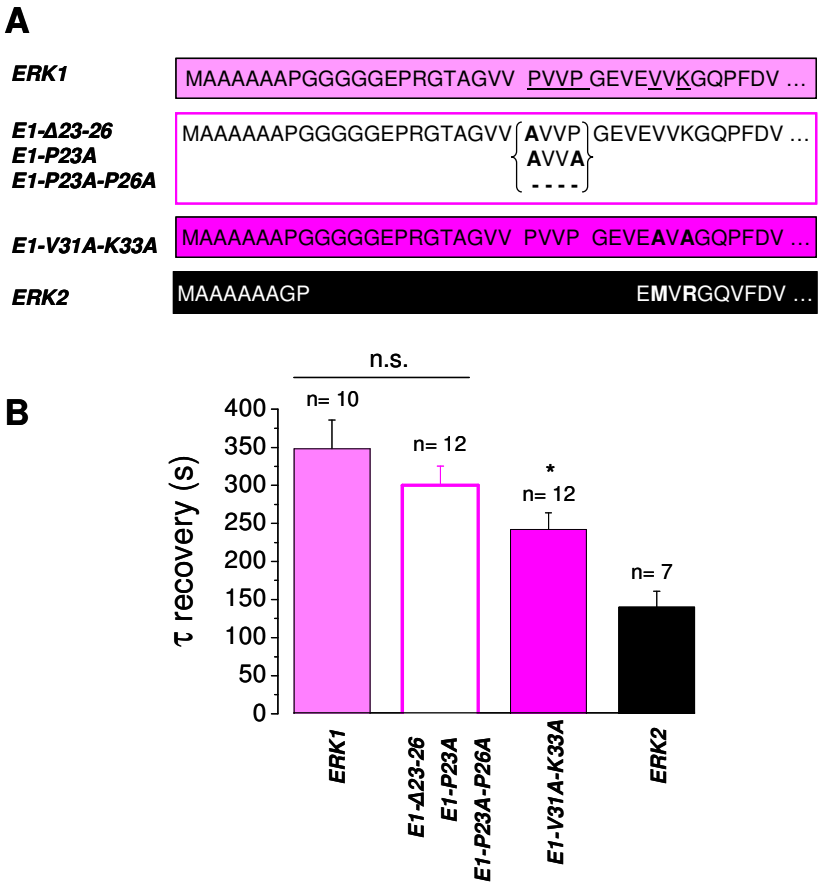

Figure 41

A) Aminoacidic composition of the mutagenized N-terminal portions of ERK1.
All the mutants have been fused either to the N- or C- terminus of GFP, obtaining identical results.
B) Cumulative data of the shuttling time constants. Only the mutant E1-V31A-K33A showed a faster shuttling respect to the control ($p<0.05$). There were not differences between all the modified E1-terminus at the PVVP, so I pooled together all the data. Comparing E1-V31A-K33A and the modified E1-terminus at the PVVP, I did not find any differences (n.s.: not significative, $p>0.05$).

Effects of the shuttling rate on ERK phosphorylation: a quantitative model

What are the functional consequences of the slower trafficking of ERK1? Since ERKs are activated in the cytoplasm but are continuously inactivated in the nucleus, the pool of nuclear phospho-ERK needs to be continuously replenished from the cytoplasm in order to maintain a sustained nuclear phosphorylation level (Costa et al., 2006; Volmat et al., 2001). The low nuclear permeation of ERK1 suggests that during steady stimulation and translocation, a large fraction of nuclear ERK1 is inactivated and is therefore unable to exert downstream effects. This qualitative observation was modeled in order to quantitatively estimate the effects of nuclear inactivation and trafficking speed on the nuclear ERK phosphorylation. The basic assumption of the model considers an equilibrium among 4 different states regulated by first order kinetics as detailed in the following reaction scheme:

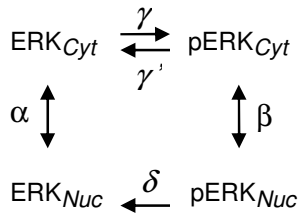

where pERK and ERK indicate the concentration of the phosphorylated and not-phosphorylated pools, respectively, either in the cytoplasm (Cyt) or in the nucleus (Nuc). When the cells are at steady state, either before stimulation or at the plateau of the translocation response, the net flux across the nuclear membrane is zero.

The following parameters were included in the model:

- rate constants α and β, from the time constant of recovery of FRAP experiments. Since the FRAP experiments suggest that nucleoporins provide for a bidirectional passage of molecules, the same rate to the influx and efflux was assigned;
- phosphorylation rates in the cytoplasm γ and in the nucleus δ;
- dephosphorylation rate in the cytoplasm γ' (in the nucleus it has been assumed that the dephosphorylation rate ≈ 0).

It has been developed a simulator that computes the temporal evolution of the system under arbitrary changes of the parameters of the state population (see Methods).

Initially, the imaging data reported in figure 26, on cells transfected with ERK2-GFP, were fitted with the model in order to estimate the rate of dephosphorylation. To this effect I have modeled the data obtained in a recently published experiment (Costa et al, 2006). Here, cells were treated with FGF for 15 min, until the translocation response reached the plateau level. At this point the MEK inhibitor U0126 was administered, causing the rapid inactivation of ERK with the consequent loss of ERK2-GFP from the nucleus. During inhibition, the phosphorylation rates tend to 0 and I can fit the model prediction of the actual time course of protein localization to obtain an estimate of the de-phosphorylation rates in nucleus and cytoplasm. As shown in figure 29 A, the model fitted the data with great accuracy and provided that $\gamma' \approx 0.003$ corresponding to t=170 s. Then, I used the model to predict the outcome of an identical experiment performed with the ERK1 fusion protein. In this new computation I used the de-phosphorylation rate I just estimated and I inserted the translocation rates α and β measured in the FRAP experiments with the ERK1-GFP construct. This time lapse experiment showed that ERK1 was retained in the nucleus for a much longer time than ERK2, and the modeling suggest that this is due to the lower rate of the ERK1 shuttling, that is especially slow for the non-phosphorylated protein. Next, I used the model to compute the percentage of activated ERK in the nucleus for ERK1, ERK2 and for proteins with varying shuttling rates. As it is shown in figure 42 B nuclear phosphorylation decreased in parallel with decreasing speed of nucleo-cytoplasmic shuttling. This indicates that even if ERK1 and ERK2 are subjected to identical rates of activation and inactivation, ERK2 maintains better its state of phosphorylation because of its faster nucleo-cytoplasmic shuttling.

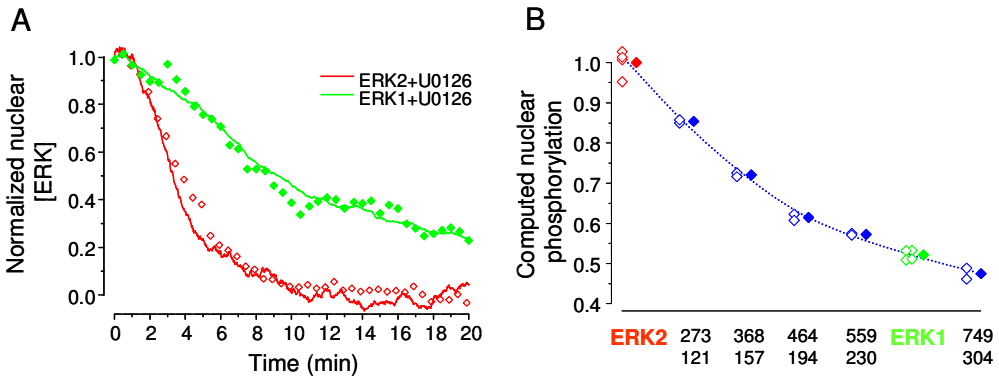

Figure 42
Computational estimate of the functional consequences of the different shuttling rates of ERK1 and E2.
A) By fitting the time course of the decay of nuclear ERK2-GFP in cells stimulated with FGF for 15 min and afterward treated with U0126 (empty red diamonds) with the model output (continuous red line), we could estimate the dephosphorylation rate. This estimate was included in the model together with the shuttling rates measured for ERK1 to predict the outcome of this experiment practiced on the cells transfected with ERK1-GFP. The model prediction (green line) describes with great accuracy the experimental points (filled green symbols).
B) The model was used to compute the phosphorylation in the nucleus as a function of the shuttling speed. The empty symbols represent the result of a single simulation run and the filled symbols are the averages of each group. The phosphorylation level has been normalized to ERK2, therefore the computation shows that the total level of phosphorylation of ERK1 is only about half of ERK2. The numbers under each set of data points are the time constants (in seconds) of nuclear shuttling in the starved (above) and stimulated conditions (below).

The results of both the imaging experiments and the simulations suggested that in stimulated cells the fraction of phosphorylated ERK1 is smaller than the fraction of activated ERK2. To verify this idea I studied the intensity/response relationship in cells treated with four increasing concentrations of serum (1%, 2%, 5% and 10%) for 15 min (Fig. 43). The gels have been blotted and probed with the phospho-specific ERK antibody and then analyzed with a phospho-imager to ensure linearity. The relative phosphorylation was evaluated by measuring the pERK1 and pERK2 signals and by computing the ratio pERK2/pERK1. If the two kinases were following the same activation profile I should expect that the ratio of activation would remain constant. On the contrary, I found that at low serum doses, ERK2 activation is larger than ERK1 indicating a better sensitivity (Fig. 43 A). According to our model this difference may largely be dependent on the action of nuclear phosphatases that affect more ERK1 because of its longer

retention time in the nucleus. If this were true, one could expect that the inhibition of phosphatases should attenuate the difference in activation between ERK1 and 2.

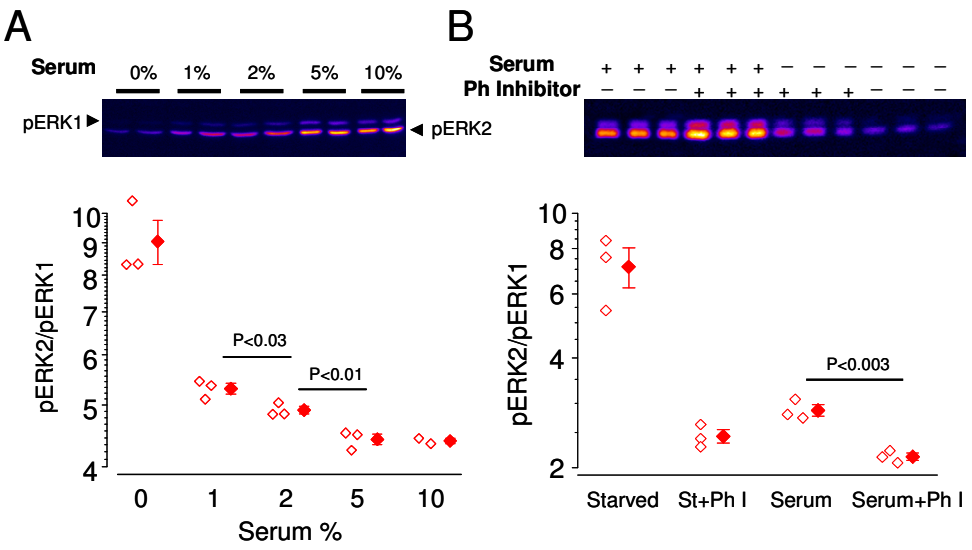

Figure 43
Comparison between the activation of ERK1 and ERK2.
A) NIH 3T3 cells have been starved for 24 hr before treatment for 15 min with increasing concentrations of serum, as indicated. The densitometric analysis of the gel blotted with the phospho-specific antibody has been performed with a linear imager to quantify the intensity of the phospho-ERK1 and 2 signals. From each experiment I computed the ratio pERK2/pERK1 which is a measure of the relative activation of the two kinases. The graphs shows that ERK1 activation lags behind ERK2.
B) Effects of phosphatase inhibition on the relative activations of ERK1 and ERK2. Cells have been starved for 24 hr before a 30 min treatment with serum 10% and/or a cocktail of phosphatase inhibitors. Inhibition of phosphatases in presence of serum caused a further increase of phosphorylation compared to serum only. This increase was larger for ERK1, indicating a stronger dependence of ERK1 on de-phosphorylation.

This idea was tested by assaying ERK1 and 2 activation by immunoblotting. Cells were harvested in either starved conditions or after 30 min in 20% serum, in presence or in absence of a cocktail of phosphatase inhibitors (cocktail 1 and 2 cat. n. respectively P2850 and P5726, Sigma). As predicted, figure 43 B shows that the inhibition of phosphatases decreased the difference between ERK1 and 2, indicating that in normal conditions ERK1 is more subjected to the action of phosphatases than ERK2.

In conclusion, these data suggest that:

1) ERK1 activation lags behind ERK2, as demonstrated by the lower response of ERK1 to non saturating stimuli.
2) This differential activation of ERK1 is reduced after inhibition of phosphatases.

Toward a functional interpretation

These conclusions are fully compatible with the theory that a prime reason for the functional differences between ERK1 and 2 is the slower trafficking of ERK1 that makes it more vulnerable to phosphatase inhibition in the nucleus and contributes to make ERK1 less competent than ERK2 in activating the downstream nuclear targets. It is now important to understand which are the functional implications for cells.

Since there is roughly a 1 to 1 relationship between the abundances of ERK1/2 and MEK, it is expected that during activation ERK1 and 2 compete for the upstream partner MEK. Therefore, I can expect that in conditions of strong activation, when the rate of the reaction ERK>>MEK>>pERK is very fast, the overexpression of ERK1 would act as an inhibitor of the pathway, while the overexpression of ERK2 would facilitate signaling to the nucleus. Viceversa, overexpressing the swapped proteins (E1Δ^{7-39} and Δ^{39}E2) it would revert the corresponding effects. To fully demonstrate this idea is necessary to devise experiments useful to evaluate the cellular response to ERK activity in cell systems overexpressing ERK1 and ERK2 or the swapped E1Δ^{7-39} and Δ^{39}E2. One possible strategy is offered by the experimental approach followed by Vantaggiato and colleagues (Vantaggiato et al., 2006): the colony formation assay in NIH 3T3 cells.

A collaboration was started with their laboratory staff in order to verify this hypothesis (see Box 8). The colony growth experiments with cells expressing the construct generated by myself, were performed in Milan. I think it is fitting to mention the result of these experiments because they nicely close the deductive process I followed during this study. The results of these experiments are narrated in Box 8.

BOX 4: Correlation between the time constant and the concentration of ERK2-GFP

ERK seems to directly interact with components of the nucleoporin complex that are enriched in FG repetitions and that are known to be involved in facilitated diffusion (Whitehurst et al., 2002; Matsubayashi et al., 2001). Given that nucleoporins and the FG sites are present in a limited number, the facilitated diffusion process should be affected by saturation, depending of the overall amount of cargo to be transported. I performed some experiments to evaluate the degree of correlation between the time constant and the concentration of ERK2-GFP. Such correlation appeared to be almost completely absent in the concentration range of ERK2-GFP considered (≤150 nM) in all of my experiments (Fig. Box 4.1).

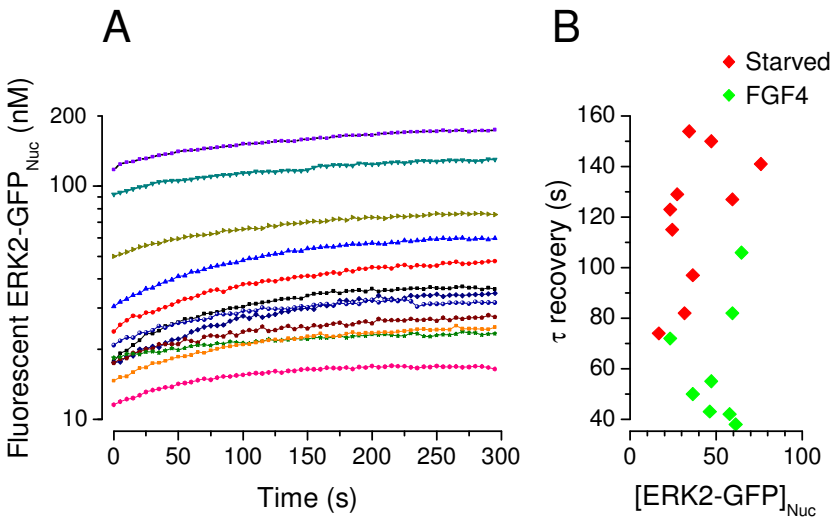

Figure Box 4.1
A) For weakly expressing cells (≤150 nM), the rate of ERK2-GFP exchange is independent on the concentration of the chimera. The panel shows typical recordings from starved cells: fluorescence was converted in average nuclear concentration of ERK2-GFP according to the calibration (see Methods). Logarithmic plot exponentials of similar τ are parallel.
B) The time constant of the recovery is independent on the average concentration of ERK2-GFP; no evident correlation is shown.

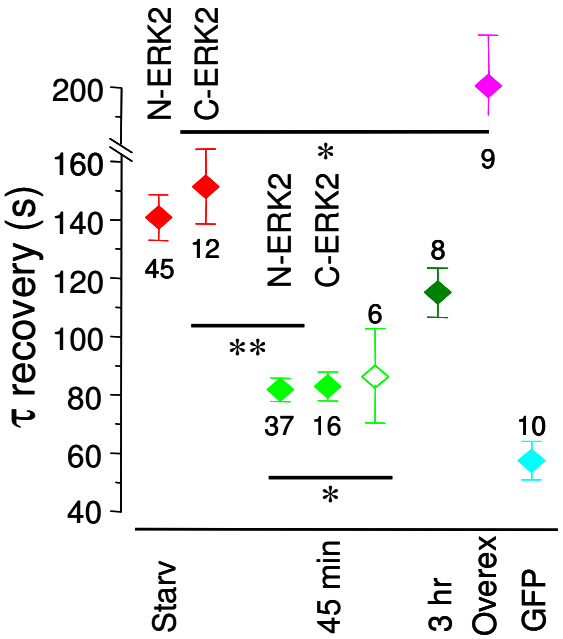

Figure Box 4.2
Averaged τ of recovery for starved cells (red symbols) or after stimulation (45 minutes: green; 3 hours: dark green). Starved over-expressing are represented in magenta. Time constants have been measured in cells transfected with both the N- and C-terminal fusions. ***P*≤0.0001; **P*≤0.003

However, the situation changed in cells strongly overexpressing ERK2-GFP. I found that the turnover was significantly slower (Fig. Box 4.2), indicating saturation of the machinery presiding at nuclear import and export. These data stress the importance of operating on cells with minimal expression of ERK2-GFP.

BOX 5*:* ERK2 immobile fraction in the nucleus

The asymptotic value of the recovery would be equal to 1 if the pool of nuclear protein was completely exchangeable with the cytoplasm, and it would be less than 1 in presence of a fraction of protein immobilized in the nucleus. The IF in over-expressing cells was zero (IF=0.01, $P \leq 0.001$; Fig. Box 5.2), indicating that ERK2-GFP accumulation was not because of immobilization in the nucleus. This is demonstrated also by the detection of a low signal of pERK in the nucleus (Fig. Box 5.2).

Starved cells expressing ERK2-GFP showed a small IF, significantly different from zero (4%) ($p \leq 0.0001$, t-test); after 45 minutes from the administration of the stimulus the IF increased to 12%; finally, after 3 hours I evidenced a decrease to 5% (Fig. Box 5.2).

The IF measured in the nucleus simply evaluated the pool of nuclear ERK that is not available to be exchanged with the cytoplasm. Presumably, this is due to the binding of ERK with some nuclear component which impairs its capability to cross the nuclear membrane. This explanation is also supported by the fact that I cannot detect any loss of fluorescence localized in the bleached region. Indeed, even if the bleach is performed in a small central region of the nucleus (see Methods, for more details), 5 s after bleach we observe that the loss of fluorescence is distributed rather uniformly through the entire nucleus, suggesting that ERK can freely move in the nuclear volume.

It is interesting to notice that the IF in overexpressing cells is close to zero, in contrast to the IF (5%) detected in starved cells at lower levels of expression. This demonstrates that immobilization occurs on a limited availability of binding sites.

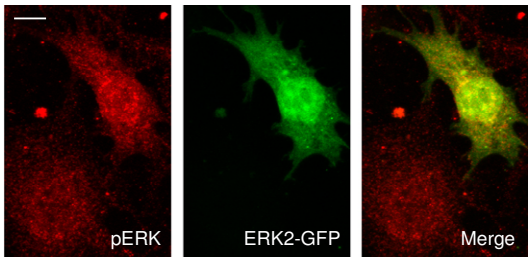

Figure Box 5.1
Starved cells with a high expression of ERK2-GFP exhibited strong nuclear localization of the chimera (green). In contrast, the pERK immuno-histochemistry (red, anti-pERK) did not show neither an appreciable phosphorylation nor nuclear accumulation. This indicates that nuclear accumulation in overexpressing cells occurs independently from phosphorylation. Bar 20 µm.

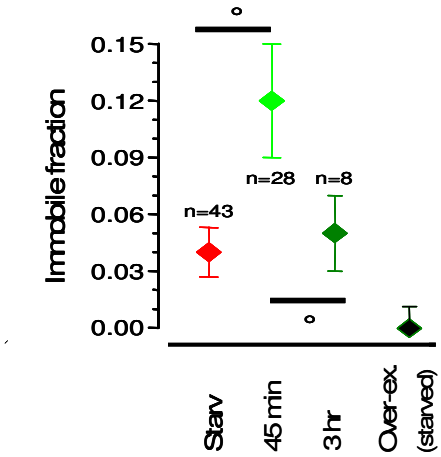

Figure Box 5.2
Cumulative data for Immobile Fraction (IF) from FRAP experiments.
Averaged IF for starved cells (red symbols) or after stimulation (45 minutes, green; 3 hours dark green); black symbols represent over-expressing cells measured in starved condition. (°$P \leq 0.05$).

BOX 6: Mechanism at the basis of ERK2-GFP nuclear accumulation

Inactive wild-type ERK is bound to MEK1 and the presence of a canonical NES in MEK has suggested that MEK might serve as an export shuttle for ERK (Fukuda et al., 1997). This suggestion is partially based on experiments using Leptomycin B treatment, which causes nuclear accumulation of both MEK and ERK (Adachi et al., 2000; Yao et al., 2001). This mechanism also operates on the ERK2-GFP chimera as demonstrated by the onset of a gradual accumulation of ERK2-GFP in the nucleus during treatment with the inhibitor leptomycin B (Kudo et al., 1999) (Fig. Box 6.1 A,B).

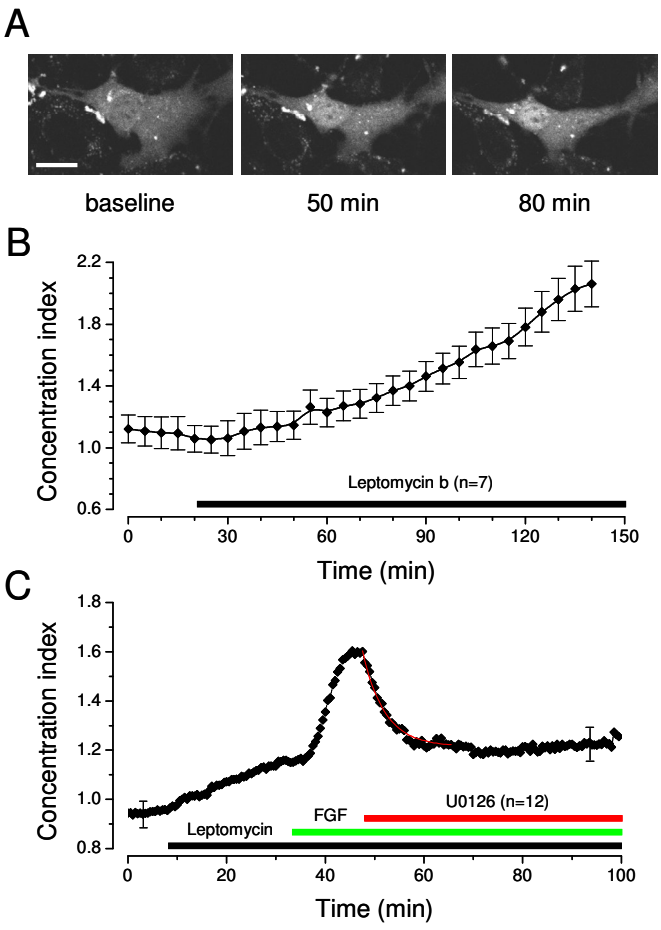

Figure Box 6.1
ERK2-GFP is extruded from the nucleus by CRM1-mediated export

A) Imaging of a NIH3T3 cell after starvation in 1% serum and during treatment with the CRM1 blocker leptomycin B (5 ng/ml). Bar 20 µm.
B) Time course of the translocation index averaged on 7 cells. Leptomycin caused a gradual accumulation of ERK2-GFP beginning after about 20 min from treatment onset.
C) Combined effect of Leptomycin, FGF and U0126 measured in 12 cells. Starved cells were pre-treated with leptomycin, then was added FGF4 and finally U0126 as indicated by the bars. The red curve is an exponential fit used to evaluate the rate of loss of nuclear ERK2-GFP (τ=4.47±0.20 min, R^2=0.98) during inhibition of the ERK pathway and CRM1-mediated export.

Thus, the cytosolic localization of ERK in starved cells is because of the efflux mediated by CRM1. Although it is well established that CRM1 is required for the depletion of ERK from the nucleus in starved cells, nothing is known about its role in controlling ERK efflux after stimulation. I tested this by pre-treating cells with leptomycin, followed by treatment with FGF and U0126 (Fig. Box 6.1C).
If CRM1-mediated export was the main vehicle of ERK export in activated cells I should observe an inhibition of the response to U126. By contrast, I observed that treatment with U0126 caused an immediate reduction in the nuclear concentration of ERK2-GFP, even if CRM1 export is ihibited.
Although this process might be slightly slower than observed in control conditions (τ=4.47 min *vs.* 3.0 minutes in control, as from Fig. 29 D), these data suggest that a large fraction of ERK2 exit occurs because of bidirectional facilitated diffusion across the nucleoporins independently of CRM1. This is in accordance with FRET studies (Burack and Shaw, 2005) on the binding between ERK and MEK. In this work ERK was fused to YFP and MEK to CFP; when ERK and MEK are bound together the two fluorescent proteins get near to each other and a FRET signal can be detected; while when ERK detaches from MEK, such signal is lost. No FRET effects were detected between MEK and ERK in the nucleus and ERK did not accumulate in the nucleus after energy depletion (the NES-dependent export requires energy); all these data suggest that the MEK/CRM1 system does not mainly contribute to the export of ERK from the nucleus.
Furthermore, the special role of CRM1-mediated export is that it can operate against a gradient. When ERK2 is strongly overexpressed there is a sizable fraction of ERK2 not bound to MEK1 and that is therefore unable to be exported by CRM1. In these conditions ERK2 accumulates in the nucleus and this requires that either its influx occurs against a gradient or that its mobility once in the nucleus is reduced.
The mobility of ERK2-GFP can be also measured by FRAP experiments. Here, I verified whether the effective diffusion coefficient (D_{eff}) of ERK2-GFP depends on its phosphorylation state, since this would influence the activity-dependent translocation process. I have studied ERK2-GFP mobility by bleaching a small spot of the nucleus with a brief laser pulse (250 milliseconds) and imaging the recovery process in starved cells and after stimulation with FGF4 (Fig. Box 6.2).

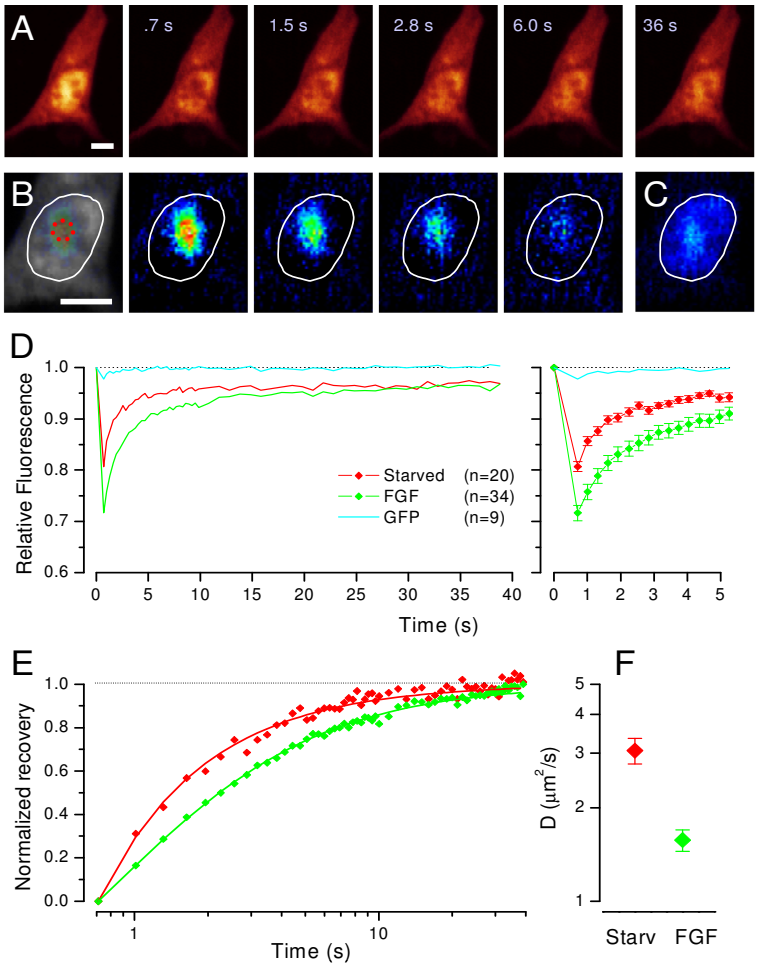

Figure Box 6.2

Reduced mobility of ERK2-GFP in the nucleus.

A) Imaging of a cell before and after the photobleaching of a small area of the nucleus (dotted circle in the magnified image in B) and at the indicated time during recovery. **B)** False colour representation of the difference with the last frame of the sequence. Bar 10 μm. **C)** Difference between the pre-bleach image and the last image of the recovery sequence (36s). The signal in the nucleus indicates that the pre-bleach fluorescence is still recovering: this requires the slower equilibration through the nuclear envelope. **D)** Time course of the normalized fluorescence recovery in the nuclei of starved (red) and stimulated (green) cells. GFP recovery is shown in light blue. Estimate of the asymptotic value reached by the recovery showed the presence of a small, but significative ($p \leq 0.0001$) immobile fraction (% of total normalized fluorescence: 3.3±0.6 starved, 3.2±0.7 FGF). **E)** ERK activation caused a considerable decrease of the recovery speed. The data in E have been normalized to allow a better comparison of the time course, and have been fitted with an approximate solution of the diffusion equation (continuous lines). **F)** Computed effective diffusion coefficient for starved and stimulated cells.

This technique is a very effective tool for measuring the diffusion of nuclear protein and it does not inflict any damage on the analyzed cells (Koster et al., 2005; Phair and Misteli, 2000).
The rate of fluorescence recovery is correlated with the mobility of the fluorescent reporter, with a faster time course being associated with a larger diffusion coefficient (Carrero et al., 2003; Lippincott-Schwartz et al., 2001).
The qualitative inspection of the fluorescence recovery indicates that ERK is substantially less mobile than GFP (Fig. Box 6.2 D,E): the result differs from previous studies (Burack and Shaw, 2005). Indeed, the recovery of GFP fluorescence is almost completed during the time elapsed from the end of photobleaching to the beginning of imaging (0.71 s). At the same time point the bleaching of ERK2-GFP is still very pronounced, demonstrating a much slower diffusion. Cell stimulation caused a clear decrease in ERK2-GFP mobility, as shown in Fig. Box 6.2 E by the comparison between the normalized recovery of starved and stimulated cells.
I have estimated ERK2-GFP D_{eff} by fitting the recovery with an approximate solution of the diffusion equation (continuous lines) (Feder et al., 1996). The diffusion coefficient of ERK2-GFP is well within the methodology sensitivity and was found to decrease by a factor of two upon stimulation (from 3.1 $\mu m^2/s$ to 1.6 $\mu m^2/s$, Fig. Box 6.2 F).
The small residual recovery of GFP only allowed a rough estimate of a lower limit for GFP diffusion coefficient (≈15 $\mu m^2/s$), which is consistent with published values (D_{GFP}>20 $\mu m^2/s$) (Chen et al., 2002).
The meaning of the IF measured in this experiment is different from the IF found in the whole-nucleus experiment. The IF observed in the whole-nucleus photobleaching measures the fraction of ERK that is unable to leave the nucleus, but which is not necessarily immobile within the nucleus. For example, this could be caused by the formation of large complexes to which the membrane is impermeable. By contrast, the spot FRAP experiments measure the fraction that is truly immobilized. These data are consistent because the IF measured in the spot experiments must be ≤ to the IF measured in the whole-nucleus experiments (starved $IF_{WholeNuc}$=4.0%, IF_{Spot}=3.3%; FGF $IF_{WholeNuc}$=12%, IF_{Spot}=3.2%).
The slow diffusion of ERK2 in the nucleus is probably because of the phosphorylation-dependent binding of ERK2 to sites of low mobility. Since these sites would be saturated by elevated concentrations of ERK2, I should expect that in strongly overexpressing cells most ERK2-GFP would diffuse freely. Since the temporal resolution of the previous assay was insufficient to measure the fluorescence recovery of freely diffusing molecules, I employed a different technique based on the line scan of the cell (Fig. Box 6.3).
In this experiment I bleached a thin stripe centred on the nucleus for 300 ms and I imaged the recovery process at high speed. These measures confirmed that ERK- GFP is much slower than GFP alone; in contrast to our data, earlier experiments did not find any difference between the mobility of ERK2-GFP and GFP alone (Burack and Shaw, 2005).

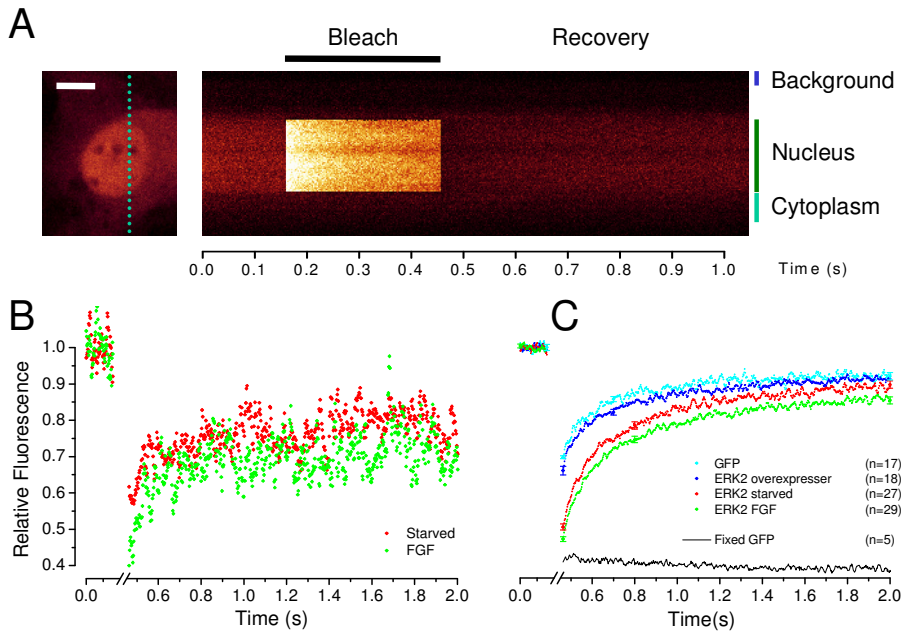

Figure Box 6.3
High speed FRAP measures
A) The cell is repeatedly imaged along the dotted line at high frequency (400 Hz). Bleaching is performed along a strip covering the nucleus for 300 ms. Fluorescence is corrected for background and divided by the cytoplasm fluorescence to compensate for imaging bleaching.
B) Recovery of fluorescence for the same cell before (red) and after stimulation with FGF4. Fluorescence has been normalized to the pre-bleach value.
C) Cumulative results. At this temporal resolution the recovery of GFP (starved cells) is clearly discernible and it almost overlaps with the recovery of ERK2-GFP measured in strongly over expressing cells (blue, stimulation did not cause any change). Photobleaching in low-expressing cells is larger and the recovery is slower, indicating lower mobility, which is dependent on ERK activation.

I believe that the cause of such difference resides in the experimental conditions used to measure the mobility by FRAP, indeed, those experiments were performed in strongly overexpressing cells (the right balance between MEK and ERK were rescued only coexpressing both the two fusion proteins), and therefore the impeded mobility of ERK2 was hidden by the saturation of the binding sites.

Accordingly, I have demonstrated that the fluorescence recovery of ERK2-GFP in strongly overexpressing cells almost overlaps with the recovery of GFP alone (Fig. Box 6.3C), confirming that the reduced mobility of ERK2 in the nucleus occurs because of the operation of saturable mechanisms. I have failed to see any phosphorylation-dependent change in mobility in these cells. Since the saturation of MEK1 causes a certain amount of nuclear translocation in overexpressing cells, the low-mobility sites in the nucleus must saturate at a higher concentration of ERK2 than MEK1. Once again, this fact highlights the importance of operating on cells minimally perturbed with low levels of expression.

BOX 7: Mapped domains of ERK

Here I show some of the most relevant domains of ERK. The primary sequences of ERK1 and ERK2 are displayed after alignment (ERK1 in the first line and ERK2 in the second line); bold characters on ERK1 sequence represent the divergences from ERK2 sequence. As it can be seen, the most important domains are almost perfectly conserved between the two kinases.

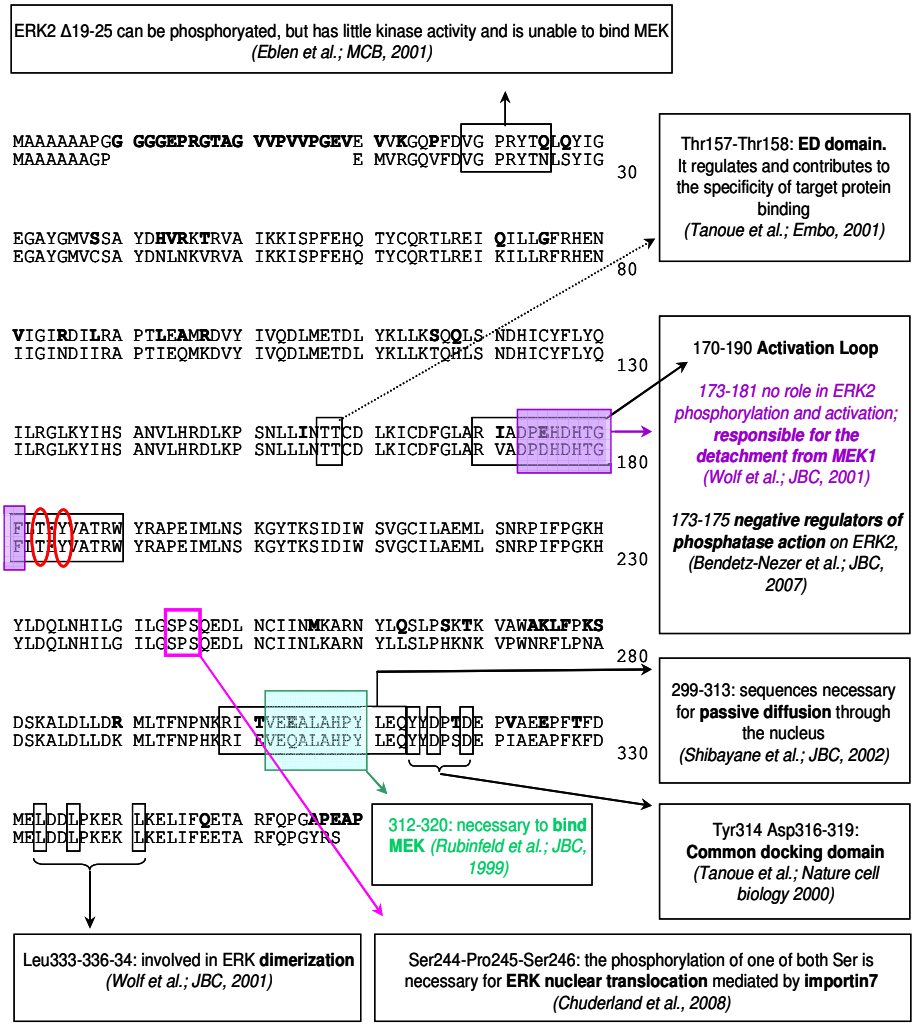

BOX 8: Functional consequences of ERK trafficking speed

Recently it has been demonstrated that ablation of ERK1 in mouse embryo fibroblasts and NIH 3T3 cells, by gene targeting and RNA interference, results in an enhancement of ERK2-dependent signaling and in a significant growth advantage. By contrast, knockdown of ERK2 almost completely abolishes normal and Ras-dependent cell proliferation (Vantaggiato et al., 2006). Besides, ectopic expression of ERK1 but not of ERK2 inhibits oncogenic Ras-mediated proliferation in NIH 3T3 cells and it is sufficient to attenuate Ras-dependent tumor formation in nude mice (Vantaggiato et al., 2006). Since these phenotypes are independent of the kinase activity of ERK1 (expression of a catalytically inactive form of ERK1 is equally effective) I hypothesized a relationship between the functional effect on cell growth and the shuttling properties I found out.

I demonstrated the changes of nucleo-cytoplasmic exchange are controlled by the N-terminus of ERK1, so I asked whether the deletion of this domain, by providing ERK1 with a faster turnover ($E1\Delta^{39}$), would also convert ERK1 in a kinase functionally similar to ERK2. If our prediction was right, I would also expect the reverse, i.e. a conversion of ERK2 mutant with a slow turnover ($\Delta^{39}E2$) into an ERK1-like molecule. This hypothesis was challenged with a colony formation experiment in collaboration with Brambilla's groups in Milan, who tested these ERK mutants for their effect on Ras-dependent cell growth (Fig. Box 8.1).
NIH 3T3 cells have been transfected with ERK1, ERK2, $E1\Delta^{39}$ or $\Delta^{39}E2$ (fused to GFP) alone or each one co-transfected with a constitutive activated form of Ras (Q61L), in order to test a system that is maximally stimulated; then the number of colony formed under each condition were quantified, by using a parameter directly proportional to the growth capability, so, indirectly, to the success in activating nuclear substrates and induce the cell cycle progression.

The N-terminus deletion of ERK1 ($E1\Delta^{39}$) failed to inhibit the proliferation caused by oncogenic Ras expression; in contrast, the fusion of the N-terminus of ERK1 with ERK2 ($\Delta^{39}E2$) results in a protein able to negatively affect Ras-mediated colony formation.

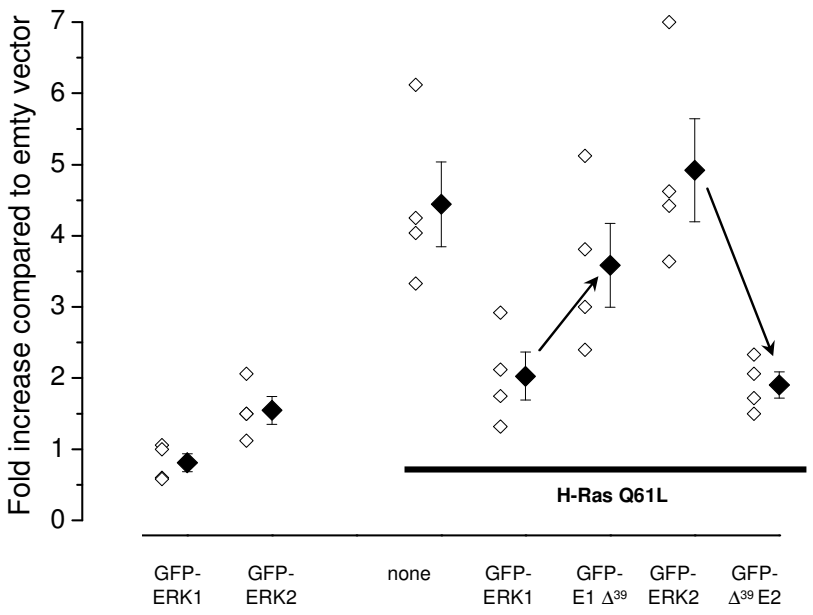

Figure Box 8.1
Number of colonies counted after transfection with the specified vector, normalized to the colonies transfected with the empty vector. Expression of constitutively active H-Ras Q61L causes a large increase in proliferation that is inhibited by co-expressing ERK1, but not by ERK2. The mutant of ERK1 characterized by fast shuttling ($E1\Delta^{39}$) did not prevent H-Ras Q61L-induced proliferation behaving similarly to ERK2. In contrast the slow mutant of ERK2 ($\Delta^{39}E2$) inhibits proliferation.

DISCUSSION

Use of fluorescent probes to study cellular processes in living cells

The approach of making proteins visible to study their involvement in intracellular events belongs to a complex inter-disciplinary field, which includes expertise in molecular biology, fluorescence-based microscopy and, eventually, computational modeling. This method of investigation can be applied to the study of every cellular process and provides the possibility to follow in real time what is happening inside a living cell.

I studied the dynamical aspects of the ERK pathway and I compared the behavior between ERK1 and 2, by expressing GFP-tagged ERK1 or ERK2 in cells and then following their localization and trafficking between different intracellular compartments.

In this paragraph I want to discuss the major characteristics of this approach for the study of ERK dynamics.

This method requires preliminary controls to validate the new fusion proteins. Notwithstanding the fact that this point is not always properly covered in the published literature, I deemed necessary to address two major aspects: A) the biochemical characterization and B) the control of the concentration level of the fusion protein.

A) At the basis of this method there is the assumption that the fusion protein should mimic the endogenous form, indeed only in this case it would be possible to get information about the real behavior of the wild type protein. In order to verify the fidelity of the chimera, it is essential to demonstrate that the fusion protein can undergo to the same post-translational modifications of the wild type protein. Furthermore, in case of an active molecule, it has to be proved also that they are catalytically active and can recognize their substrates.

Upon activation of the Ras module, ERKs are doubly phosphorylated by MEK and in turn phosphorylate their targets in the nucleus and in the cytoplasm. I demonstrated that GFP-tagged ERK1 and 2 can be correctly phosphorylated upon FGF stimulation (Fig. 14) and that they can properly phosphorylate a well known ERK target as MBP (Fig. 15). These assays are fundamental to exclude possible interference due to the proximity of the fused GFP. Indeed, the fluorescent tag could disturb or modify the structural properties of the protein of

interest, leading, for example, to their ectopic localization or impairing their capability of interacting with other important partners of the pathway.

Given that the ERK phosphorylation assay was performed *in vitro,* it cannot account for the intracellular localization of the chimeras; for this reason, I confirmed the result by immunocytochemistry experiments (Fig. 16). The chimera localization perfectly reflected the state of activation/inactivation of ERKs, demonstrating that ERK changes in localization are effectively promoted by phosphorylation of the fusion proteins. Specifically, cytoplasmic localization of the chimera is associated with a low level of phospho-ERK signal (in red, Fig. 16), while in stimulated condition nuclear accumulation of ERK-GFP (in green, Fig.16) colocalizes with a high pERK signal in the nucleus. All these results demonstrated that the two fusion proteins are functional: they can mimic the biochemical features of the corresponding wild types and they can be correctly controlled by the pathway, once expressed in living cells.

B) The second important issue to take into account is the level of expression in cells; the overexpression has two main effects on the pathway: the alteration of the stoichiometric ratio with binding partners and/or a possible saturation of binding sites.

I selectively studied cells with very low levels of expression that were compatible with a normal ERK localization in nucleus and cytoplasm. The expression level was evaluated by measuring the fluorescence of the chimera after a calibration performed on micelles, loaded with known amounts of recombinant GFP (see Methods). Successively, I correlated the concentration with a parameter estimating the distribution of the protein between nucleus and cytoplasm in resting conditions.

Figure 17 shows that the increase of ERK concentration causes the ectopic accumulation of the protein in the nucleus. This was due to the alteration of the stoichiometric balance with endogenous MEK, as it has been already demonstrated by several laboratories (Burack and Shaw, 2005; Stork and Schmitt, 2002). This experiment was instrumental to identify an upper limit for the concentration of ERK-GFP (150 nM) that was low enough to be compatible with normal localization, but sufficiently high to allow confocal imaging.

The overexpression of GFP-tagged ERK can heavily affect the evaluation of important cellular processes. For example, Burack et al. used live cell imaging to examine the interaction between CFP-MEK and YFP-ERK by means of FRET

effect (Burack and Shaw, 2005). In this experiment, they rescued the stoichiometric unbalance between MEK and ERK, by introducing large amounts of both proteins. Although this procedure might address the unbalance between ERK and MEK, it does not fix the unbalance with other binding partners. Indeed, I have demonstrated that the strong overexpression of ERK2-GFP considerably slowed down trafficking (Fig. Box 4.2), indicating the saturation of the machinery presiding at nuclear import and export. This interference of the trafficking mechanisms, due to the overexpression, might explain why Burack and colleagues did not observe the dependency of ERK turnover on its phosphorylation, in contrast with what I and others have found (Ando et al., 2004; Costa et al., 2006).

The majority of the cells included in my study showed a concentration of ERK-GFP less than ≤100 nM and since ERK levels in mammalian cells have been estimated to be in the 1-3 μM range (Ferrell and Bhatt, 1997; Whitehurst et al., 2002), ERK-GFP was much less abundant than the endogenous protein with consequently minimal perturbation of the biological homeostasis.

Dynamics of ERK activation/deactivation

The ERK1/2 pathway integrates various cytosolic signals depending on the cellular context (Bhalla and Iyengar, 1999; Chuderland and Seger, 2005). This plethora of incoming signals is converted to a variety of actions, owing to the phosphorylation of downstream effectors both in the cytoplasm and in the nucleus.

The translocation of ERK within the cell represents one level at which the specificity of ERK signaling pathway might be regulated. In particular, cytoplasmic-to-nuclear movement of ERK has been suggested to be important for the long-term consequences of ERK activation in multiple cellular processes, such as cell growth, differentiation and neuronal plasticity (Marshall, 1995).

In this work I studied ERK translocation process under different aspects, paying particular attention to the regulatory mechanisms that control the on/off switching of the cascade and measuring the temporal pattern of ERK localization.

I followed ERK nuclear translocation, after serum or FGF stimulation, with time lapse recordings, capturing all the crucial phases of the processes and measuring their temporal profiles. Nuclear accumulation is biphasic: the latency phase of approximately 2 min is followed by a rapid accumulation of the protein

(Fig 19). The observed time lag correlates with recent data which showed that ERK2 unbinds from MEK1 within 90 s from the stimulus onset (Burack and Shaw, 2005). Afterwards, nuclear accumulation follows a sigmoidal rising phase that concludes in a plateau in about 15 min.

The general characteristics of this process are highly conserved in different replicating cell lines (L1 3T3 and primary mouse fibroblasts; Fig. 20), even if the timing is variable.

Interestingly, at longer times (more than 15-20 min from stimulation) different stimuli led to diverse responses. A continuous stimulation with FGF gave a sustained nuclear accumulation of ERK, while serum provoked a transient maximal accumulation, which soon after declined and stabilized on a lower plateau (Fig. 21). This difference probably reflects the high variety in composition of serum, which contains many active molecules, and some of these may influence phosphatase activity or other molecules responsible of the negative feedback mechanisms which switch off ERK activation.

The steady response to a constant stimulus is potentially capable of controlling gene expression with noteworthy rapidity; for example, the transcriptional effects of activated ERK on MKP expression can already be detected 15-30 min after stimulation (Bhalla et al., 2002). This regulatory mechanism implies that, in the appropriate context, the degree of ERK activation and its translocation might follow complex temporal patterns with a bandwidth of few minutes and that ERK might undergo burst-like episodes of activation lasting 15-20 minutes.

Conversely, I showed that a brief presentation of FGF, lasting 4 min, caused only transient ERK nuclear translocation, which would not be sufficient to maintain a steady state activation of nuclear targets (Fig. 22). Indeed, it has been demonstrated that sustained, but not transient, activation of ERK is required for quiescent fibroblasts to begin to proliferate (Balmanno and Cook, 1999; Dobrowolski et al., 1994) Furthermore, whereas both transient and sustained activation of ERK induce transcription of immediate early genes (e.i. Fos, Jun, Myc, Egr1), only sustained ERK activation causes phosphorylation and stabilization of the proteins they encode (Murphy et al., 2004; Murphy et al., 2002).

In the FGF pulse experiment there is another level of complexity: the internalization of the growth factor inside the cell (Wiedlocha and Sorensen, 2004) and the consequent persistency of the active signaling complex

FGF/receptor/scaffold-proteins/ERK module. This could lead to prolonged activation of the pathway, which depends no more on the presence of the signal in the extracellular environment. In conclusion, these observations suggest that there might be a minimal temporal window to start and establish the molecular mechanisms necessary to maintain ERK signaling over long time periods.

The temporal pattern of ERK phosphorylation and translocation is finely tuned; if a certain threshold of ERK activation is overcome, mechanisms like stabilization of early genes products, auto-catalytical activation and positive feedback events are favored, and all of them might contribute to stabilize and complete the long term events involving gene transcription. Otherwise, the cascade is rapidly shut down to restore the basal conditions, getting the cell ready for a new burst of activation.

The long term ERK nuclear accumulation I observed after FGF is compatible with the instauration of positive feed back mechanisms; ERK has been reported to phosphorylate already active Raf, increasing its activity 4-fold (Balan et al., 2006), even if hyperphosphorylation prevents Raf interaction with the Ras GTPase and promotes its dephosphorylation by PP2A (Dougherty et al., 2005). In addition, ERK has been demonstrated also to phosphorylate MPK-3 at two serine residues, targeting the phosphatase for degradation in the proteosome (Marchetti et al., 2005), thus reducing the level of ERK inactivation.

Conversely, I can hypothesize that negative feedback loops predominate in the transient response to a brief exposure of FGF and/or in the rapid ERK efflux from the nucleus after U0126, contributing to restore the ERK cytoplasmic localization. It has been reported that MEK can be inhibited by ERK phosphorylation at Thr 292 (Eblen et al., 2004) and Thr 212 (Sundberg-Smith et al., 2005) preventing further enhancement of its catalytical activity by PAK1 (Slack-Davis et al., 2003). In addition, ERK can phosphorylate also Sos, inhibiting its interaction with Grb2, thus preventing Sos recruitment to the membrane, thereby reducing Ras activation (Douville and Downward, 1997).

I determined that ERK activation and localization are rapidly and dynamically regulated by concurrent processes of phosphorylation and dephosphorylation that also occur in the absence of extracellular stimulation. Indeed, there is a continuous balance between MEK and phosphatases; this push-pull mechanism exerts a tight control of the phosphorylation state of the protein that can be rapidly regulated. This fine tuning seems to be necessary to prepare the cell to

promptly answer to different extracellular stimuli or to the changing environmental conditions; all of these factors can heavily influence cell survival.

The proteins directly involved in ERK activation/inactivation are essentially: MEK and phosphatases. There is a large family of dual-specificity phosphatases (MKP) known to dephosphorylate ERK1/2 even if their action show a high degree of cross-talk with other MAPK, like JNK or p38. Indeed, it is getting clear that it does not exist any specific phosphatase for ERK1/2 or other kinases, but rather, there are phosphatases which are more affine for one or more substrates respect to others. Anyway, it has been demonstrated that ERKs are dephosphorylated by 3 cytoplasmatic (PP2A, MKP-X, MKP-3) and 4 nuclear (MKP-1, MKP-4, Pac-1, hVH3) phosphatases [reviewed in (Kondoh and Nishida, 2007)].

I designed a set of experiments to better elucidate the modality and the kinetic properties of the processes which control ERK fate, by using drugs which interfere with the two main regulators of ERK. While it exists a specific and potent MEK inhibitor (U0126), it is not available any specific substance blocking the activity of a specific phosphatase; in addition, as I reminded before, there are several phosphatases acting on ERK, so I applied a general phosphatase inhibitor, sodium orthovanadate, to interfere with ERK inactivation.

By treating starved cells with sodium orthovanadate I unmasked a small level of basal MEK activity that caused a slow phosphorylation of ERK in absence of any stimulation. ERK slowly accumulated into the nucleus (Fig. 24) because the fraction of activated ERK cannot be dephosphorylated any more by nuclear and cytoplasmic phosphatases.

In resting conditions cells do not completely stop the ERK pathway, providing for a more efficient reaction to extracellular stimuli. Indeed, if a residual activity is always present, the pathway can provide for a quicker response, skipping some of the start up operations.

I demonstrated that the slow rate of ERK accumulation detected in the experiment of figure 24, was not influenced by the speed of permeation of the inhibitor inside the cell, but it reflected the real kinetics of the occurring process. Indeed, cells pretreated with FGF and then exposed to orthovanadate (Fig. 28) showed a faster ERK accumulation in the nucleus (τ=4 min *vs.* 26 min), indicating that ERK shows different rate of activation by MEK, depending on cellular conditions.

This last experiment gives some other important clues to the understanding of the complex network regulating ERK localization and activation. Indeed, while neither FGF nor serum stimulation provoked a maximal activation, in cells previously stimulated with FGF and then treated with the phosphatase inhibitor, the plateau of ERK nuclear concentration achieved after FGF was further lifted after orthovanadate administration. Therefore, the blockage of phosphatases, unmasked the small fraction of ERK which is continuously dephosphorylated, even in presence of sustained stimulation (Fig. 28). This means that the process of ERK recycling is continuous and a new equilibrium between activation and inactivation is established, in order to make the system plastic for further changes.

Conversely, I unmasked phosphatases actions, blocking MEK activity with U0126 in cells at the maximum of their stimulation (Fig. 26). I observed a fast decrease of ERK2 concentration in the nucleus due to ERK dephosphorylation by nuclear phosphatases. The two processes of ERK phosphorylation and dephosphorylation are dynamically controlled by feedback mechanisms acting as bridges which interconnect the activity of diverse proteins and make possible the communication between them. ERK itself intervenes in loops of auto-catalytical activation/inactivation; for example, it has been reported the physical and functional association of ERKs with PAC-1 and MPK-3, whose binding increases their dephosphorylative activity (Camps et al., 1998; Dickinson and Keyse, 2006; Muda et al., 1998; Rohan et al., 1993; Sharma et al., 2002). Furthermore, ERK can influence also the level of expression of phosphates such as MPK-2 (Brondello et al., 1997) and MKP-1 (Charles et al., 1992; Keyse and Emslie, 1992; Noguchi et al., 1993), which is rapidly induced after exposure of growth factors, heat shock and oxidative stress. Finally, a study has shown that hVH3 (both in an active or inactive conformation) causes ERK translocation and sequestration in the nucleus (Mandl et al., 2005), suggesting that hVH3 can function as a nuclear anchor for ERK.

ERK2 nuclear entry/exit

The nucleus represents the end station for the action of every signaling pathway that controls gene expression in response to changes of the extracellular environment.

The process which mediates the entrance and exit of ERK from the nucleus has been object of numerous studies and several model mechanisms have been invoked to explain such influx/efflux. For the entrance of ERK in the nucleus, the following 3 mechanisms have been proposed.

1. Khokhlatchev et al. studied the nuclear accumulation of ERK after activation of the pathway and they showed that it depends on ERK phosphorylation state rather than its activity. They proposed that pERK dimerizes with phosphorylated and unphosphorylaed ERK partners; accordingly, mutants unable to dimerize showed a minor capability to translocate (Khokhlatchev et al., 1998); this is in contrast with previous results which excluded the dependency from phosphorylation (Lenormand et al., 1993). However, it still remains unclear if dimerization is required for the rapid, agonist-induced entry of ERK into the nucleus, and the most recent opinions tend to consider this mechanism not really probable.
2. Adachi and coworkers added that ERK can cross the nuclear barrier by passive diffusion (Adachi et al., 1999), concluding that there are at least two pathways for ERK entry in the nucleus: the passive diffusion as a monomer and the active transport of a dimer.
3. Finally, Matsubayashi et al. proposed that ERK passes through the nuclear pore by directly interacting with the nuclear pore complex, independently from cytosolic factors such as the importin beta family protein and Ran (Matsubayashi et al., 2001). Indeed, ERK has been demonstrated to be one of the proteins which is not imported by either classic or non-classic NLS systems, like β-catenin (Fagotto et al., 1998) and SMAD 2,3 and 4 (Xu et al., 2003; Xu et al., 2000). It has been shown that ERK2 is able to interact directly with CAN/Nup214 and Nup153 (Matsubayashi et al., 2001; Whitehurst et al., 2002). Nucleoporins containing FG repeat motifs are thought to be common docking sites for molecules that pass through the NPC [reviewed in (Peters, 2005)]. The FG repeats would be displaced along the internal wall of the pore channel in order to follow a favorable affinity gradient until reaching the end of the channel. The molecular and biophysical details of this process are still completely missing.
Recently, it has been identified a 3 aminoacid domain (SPS), phosphorylated upon stimulation, that it has been shown to interact with the importin7, which in turn mediates ERK nuclear translocation (Chuderland et al., 2008). The

phosphorylation can occur on only one or both the serines, and these events are indipendent from the phosphorylation of Thr and Tyr by MEK (**T**E**Y**). In accordance with the model proposed by Chuderland and collegues, the **T**E**Y** phosphorylation (detected within 5 min from the stimulus) is important for the detachment from cytoplasmic anchors, while the subsequent SPS phosphorylation (detected after 15 min) should plays a role in the nuclear translocation.
Interestingly, if SPS is mutated in APA (not phopshorylable) the interaction of ERK with the Nup153 is increased, suggesting that this specific interaction might be mediated by other residues and that the pSPS is required for a faster release of ERKs from the NUPs. This domain has been found also in other shuttling proteins, suggesting that it might be a general signal sequence for nuclear translocation.

Concerning ERK exit, previous data proposed that this process uniquely depends on MEK. This upstream kinase acts as a nuclear export shuttle, given that it carries a NES and it is actively extruded by a CRM1-dependent mechanism (Adachi et al., 2000; Fukuda et al., 1996; Fukuda et al., 1997).

I demonstrated that ERK1/2 can shuttle across the nuclear envelop (Fig. 30, 32); this passage of signaling molecules does not occur only at the time of activation but continuously, because a steady flux accounts for the biochemical communication between nucleus and cytoplasm. I measured the rates of shuttling with the FRAP imaging. The shuttling rate is determined by the steady state equilibrium between two simultaneous fluxes, one towards the nucleus and the other one towards the cytoplasm. I propose that, in addition to the mechanisms of entrance and exit that I have described above, ERK must be capable of diffusing though the nuclear pore bidirectionally. There are several evidences supporting this theory: first of all the very small quantity of MEK present in the nucleus, clearly shown in figure 44, both in starved and stimulated conditions. Indeed, given that the binding between ERK and MEK follow a 1:1 stoichiometry, it is unlikely that the few MEK molecules present in the nucleus might rapidly export the high quantity of ERK present after translocation.

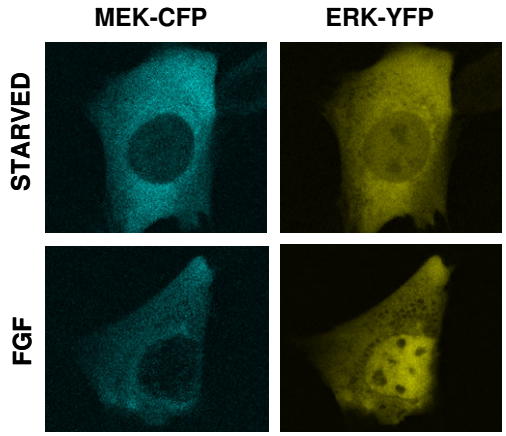

Figure 44
NIH 3T3 cells co-expressing MEK-CFP (cyan channel displayed in the first column) and ERK2-YFP (yellow channel displayed in the second column). While in starved condition ERK localization is overlapped to MEK, after stimulation ERK predominantly localized in the nucleus and MEK remained mostly in the cytoplasm.

This might happen only if MEK would show a very fast turnover across the nuclear barrier, but this is really unlikely, given that it has a high MW (45 kDa) and it carries a NES, which would definitely not endow MEK with any special facilitation in entering the nucleus. Furthermore, the presence of the exclusion signal suggests that MEK has a more important role as ERK activator in the cytoplasm, rather than as ERK exporter from the nucleus.

Consequentially, all these considerations indicate that ERK outflux should occur mainly by passive diffusion, while the influx is probably formed by at least two components: passive diffusion and an active import mediated by importin7 (Chuderland et al., 2008). The relative size of this fluxes and the reversibility of the importin-mediated flux remain to be determined. This implies that nucleoporins must allow the bidirectional passage of ERK. In support to this theory, a recent paper demonstrated that nucleoporins let access molecules in both directions with the same probability, in permeabilized cells (Kopito and Elbaum, 2007). Notwithstanding this, it is usually accepted the notion that ERK exits from the nucleus uniquely by MEK binding; an indication that CRM1-mediated export cannot be the only vehicle of ERK export in cells, comes from the experiment in which pre-treated cells with leptomycin were then sequentially treated with FGF and U0126 (Fig. Box 6.1). If CRM1-mediated export was the main vehicle of ERK export in activated cells, I should have observed an inhibition of the response to U0126. In contrast, I observed that the treatment with U0126 caused an immediate reduction of the nuclear concentration of ERK2-GFP, indicating that efflux is still present even after the blockage of active export. However, since, this process was slightly slower than observed in control conditions (τ=4.47 min *vs.* 3.0 min in control, Fig. Box 6.1C), it is possible that

there might be a small component of the efflux mediated by CRM1. I can exclude that the treatment with U0126 interferes with MEK export, since the characterization of the inhibitor interaction showed that U0126 can bind with identical affinity the free enzyme and the MEK-ATP complex, and this is also capable to bind the entire complex MEK-ERK (Favata et al., 1998). This binding has been reported to be noncompetitive and that it minimally perturbs the affinity of MEK for its binding partners. This means that MEK should be capable to bind CRM1 and ERK even if already bound to U0126.

I can conclude that ERK can enter as (see summary in Fig. 45):

1. pERK monomer (Fig. 45 a), with an energy-independent and -dependent mechanism (Costa et al., 2006; Ranganathan et al., 2006);
2. ERK not phosphorylated (Fig. 45 b), with an energy-independent way (Adachi et al., 1999; Costa et al., 2006).
3. ERK (pSPS), bound to importin7 (Chuderland et al., 2008), independently from the phosphorylation on **T**E**Y** (Fig. 45 a/b).

Concerning the exit:
only a small fraction of ERK exits by a CRM1-mediated mechanism (Fig. 45 c), while the majority of the outward flux must occur though the nuclear pores, in a energy-independent way (Fig. 45 a/b).

ERK can shuttle back and forth from the nucleus and the speed of shuttling determines the capability of nuclear targets to sense the extracellular environment, representing a possible locus for the fine tuning of the pathway activity.
It is conceivable that the biological advantage of this way of communication is that, since the signaling elements are continuously moving between the two compartments, the system has a better time responsiveness to the external environment.

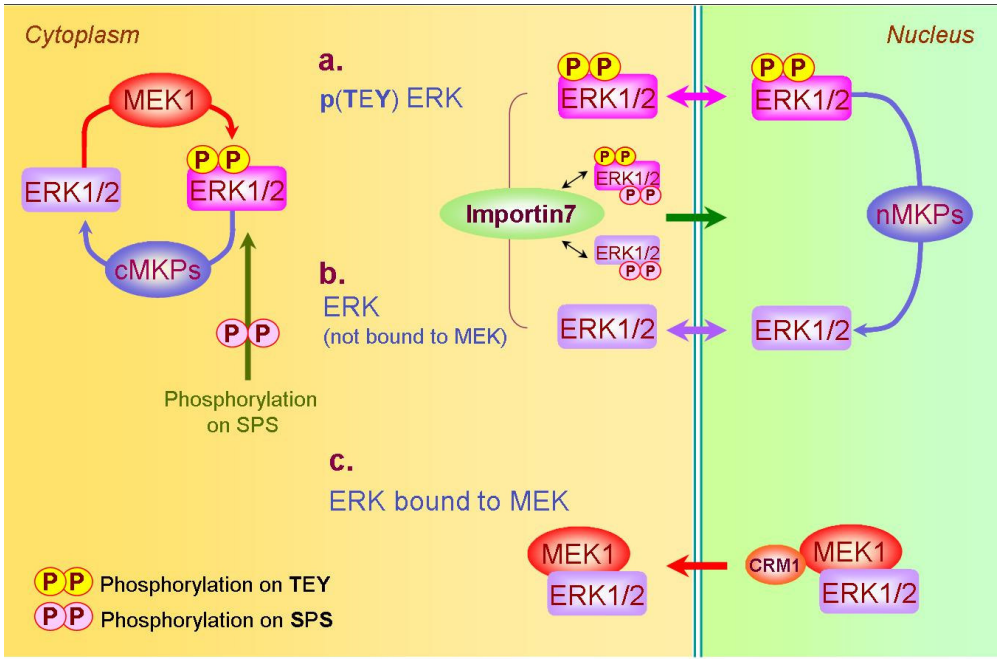

Figure 45
ERK import/export is regulated by the following mechanisms:
a. Study conducted with GFP-tagged ERK2 in permeabilized cells demonstrated that p(TEY) ERK can be imported and exported from the nucleus in the absence of transport factors and energy (Ranganathan et al., 2006); but, given that it has been observed a dramatic increase in nuclear import of thio-pERK2 when energy was included in the import mixture, Ranganathan concluded that the import of pERK2 occurs predominantly by an energy-dependent process.
FRAP experiments on ERK2 nuclear shuttling in stimulated cells (Fig. 30, 32) suggest a bidirectional passage of ERK through the nuclear pores (Costa et al., 2006).
b. It has been reported that ERK can cross the nuclear barrier by passive diffusion (Adachi et al.; 1999).
Ranganathan demonstrated that non phosphorylated ERK2 is imported in an energy-independent way (Ranganathan et al., 2006).
Matsubayashi et al. proposed that ERK passes through the nuclear pore by directly interacting with the nuclear pore complex, independently from cytosolic factors (Matsubayashi et al., 2001). It has been shown that ERK is able to interact with CAN/Nup214 and Nup153 (Whitehurst et al., 2002; Matsubayashi et al., 2002).
Export of ERK2 occurs even with impaired MEK1 binding (Ranganathan et al., 2006). FRAP experiments on ERK2 nuclear shuttling in starved cells (Fig. 30, 32) and the dynamics of ERK change in localization following Leptomycin and U0126 administration (Fig. 6.1C) suggest a bidirectional passage of ERK through the nuclear pores (Costa, 2006, JCS).
a./b. A recent research has demonstrated that the phosphorylation of the SPS peptide (in the Kinase Insert Domain, KID) allows ERK nuclear translocation by importin7 (Chuderland et al., 2008), and this mechanism is independent from the phosphorylation on TEY by MEK.
c. ERK bound to MEK is actively extruded by a CRM1-dependent mechanism (Fukuda et al., 1997; Adachi, et al., 2000; Fukuda et al., 1996).

To draw a complete scheme of all the mechanisms contributing to the change of ERK localization I cannot ignore a further aspect: the mobility of ERK in the nucleus. I have reported that when the pathway is activated, ERK accumulated in the nucleus and concomitantly, its mobility significantly decreased (D values: 3.06 ± 0.30 $\mu m^2/s$ in starved cells *vs.* 1.57 ± 0.10 $\mu m^2/s$ in stimulated cells; as I measured by spot FRAP; Fig. Box 6.2 E,F). This suggests that pERK has an increased affinity for nuclear anchors and for this reason it spends more time in the nucleus.

ERK1 and ERK2 shuttle across the nuclear membrane with different rates

For a long time it has been believed that ERK1 and 2 were interchangeable. This notion was originated by their vast sequence homology (Fig. 34) and by the identity of the upstream activator and of the identified substrates. Only recently it has become clear that while ERK2 is the most active kinase form, ERK1 contributes far less to the overall signaling output; indeed, it has been recently proposed that ERK1 functions as a partial agonist of ERK2 for MEK binding (Vantaggiato et al., 2006). However, the mechanism and the domain responsible for the differences between ERK1 and ERK2 have not been yet identified.

Most of the functional domains that have been mapped on ERK sequences are present on both ERK1 and 2, including a consensus region for MEK (Brunet and Pouyssegur, 1996; Robinson et al., 2002), the catalytic domain (Tanoue et al., 2000) and a region considered the interacting site for the nucleoporins (Matsubayashi et al., 2001; Whitehurst et al., 2002). Surprisingly, notwithstanding all these similarities, I found that ERK1 shuttles about three times more slowly than ERK2, although the turnover acceleration after stimulation is preserved (Fig. 32). I observed that translocation after stimulation followed a similar temporal pattern for both ERK1 and 2 (Fig. 29B). This is not surprising given that the time constants of nucleo-cytoplasmic shuttling of ERK1 and 2 in stimulated conditions are both smaller than the time constants of ERK translocation (respectively, 170 s ERK1, 84 s ERK2 and about 180 s for the translocation of both ERK1 and 2).

Conversely, the time constant of the net efflux following acute inactivation of MEK (Fig. 29D) is much slower and it can be effectively limited by the far slower shuttling rate of ERKs in starved conditions.

After U0126 administration MEK is inhibited and so the cell returns to the condition preceding the stimulation. As dephosphorylation proceeds, the rate of ERK shuttling drops: ERK1 in the dephosphorylated form moves very slowly,

strongly affecting the speed by which ERK1 distribution returns to the initial state. Indeed, the mean time constant of ERK1 shuttling in starved conditions (τ=10.9 min) is very similar to the time constant of the protein redistribution after U0126 administration (τ=9.3 min), like the faster efflux of ERK2 (τ=3.1 min) reflects its faster turnover (τ= about 3 min).

ERK1 N-terminus is the domain causing the slowing down ERK1

ERK1 is slowly exchanged between the two main compartments, nucleus and cytoplasm; I tried to find the main cause of such phenotype comparing the primary aminoacidic sequences of the two kinases. Observing figure 34 it is evident that ERK1/2 are very similar, displaying over 85% of sequence homology and sharing almost all the mapped functional domains (Box 7). Thus, there are no clear reasons why the two proteins should shuttle as differently as they do. The larger sequence divergence is a region of about 39 residues, located at the N-terminus of ERK1, that has not been associated to any specific function to date. I decided to test the hypothetical involvement of this region in ERK shuttling behavior by either removing, transposing on ERK2, or mutating specific portions. For simplicity, I divided ERK1 N-terminus in three main regions (see Fig. 35):

1. an alanine rich cap, in common with the two kinases except for the inversion of P_8G_9 of ERK1 in G_8P_9 of ERK2 (in mouse this region spans aa 1 to 8);
2. a region present only in ERK1 (aa 9-29);
3. a homologous region (aa 30-39) which differs of only three single non consecutive aa (Val_{31}, Arg_{33} and Pro_{36}).

As I have already pointed out, ERK1 and 2 have been considered for a long time as isoforms and thus, most studies about functional or active domains have been conducted only on ERK2 (se Box 7), consequently no information are available about the putative role of the N-terminus of ERK1.

First of all, I generated a series of deleted derivatives of ERK1 N-terminus, by removing region 1, both regions 1 and 2 and all three regions (Fig. 36A). The resulting proteins gave different results in terms of nuclear shuttling (Fig. 36B).

The removal of the alanine rich cap did not affect the time constant of shuttling which resulted not significantly different from ERK1 wt; the same results were obtained also if the poly-alanine sequence was removed from ERK2 (data not

shown). These results demonstrate that region 1 is not involved in controlling the shuttling. In parallel, it has been demonstrated for ERK2, that this region is not involved in other functional properties, such as the capability to be phosphorylated and the catalytic activity (Eblen et al., 2001).

Conversely, the removal of region 2 or both 2+3 drastically reduced, to different extend, the value of τ. The removal of both regions 2+3 ($E1\Delta^{7-39}$) made ERK1 shuttling identical to ERK2, while the removal of region 1+2 ($E1\Delta^{26}$) caused a partial acceleration of the shuttling (Fig. 36). This suggest that both region 2 and 3, cooperate and are necessary to define the slower phenotype of ERK1.

Region 2 and 3 are not only necessary for the slowing down of shuttling, but they are also sufficient since, fusing region 2+3 of ERK1 on the N-terminus of ERK2 ($\Delta^{39}E2$) causes a large slowing down of the shuttling (Fig. 37). These data suggest that differences between ERK1 and 2 present elsewhere than on the N-terminus are non-consequential to the shuttling differences that I observed.

One possible explanation for this phenotype might be that this terminal region masks some critical sites on the ERK ternary structure, responsible of the interaction with nucleoporins, which are at the basis of facilitated diffusion. However, since the fusion of the N-terminus to GFP dramatically slows down the trafficking of GFP, I must conclude that this domain is able *per se* to slow down the speed of exchange across the nuclear envelope (Fig. 38 B).

Furthermore, the direct fusion of all the three N-terminal regions 1+2+3 to GFP (GFP-ΔN_{1-39}) decreased GFP shuttling rate to a different extent compared to the fusion of only region 1+2 (GFP-ΔN_{1-27}). Specifically, region 1+2 (GFP-ΔN_{1-27}) was faster than region 1+2+3 (GFP-ΔN_{1-39}), but it is significantly different from the GFP and from the random sequence. Putting together these data, I can conclude that the slow phenotype observed is due to the combination of at least two factors, one connected with region 2 (aa 9-29) and the other one related to region 3 (aa 30-39).

The slowing down effect that the N-terminus induced on GFP trafficking is surprising since it cannot be due to the higher molecular weight of this fusion protein (32 kDa). It is widely acknowledged that globular molecules smaller than about 40 kDa can freely permeate thought the nucleoporin [reviewed in (Patel et al., 2007)], thence, the GFP monomer (27 kDa) can equilibrate between nucleus and cytoplasm by simple passive diffusion. It seems unlikely that the addition of only 39 residues might cause any change in passive diffusion. Furthermore the

observation that a scrambled sequence of the size of region 2+3 has not effect whatever of GFP trafficking, suggests that the slow permeation is caused not by steric hindrance but rather by specific binding with other components. It is probable that an interaction might occur between ERK1 N-terminus and some binding partner, yet to be identified, that slowed down the permeation of the protein. This interaction, would be directly responsible for the differences in trafficking that have been observed between ERK1 and 2. The analysis of the sequence of the N-terminal region, suggests 2 possible candidates involved in the interaction: A) a putative SH3 recognition domain in region 2 and B) three aminoacids in region 3 which differ between ERK1 and 2.

A) The presence of a putative SH3 domain in region 2 (residues 23-26 PVVP; Fig. 39) was assed by the probabilistic calculation generated with a web server (Ferraro et al., 2007) specialized in the recognition of SH3 interaction sites.

It is possible that PVVP site might specifically interact with a SH3 binding partner and that this interaction might be somehow responsible for the slower permeation. However, the experiments clearly showed that any kind of manipulation on the PVVP site (mutations targeted to one or both the prolines or the deletion of the whole region PVVP) did not confer any acceleration to the protein. Therefore, even if I cannot conclude that there are no SH3 interactions occurring at this site, I can exclude that this putative interactions are not involved in nuclear trafficking.

B) Comparing the region 3 of ERK1 and the respective homologous of ERK2, it is evident that there are only three differing aminoacids (Val_{31}, Arg_{33} and Pro_{36}; Fig. 39). Therefore, I expected that one or all of them were crucial determinants, even if not uniquely responsible, for the different trafficking.

Indeed, the results obtained by converting both Val_{31} and Arg_{33} in Ala, either in the N-terminus alone or in the entire sequence of ERK1 (Fig. 36 and 39), demonstrated that these two aminoacids are heavily involved in controlling nuclear trafficking.

At this point a question arises: what could be the mechanism that links the presence of a putative binding site to the slowing down of the facilitated diffusion process? I can hypothesize that this domain might interact with specific consensus regions of nucleoporins, influencing ERK1 rate of passage through the pore channel. More specifically, I expect that this interaction increases the residency time of the protein inside the channel, thus decreasing the overall flux.

ERK2 is known to directly interact with some nucleoporins [reviewed in (Xu and Massague, 2004)], so it is likely that also ERK1 establishes similar interactions. In addition, it can be hypothesized that its N-terminus affects the binding, presumably inducing a longer residence time in the pore channel. Interestingly, although GFP can cross the nuclear barrier without any need of the facilitated diffusion mechanisms, it slowed down when tagged with ERK1 N-terminus. One possible explanation could be that GFP becomes more sticky to the pore walls increasing its residence time inside the nuclear pore (Fig. 38 B).

Interestingly, the N-terminal peptide shows a high degree of hydrophobicity that can favor and increse the affinity for certain domains of the pore wall, for example, the repetitive stretches of Phe-Gly residues (Rout and Wente, 1994) which are thought directly to interact with ERK2. An alternative explanation is that the N-terminus binds to a yet unidentified partner not belonging to the nucleoporin, that increases the size of the protein with a corresponding decreased permeation. Regardless of the details of the molecular interactions involved, these results are in accordance with the idea that the N-terminus *per se* interferes with nuclear shuttling, because of direct molecular interactions, rather than by masking specific sites on the ternary structure of ERK.

The striking difference obtained by targeting region 3 with the conversion of the two aminoacids in alanine is surprising given that they share the same chemical properties, respectively Val_{31} in ERK1 versus Met in ERK2 are both hydrophobic, and Arg_{33} in ERK1 versus Lys in ERK2 are both positively charged. This observation strongly suggests that these residues (one of them or both) represent the site of an interaction which requires their specific chemical structures and cannot be supported by similar aminoacids.

I did not mutate also the third aminoacid (Pro_{36} of ERK1 *vs.* Val of ERK2) because the neutralization of the first two aminoacids was sufficient to obtain a strong difference in shuttling rate. Given that, I demonstrated that also region 2 is necessary to completely revert ERK1 phenotype into ERK2, I expect that the additional neutralization of the Pro_{36} would not dramatically change the effect.

Phosphorylation levels of ERK1 and 2 in the nucleus and consequent functional outputs

Since MEK is mainly localized in the cytoplasm (Adachi et al., 2000), the maintenance of a functional level of activated ERK in the nucleus depends

crucially on the inflow of phosphorylated ERK. I speculated that the different efficacies of ERK1 and ERK2 might be due, at least in part, to some differences in their nuclear trafficking.

ERK1 permeates the nuclear membrane far more slowly than ERK2 and this causes a longer permanence of ERK1 in the nucleus, as exemplified by the slow loss of nuclear accumulation following MEK1 blockage (Fig. 42). What are the consequences of the slower trafficking? Computational simulations predicted that the longer residency time of ERK1 in the nucleus, where inactivation predominates over activation, causes a pronounced dephosphorylation of ERK1 compared to ERK2. The available evidences therefore suggest that ERK1 and 2 differ in the capability of maintaining their phosphorylation state in the nucleus. Indeed, if phosphatases are inhibited in presence of serum (Fig. 43 B) I observed a further increase of ERK phosphorylation, that is larger for ERK1 respect to ERK2, indicating that the activation state of ERK1 is more affected by de-phosphorylation than ERK2.

In conclusion, I found the following:

1. ERK1 turnover is slower than ERK2, and this is due to its N-terminus, which probably impairs ERK1 facilitated diffusion mechanism;
2. ERK1 slower trafficking causes a longer residence time of ERK1 in the nucleus, which makes the kinase more vulnerable to the phosphatase action. Consequently, in the nucleus ERK1 is more dephosphorylated than ERK2;
3. the minor percentage of phosphorylated ERK1 (active form) makes ERK1 less capable of activating nuclear substrates and of inducing the cell cycle progression (Fig. Box 8.1).

I can conclude that ERK1 results to be less competent in activating nuclear targets respect to ERK2. This is caused by its N-terminus, which, by impairing the passage through the nuclear envelop, increases its residence time in the nucleus decreasing its state of activation.

CONCLUSIONS and FUTURE DIRECTIONS

I have studied the mechanisms at the basis of ERK regulation, focusing on the spatio-temporal patterns of ERK trafficking in living cells, by live imaging of fluorescently tagged proteins. I have then measured the nucleo-cytoplasmic shuttling of ERK1 and 2 finding out that ERK1 and 2 drastically differ in their capability of crossing the nuclear envelope and that this difference is caused by a short domain located at the N-terminus of ERK1. Since the nucleus is a site of inactivation for signaling originating at the cell membrane, the speed of permeation through the nuclear envelope is a critical determinant of the efficiency of the communication between cytoplasm and nucleus.

I have provided computational, biochemical and functional evidence that ERK1 and 2 have different signaling capabilities and I have showed that the rate of nucleo-cytoplasmic shuttling and its possible modulations are crucial regulators of signaling to the nucleus and represent a novel possible target for the molecular control of this pathway.

Furthermore, I have demonstrated that the N-terminus of ERK1 is necessary and sufficient to cause the differences of permeation and functional properties between ERK1 and 2. By directed mutagenesis I have identified some crucial residues responsible of the slow permeation of ERK1.

My data suggest that the N-terminus of ERK1 might represent a domain interacting with some not yet identified partner; it is probable that it could bind specific sites present on subunits of the nucleoporins, increasing the residence time inside the pore channel and slowing down ERK1 in respect to ERK2.

The next steps will be directed to identify the putative binding partners of ERK1 N-terminus, by using a combination of techniques of structural biology and biochemistry.

Computational methods, based on structural informations like crystallography and molecular dynamics, will be helpful to study the conformation of this terminal region in terms of stability, folding and steric hindrance. To date, only ERK2 has been crystallized (Zhang et al., 1994) and given that part of ERK1 N-terminus is completely absent in ERK2, I can only speculate with in silico models about the real configuration of this region. These studies will guide the future experiments, permitting to select specific targets restricting the enormous variety of possible interactions which could occur on this domain.

MATERIAL and METHODS

Plasmid preparation

GFP-ERK2 and YFP-ERK2

cDNA was obtained by one-step reverse transcription-polymerase chain reaction (RT-PCR), performed with a template on 100 ng of total RNA extract from rat brain.

Forward primer: 5'-ACGTCTCGAGATGCTGTGCAGCCAAC**ATG**G-3',
incorporating *XhoI* site (underlined) and the ERK2 ATG start codon (in bold);
Reverse primer: 5'-ACGTGGATCCT**TTA**AGATCTGTATCCTGGC-3'
incorporating *BamHI* site (underlined) and the ERK2 stop codon (in bold).

The amplification product was purified and cleaved with *XhoI/BamHI*, then it was ligated into the corresponding restriction sites in the Clontech vectors pEGFP-C2 and pEYFP-C1 to fuse the fluorescent reporter to the N-terminus of ERK2 (N-ERK).

A similar N-terminus fusion of mouse ERK2 with YFP (ATCC cat. N°9830384) was purchased from ATCC (American Type Culture Collection).

Verification of correct sequence and framing of all the engineered constructs used in this work was obtained from forward and reverse automated fluorescence sequencing.

ERK2-YFP

The C-terminal fusion protein was obtained by digesting with *XhoI* and *PstI* the plasmid pECFP-C1 (Clontech) carrying the fusion rat ERK2-EYFP in frame at the C-terminal of the ECFP. The fragment containing ERK2 was then ligated to the pEYFP-N1 vector (Clontech). Most experiments were performed with the N-terminal fusion with either GFP or YFP with identical results. Selected experiments were performed with the C-ERK fusion with identical results.

GFP-ERK1

cDNA was obtained by one step RT-PCR performed with a template on 100 ng of total RNA extract from rat brain.

Forward primer: 5'-ACGTCTCGAGCGCAGTGGAG**ATG**G-3', incorporating *XhoI* site (underlined) and the ERK1 ATG start codon (in bold).

Reverse primer: 5'-ACGTGGATCCTGC**TTA**GGGGGCCTCTGGTGC-3'
incorporating *BamHI* site (underlined) and the ERK1 stop codon (in bold).
The amplification product was purified and cleaved with *XhoI/BamHI*, then it was ligated to the corresponding restriction sites in the vector pEGFP-C2 (Clonetech) to produce the fusion of GFP at the N-terminus of rat ERK1.
A similar N-terminus fusion of mouse ERK1 with YFP (ATCC cat. N° 9891061) was purchased from ATCC (American Type Culture Collection).

ERK1-GFP

We produced a ERK1-GFP fusion at the C-terminus of ERK1 by amplifying ERK1 from the ATCC plasmid with following primers:
Forward primer: 5'-CCGCTCGAGAGCCAAC**ATG**GCGGCGGCG-3',
incorporating *Xho*I site (underlined) and the ERK1 ATG start codon;
Reverse primer: 5'-CGGGATCCGGGGCCCTCTGGCGCCC-3' incorporating *BamHI* site (underlined) and not carrying ERK1 stop codon.
The amplification product was purified, cleaved and ligated to the corresponding restriction site in the vector pEGFP-N3 (Clonetech). All crucial experiments were repeated using both the N- and C-terminal fusion proteins with identical results.

Swapped ERK clones

GFP-Δ^{39}E2

ERK2 mouse cDNA was amplified by PCR introducing an *ApaI* restriction site in the forward primer (underlined), upstream the kinase domain (aa 19-25):
Forward primer: 5'-AAGGGCCCGCGCTACACCACCCTCTC-3'
Reverse primer: 5'-CGGGATCC**TTA**AGATCTGTATCCTGGCTG-3'
BamHI site is underlined, the stop codon is displayed in bold. The amplified fragment was cloned in *ApaI/BamHI* of rat ERK2/EGFP-C2.

GFP-E1Δ^{39}

obtained by digesting *ApaI/BamHI* rat ERK1 cDNA and cloning it in pEGFP-C2

YFP-E1Δ^{7-39}

obtained by digesting *ApaI/BamHI* rat ERK1 cDNA and cloning it in pEYFP-C1 maintaining the aa 1-7 common to ERK1 and 2.

YFP-E1Δ^{27}

obtained by digesting *SmaI/BamHI* rat ERK1 cDNA and cloning it in pEYFP-C1.

YFP-E2Δ^{7}

obtained by digesting *ApaI/BamHI* rat ERK2 cDNA and cloning it in pEYFP-C1.

Deleted clones

GFP-ΔN_{1-39} and GFP-ΔN_{1-27}

obtained by digesting pEGFP-C2- rat ERK1 with *HindIII/BamHI* and cloning the extracted fragment of ERK into pEGFP-C2 by using the same restriction enzymes. Then the resulting construct was digested with *ApaI* (ΔN_{1-39}) or *SmaI* (ΔN_{1-27}) and the plasmid were ligated to let its re-circularization.

ΔN_{1-39}-GFP

obtained digesting the construct carrying ERK1 fused to the N-terminal of GFP (ERK1-GFP) with *XhoI/BamHI* and cloning the fragment of ERK N-terminus in pEGFP-N3 with the same restriction enzymes.

Mutagenized clones

Mutagenesis have been performed on the template the N-terminus of ERK1 E1Δ^{7-39} and ERK1-GFP by using the Quick Change Site-directed Mutagenesis Kit (n. cat. 200518, Stratagene) accordingly with the manufacture procedures. Pfu Turbo amplified the cDNA templates with the following primers (mutagenized bases are shown in bold):

Δ23-26

Forward primer: 5'-CTGCTGGGGTCGTC**...**GGGGAGGTGGAGG-3'

Reverse primer: 5'-CCTCCACCTCCCCG**...**GGGACCCCAGCAG-3'

It has been deleted 12 pb codifying for the aminoacid 23-26 (PVVP).

P23A

Forward primer: 5'-CTGCTGGGGTCGTC**G**CGGTGGTCCCCGG-3'

Reverse primer: 5'-CCGGGGACCA**C**CGCGACGGGAGCAG-3'

P23A-P26A

Forward primer: 5'-GCTGGGGTCGTC**G**CGGTGGTC**G**CCGGGGAGGTG-3'

Reverse primer: 5'-CACCTCCCCGG**C**GACCACCG**C**GACGACCCCAGC-3'

V31A-K33A

Forward primer: 5'-CGGGGAGGTGGAGG**C**GGTG**GC**GGGGCAGCCATTC-3'

Reverse primer:5'-CGAATGGATGCCCC**GC**CACC**G**CCTCCACCTCCCCG-3'

Cell culture and transfection

NIH 3T3 cell line were cultured in Dulbecco modified medium supplemented with 10% FBS and antibiotics (100 units/ml penicillin/streptomycin). Cells were plated on glass disks or on glass-bottomed dishes (Willco) at 60-70% confluence and transfected using Lipofectamin 2000 (Invitrogen), according to the manufacture procedures. After transfection cells were left undisturbed for 24 hrs before any further experimental manipulation. Starvation was obtained by keeping the cells for 24 hrs in 1% FBS.

Immunoblotting

Cultures of NIH 3T3 cell lines were growth to 90% confluence in Dulbecco modified medium supplemented with 10% FBS and antibiotics (100 units/ml penicillin/streptomycin) in 60 mm Petri dishes. Before treatments the cultures were starved for 24 h in 1% serum. In some experiments cells were treated with two mixtures of phosphatases inhibitors (P2850 and P5726, Sigma Aldrich). Cells were washed in cold PBS and lysed with 300 µl of RIPA buffer (1% Triton X-100, 0,5% Na deoxicolate, 0,1% SDS, 10% glycerol, 20 mM TrisHCL pH 8, 150 mM NaCl, 1mM EDTA, 1mM PMSF). Then, the samples were sonicated 3 times for 10 sec (Microsonics, ultrasonic cell disruptor) and boiled for 5 min in sample buffer. The same amount (around 10 µg) of cellular proteins were then subjected to SDS-PAGE in 10% gels and transferred to nitrocellulose membranes. Membranes were incubated 1 hour in TBS-Tween 20, containing 5% of non-fat dry milk and then exposed to a 1:1000 dilution of rabbit polyclonal antiserum anti-pERK (M-8159 Sigma) or anti-GFP (A1112, Invitrogen) at 4 C° over night. Membranes were washed and incubated with 1:3000 anti-mouse IgG (H+L) or anti-rabbit conjugated to horseradish peroxidase (Bio-Rad 170-6516) for 1 hour

at room temperature and finally revealed following the standard method for the chemiluminescence system (Bio-Rad). Gels have been exposed with the ChemiDoc analyzer and the output files were analyzed with Image J to obtain the density profiles of the bands. Quantification was performed by computing a Gaussian fit for the profiles after background subtraction. Linearity was checked by using calibration samples at known concentration of protein (Costa et al., 2006).

Immunoprecipitation, pMBP reaction and immunoblotting

NIH 3T3 cell line were cultured in 6 cm diameter petri dish at 80% of confluency and they were transfected with the vectors described in the paragraph "Plasmid preparation", by using Lipofectamine 2000 (11668-027, Invitrogen). The next day, cells were stimulated with 10% serum for 10 minutes, then they were washed in cold PBS and lysed with 0.5 ml of Triton lysis buffer (10 mM phosphate buffer, pH 7.4; 100 mM NaCl; 1% Triton X-100; 5mM EDTA) containing 1mM PMSF and 1mM of phosphatase inhibitor 1 and 2 (P2850 and P5726, Sigma Aldrich). The samples were sonicated three times for 10 sec (Microsonics, ultrasonic cell disruptor) and then they were centrifuged at 4°C 10000 rpm. The supernatant were incubated 1 hour at 4°C with 50 µl of protein A-Sepharose 4B conjugate (10-1041 Zymed Laboratories, Invitogen) for a pre-clear step. The samples were then centrifuged 1 minute at 700 rpm, 4°C and the supernatants were incubated with 1 µg of antibody anti-GFP (A1112, Invitrogen) on a rotating wheel at 4 °C O/N. The next day 50 µl protein A-Sepharose were added to each sample on a rotating wheel 1 hour at 4°C and afterwards, the samples were washed three times in 10% lysis buffer in PBS 1x.

The protein A-Sepharose conjugated with our fusion proteins were splitted in two aliquots for each sample, used respectively to assay the ERK1/2 phosphorylation and MBP activation.

<u>ERK1/2 phosphorylation</u>

Samples were assayed by western blot, following the standard procedures, and probed with anti p-ERK1/2 (M-8159 Sigma). These nitrocellulose filters were then stripped and re-probed with the anti-ERK1/2 (sc-153, Santa Cruz) to check for the overall protein amount.

pMBP assay

Samples were assayed to measure the phospho-transferase activity of our fusion proteins on Myelin Binding Protein (MBP), by using the pMBP assay (17-191, Upstate). The reactions were worked out accordingly to the manufacture procedures; In brief, the immunoprecipitated samples of active ERK preparations were mixed with Mg^{2+}/ATP cocktail, the Assay Diluition Buffer I (ADBI, n. cat. 20-108, Upstate) and the MAPK substrate cocktail II (n. cat. 20-166, Upstate); then, the reaction mixtures were incubated for 20-30 min in a 30°C shaking incubator. Samples were then analyzed by immunoblot probed using 1 µg/ml anti-phospho-MBP, clone p12 (n. cat. 20-113, Upstate).

Immunofluorescence

Mouse fibroblasts NIH3T3 were fixed in Tris buffer containing 4% formaldehyde, 1 mM orthovanadate and 30% saccarose, at room temperature for 10 minutes, then they were washed three times and kept in blocking solution (0.4% Triton X-100, 10% bovine serum albumin (BSA), 10 Mm Tris and 1 mM sodium orthovanadate) 30' at RT.

Cells transfected with ERK constructs were incubated overnight with a phospho-specific ERK1/2 antibody (dilution 1:1000, Sigma M-8159) in blocking solution at 4°C. The reaction was completed by incubation for 2 hrs in secondary antibody (Alexa Fluor 546, Molecular Probes). Hoechst 33258 was used to visualize the nucleus localization.

Calibration of protein concentration

I estimated the concentration of ERK-GFP by comparing the fluorescence of the cells with artificial cells loaded with known concentrations of EGFP. Recombinant EGFP was diluted at decreasing concentrations in saline solution. The micelles were prepared by dispersing the solution in mineral oil. Imaging was performed on the confocal microscope in controlled conditions to ensure applicability of the calibration to the experiments in living cells. Figure Met.1A shows three images of micelles at three different concentrations; quantification has been performed in the central part of the micelles to avoid spurious effects because of microlensing. Images are shown in false colours to enhance differences in brightness.

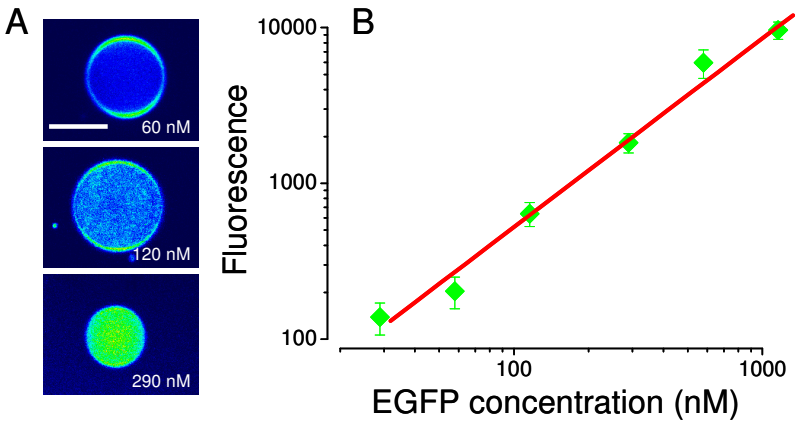

Figure Met.1
A) Images of three GFP-including micelles at different concentration. Bar, 10 µm.
B) Calibration at 6 different GFP concentration (cumulative data); fitted by a linear function.

Calibration data has been done for six different concentrations (Fig. Met.1.B). Each point is the average of at least ten measures (30 at the three lower concentrations). These measures are relative to the FV 300 microscope. Each microscope used in the study required a specific calibration curve.

Fluorescence-based recordings

Imaging experiments were performed on an Olympus Fluoview 300 or on a Leica SL confocal scanning microscope equipped with high numerical aperture objectives (Olympus water immersion 60x, 0.9 NA; Leica oil immersion HCX PL Apo 63x, 1.4 NA). In all experiments GFP fluorescence was excited at 488 nm with an Ar/K laser. In average, the laser power employed during imaging was about 30 µW. Coverslips were placed in a recording chamber that were firmly locked on the microscope stage and kept at 37°C.

All data plotting and statistical testing (one- or two-way *t*-test) have been performed with Origin 7 package. Other statistical tests were used where appropriate. Quality of fits was given by the correlation coefficient *R*.

Acquisition of pERK immunohistochemistry

Acquisitions were performed on randomly chosen fields by blind operators. Images were acquired on the Olympus Fluoview 300 microscope; this unit was equipped with visible light and with an infrared laser for 2-photon excitation (Verdi-Mira; Coherent). Combined imaging of pERK immunofluorescence and ERK2-GFP fluorescence was performed separately for the two channels to minimize cross talk. Quantification of fluorescence was performed either on the Fluoview platform or with custom software. Cells were carefully selected by measuring the fluorescence of ERK2-GFP; cells characterized by medium-high levels of expression were avoided. Given the weak fluorescence and the need to contain photobleaching, we optimized detection sensitivity by fully opening the confocal aperture and using a wide-emission bandpass. These conditions caused the frequent presence of fluorescent debris over imposed on the cells. During quantification of fluorescence these points were avoided. Average fluorescence background was evaluated on non transfected cells and was subtracted from all measurements. To evaluate the degree of nuclear localization we measured the average fluorescence of the nucleus (F_{Nuc}) and of a surrounding ring of thickness approximately equal to the nucleus radius (F_{Ring}). The CI was computed as:

$$CI = (F_{Nuc} - BG)/(F_{Ring} - BG)$$

where *BG* was the average background. All images shown in the study have been subjected only to linear adjustments.

FRAP experiments: nucleus-cytoplasm shuttling

Photobleaching was preceded by the acquisition of a pre-bleach image that was used to estimate the loss of fluorescence due to bleaching and for data normalization.

The nucleus of the cell was photobleached by repeated scans along a line centred on the nucleus at high laser power. Bleaching was applied for approximately 5 s, which was sufficient to quench most of the nuclear fluorescence. Bleaching was followed by time-lapse acquisition to measure the recovery (60 frames at 5 s intervals for ERK2 and 60 frames at 20 s intervals for ERK1).

In all the cases recovery was described by the function:

$$F(t) = \frac{F_{Tot}^{PB}}{F_{Nuc}^{PB}} \cdot \frac{F_{Nuc}(t)}{F_{Tot}(t)}$$

where F_{PB} indicates the fluorescence (corrected for background) measured before bleach in the nucleus (*Nuc*) or on the entire cell (*Tot*). This normalization corrects for bleaching caused by imaging (Phair and Misteli, 2000). In the absence of an immobile fraction, the formula has an asymptotic value of 1. The recovery of all imaged cells was accurately fitted with a single exponential defined by the time constant (τ) of shuttling and by the Immobile Fraction (IF=1-asymptotic value).

FRAP experiments: spot photobleaching

Spot photobleaching was attained by flashing a diffraction-limited spot (1µm) in a fixed central position in the nucleus for 250 ms. Recovery was measured in a time-lapse sequence imaged immediately afterwards on a Leica TCS NT microscope. Owing to the technical limitations of the scanning-head, the shortest interval elapsing from the end of bleaching until the beginning of recovery was 0.71 seconds, as determined by direct measurements with a photodiode. This delay prevented a meaningful measurement of the recovery of freely diffusible GFP in the nuclear compartment. The spatial profile of the bleached area was measured on fixed cells bleached in the same conditions as in the in vivo experiments. Normalized fluorescence was fitted by the equation provided by Axelrod et al. (Axelrod et al., 1976):

$$F(X) = e^{-Ke^{-(XW)2}}$$

where *K* defines the depth of the photobleaching and *w* its width. The mean values for these parameters were found to be K=1.63±0.10, w=2.02±0.18 µm (n=8). The effective diffusion coefficient D_{eff} was computed by fitting the recovery data to an approximate solution of the diffusion equation (Feder et al., 1996):

$$I(t) = \frac{I_0 + I_\infty \, t/t_{1/2}}{1 + t/t_{1/2}}$$

where I_0 and I_∞ are the fluorescence intensity at time zero and at the asymptote. The time to half recovery $t_{1/2}$ depends on the diffusion coefficient D_{eff}, and on the width w of the bleaching through the relationship:

$$t_{1/2} = \frac{w^2 \gamma}{2 D_{eff}}$$

where the factor γ is a weak function of the beam shape and of the bleach depth K; in our experiments γ=1.1 (Axelrod et al., 1976; Carrero et al., 2003).

Strip-FRAP

Photobleaching was preceded by the acquisition of 64 lines necessary for data normalization. The total fluorescence bleached in the imaging run was estimated by comparing a pre-bleach image of the nucleus with an image acquired at the end of the line scans. Bleaching was performed by scanning the line at high power (about 50 times larger than during pre bleach and recovery) for 160 ms. Line scan was performed at a frequency of 200 Hz and the recovery was evaluated for 2 min. Fluorescence is corrected for background and normalized for the corresponding pre-bleached regions.

Recovery curves were fitted by a double exponential function. The immobile fraction was computed by the asymptotic value of the recovery corrected for the total amount of fluorescence loss, as estimated by the comparison of the pre-bleach and post-bleach images.

Modelling

To understand how the speed of nucleo-cytoplasmic trafficking influence the equilibrium of the activation/inactivation balance of ERK we modelled the ERK system considering that the protein equilibrates among 4 different states

regulated by first order kinetics. The simulator computes the temporal evolution of the system starting from arbitrary initial conditions by means of a Montecarlo methods. In brief, the system is modelled as a collection of particles that can exists in any of the following states: ERK_{Cyt}, $pERK_{Cyt}$, ERK_{Nuc} and $pERK_{Nuc}$. At each time point of the simulation each particle can undergo the transitions admitted by its present state or remain in the present state. The probability of each transition is given by the rate (probability per second) divided by the temporal resolution of the sequence. A random number generator is utilized to decide the particle fate. The data presented have been computed on a system with 10000 particles simulated with a time resolution of 1 s and for a duration of 5000 iterations. This time was sufficient to allow a complete evolution of the system to the equilibrium condition. Convergence to a unique solution was verified as the final state was independent on the values of the initial conditions. At least 4 simulation runs were used for each set of conditions.

BIBLIOGRAPHY

Abbott, D.W., and J.T. Holt. 1999. Mitogen-activated protein kinase kinase 2 activation is essential for progression through the G2/M checkpoint arrest in cells exposed to ionizing radiation. *J Biol Chem*. 274:2732-42.

Aberg, E., M. Perander, B. Johansen, C. Julien, S. Meloche, S.M. Keyse, and O.M. Seternes. 2006. Regulation of MAPK-activated protein kinase 5 activity and subcellular localization by the atypical MAPK ERK4/MAPK4. *J Biol Chem*. 281:35499-510.

Adachi, M., M. Fukuda, and E. Nishida. 1999. Two co-existing mechanisms for nuclear import of MAP kinase: passive diffusion of a monomer and active transport of a dimer. *Embo J*. 18:5347-58.

Adachi, M., M. Fukuda, and E. Nishida. 2000. Nuclear export of MAP kinase (ERK) involves a MAP kinase kinase (MEK)-dependent active transport mechanism. *J Cell Biol*. 148:849-56.

Akaike, M., W. Che, N.L. Marmarosh, S. Ohta, M. Osawa, B. Ding, B.C. Berk, C. Yan, and J. Abe. 2004. The hinge-helix 1 region of peroxisome proliferator-activated receptor gamma1 (PPARgamma1) mediates interaction with extracellular signal-regulated kinase 5 and PPARgamma1 transcriptional activation: involvement in flow-induced PPARgamma activation in endothelial cells. *Mol Cell Biol*. 24:8691-704.

Alessi, D.R., Y. Saito, D.G. Campbell, P. Cohen, G. Sithanandam, U. Rapp, A. Ashworth, C.J. Marshall, and S. Cowley. 1994. Identification of the sites in MAP kinase kinase-1 phosphorylated by p74raf-1. *Embo J*. 13:1610-9.

Anderton, B.H., J. Betts, W.P. Blackstock, J.P. Brion, S. Chapman, J. Connell, R. Dayanandan, J.M. Gallo, G. Gibb, D.P. Hanger, M. Hutton, E. Kardalinou, K. Leroy, S. Lovestone, T. Mack, C.H. Reynolds, and M. Van Slegtenhorst. 2001. Sites of phosphorylation in tau and factors affecting their regulation. *Biochem Soc Symp*:73-80.

Ando, R., H. Mizuno, and A. Miyawaki. 2004. Regulated fast nucleocytoplasmic shuttling observed by reversible protein highlighting. *Science*. 306:1370-3.

Atwal, J.K., B. Massie, F.D. Miller, and D.R. Kaplan. 2000. The TrkB-Shc site signals neuronal survival and local axon growth via MEK and P13-kinase. *Neuron*. 27:265-77.

Avruch, J., X.F. Zhang, and J.M. Kyriakis. 1994. Raf meets Ras: completing the framework of a signal transduction pathway. *Trends Biochem Sci*. 19:279-83.

Axelrod, D., D.E. Koppel, J. Schlessinger, E. Elson, and W.W. Webb. 1976. Mobility measurement by analysis of fluorescence photobleaching recovery kinetics. *Biophys J*. 16:1055-69.

Balan, V., D.T. Leicht, J. Zhu, K. Balan, A. Kaplun, V. Singh-Gupta, J. Qin, H. Ruan, M.J. Comb, and G. Tzivion. 2006. Identification of novel in vivo Raf-1 phosphorylation sites mediating positive feedback Raf-1 regulation by extracellular signal-regulated kinase. *Mol Biol Cell*. 17:1141-53.

Balmanno, K., and S.J. Cook. 1999. Sustained MAP kinase activation is required for the expression of cyclin D1, p21Cip1 and a subset of AP-1 proteins in CCL39 cells. *Oncogene*. 18:3085-97.

Bannister, A.J., and T. Kouzarides. 1995. CBP-induced stimulation of c-Fos activity is abrogated by E1A. *Embo J*. 14:4758-62.

Barnier, J.V., C. Papin, A. Eychene, O. Lecoq, and G. Calothy. 1995. The mouse B-raf gene encodes multiple protein isoforms with tissue-specific expression. *J Biol Chem*. 270:23381-9.

Bassell, G.J., H. Zhang, A.L. Byrd, A.M. Femino, R.H. Singer, K.L. Taneja, L.M. Lifshitz, I.M. Herman, and K.S. Kosik. 1998. Sorting of beta-actin mRNA and protein to neurites and growth cones in culture. *J Neurosci*. 18:251-65.

Bayliss, R., A.H. Corbett, and M. Stewart. 2000. The molecular mechanism of transport of macromolecules through nuclear pore complexes. *Traffic*. 1:448-56.

Beck, M., F. Forster, M. Ecke, J.M. Plitzko, F. Melchior, G. Gerisch, W. Baumeister, and O. Medalia. 2004. Nuclear pore complex structure and dynamics revealed by cryoelectron tomography. *Science*. 306:1387-90.

Belanger, L.F., S. Roy, M. Tremblay, B. Brott, A.M. Steff, W. Mourad, P. Hugo, R. Erikson, and J. Charron. 2003. Mek2 is dispensable for mouse growth and development. *Mol Cell Biol*. 23:4778-87.

Bhalla, U.S., and R. Iyengar. 1999. Emergent properties of networks of biological signaling pathways. *Science*. 283:381-7.

Bhalla, U.S., P.T. Ram, and R. Iyengar. 2002. MAP kinase phosphatase as a locus of flexibility in a mitogen-activated protein kinase signaling network. *Science*. 297:1018-23.

Blume-Jensen, P., and T. Hunter. 2001. Oncogenic kinase signalling. *Nature*. 411:355-65.

Bogoyevitch, M.A., and N.W. Court. 2004. Counting on mitogen-activated protein kinases-ERKs 3, 4, 5, 6, 7 and 8. *Cell Signal*. 16:1345-54.

Bos, J.L. 1989. ras oncogenes in human cancer: a review. *Cancer Res*. 49:4682-9.

Boulton, T.G., S.H. Nye, D.J. Robbins, N.Y. Ip, E. Radziejewska, S.D. Morgenbesser, R.A. DePinho, N. Panayotatos, M.H. Cobb, and G.D. Yancopoulos. 1991. ERKs: a family of protein-serine/threonine kinases that are activated and tyrosine phosphorylated in response to insulin and NGF. *Cell*. 65:663-75.

Brondello, J.M., A. Brunet, J. Pouyssegur, and F.R. McKenzie. 1997. The dual specificity mitogen-activated protein kinase phosphatase-1 and -2 are induced by the p42/p44MAPK cascade. *J Biol Chem*. 272:1368-76.

Brondello, J.M., J. Pouyssegur, and F.R. McKenzie. 1999. Reduced MAP kinase phosphatase-1 degradation after p42/p44MAPK-dependent phosphorylation. *Science*. 286:2514-7.

Brott, B.K., A. Alessandrini, D.A. Largaespada, N.G. Copeland, N.A. Jenkins, C.M. Crews, and R.L. Erikson. 1993. MEK2 is a kinase related to MEK1 and is differentially expressed in murine tissues. *Cell Growth Differ*. 4:921-9.

Brunet, A., and J. Pouyssegur. 1996. Identification of MAP kinase domains by redirecting stress signals into growth factor responses. *Science*. 272:1652-5.

Brunet, A., D. Roux, P. Lenormand, S. Dowd, S. Keyse, and J. Pouyssegur. 1999. Nuclear translocation of p42/p44 mitogen-activated protein kinase is required for growth factor-induced gene expression and cell cycle entry. *Embo J*. 18:664-74.

Brunner, D., K. Ducker, N. Oellers, E. Hafen, H. Scholz, and C. Klambt. 1994. The ETS domain protein pointed-P2 is a target of MAP kinase in the sevenless signal transduction pathway. *Nature*. 370:386-9.

Burack, W.R., and A.S. Shaw. 2005. Live Cell Imaging of ERK and MEK: simple binding equilibrium explains the regulated nucleocytoplasmic distribution of ERK. *J Biol Chem*. 280:3832-7.

Buschbeck, M., and A. Ullrich. 2005. The unique C-terminal tail of the mitogen-activated protein kinase ERK5 regulates its activation and nuclear shuttling. *J Biol Chem*. 280:2659-67.

Campbell, D.S., and C.E. Holt. 2003. Apoptotic pathway and MAPKs differentially regulate chemotropic responses of retinal growth cones. *Neuron*. 37:939-52.

Camps, M., A. Nichols, and S. Arkinstall. 2000. Dual specificity phosphatases: a gene family for control of MAP kinase function. *Faseb J*. 14:6-16.

Camps, M., A. Nichols, C. Gillieron, B. Antonsson, M. Muda, C. Chabert, U. Boschert, and S. Arkinstall. 1998. Catalytic activation of the phosphatase MKP-3 by ERK2 mitogen-activated protein kinase. *Science*. 280:1262-5.

Carragher, N.O., M.A. Westhoff, V.J. Fincham, M.D. Schaller, and M.C. Frame. 2003. A novel role for FAK as a protease-targeting adaptor protein: regulation by p42 ERK and Src. *Curr Biol*. 13:1442-50.

Carrero, G., D. McDonald, E. Crawford, G. de Vries, and M.J. Hendzel. 2003. Using FRAP and mathematical modeling to determine the in vivo kinetics of nuclear proteins. *Methods*. 29:14-28.

Chalfie, M., Y. Tu, G. Euskirchen, W.W. Ward, and D.C. Prasher. 1994. Green fluorescent protein as a marker for gene expression. *Science*. 263:802-5.

Charles, C.H., A.S. Abler, and L.F. Lau. 1992. cDNA sequence of a growth factor-inducible immediate early gene and characterization of its encoded protein. *Oncogene*. 7:187-90.

Chen, D.Y., J.A. Deutsch, M.F. Gonzalez, and Y. Gu. 1993a. The induction and suppression of c-fos expression in the rat brain by cholecystokinin and its antagonist L364,718. *Neurosci Lett*. 149:91-4.

Chen, R.H., J. Chung, and J. Blenis. 1991. Regulation of pp90rsk phosphorylation and S6 phosphotransferase activity in Swiss 3T3 cells by growth factor-, phorbol ester-, and cyclic AMP-mediated signal transduction. *Mol Cell Biol*. 11:1861-7.

Chen, R.H., C. Sarnecki, and J. Blenis. 1992. Nuclear localization and regulation of erk- and rsk-encoded protein kinases. *Mol Cell Biol*. 12:915-27.

Chen, R.H., R. Tung, C. Abate, and J. Blenis. 1993b. Cytoplasmic to nuclear signal transduction by mitogen-activated protein kinase and 90 kDa ribosomal S6 kinase. *Biochem Soc Trans*. 21:895-900.

Chen, Y., J.D. Muller, Q. Ruan, and E. Gratton. 2002. Molecular brightness characterization of EGFP in vivo by fluorescence fluctuation spectroscopy. *Biophys J*. 82:133-44.

Chong, H., H.G. Vikis, and K.L. Guan. 2003. Mechanisms of regulating the Raf kinase family. *Cell Signal*. 15:463-9.

Chou, F.L., J.M. Hill, J.C. Hsieh, J. Pouyssegur, A. Brunet, A. Glading, F. Uberall, J.W. Ramos, M.H. Werner, and M.H. Ginsberg. 2003. PEA-15 binding to ERK1/2 MAPKs is required for its modulation of integrin activation. *J Biol Chem*. 278:52587-97.

Chuderland, D., A. Konson, and R. Seger. 2008. Identification and characterization of a general nuclear translocation signal in signaling proteins. *Mol Cell*. 31:850-61.

Chuderland, D., and R. Seger. 2005. Protein-protein interactions in the regulation of the extracellular signal-regulated kinase. *Mol Biotechnol*. 29:57-74.

Chung, J., C.J. Kuo, G.R. Crabtree, and J. Blenis. 1992. Rapamycin-FKBP specifically blocks growth-dependent activation of and signaling by the 70 kd S6 protein kinases. *Cell*. 69:1227-36.

Cohen, P. 1997. The search for physiological substrates of MAP and SAP kinases in mammalian cells. *Trends Cell Biol*. 7:353-61.

Colanzi, A., T.J. Deerinck, M.H. Ellisman, and V. Malhotra. 2000. A specific activation of the mitogen-activated protein kinase kinase 1 (MEK1) is required for Golgi fragmentation during mitosis. *J Cell Biol*. 149:331-9.

Cole, N.B., C.L. Smith, N. Sciaky, M. Terasaki, M. Edidin, and J. Lippincott-Schwartz. 1996. Diffusional mobility of Golgi proteins in membranes of living cells. *Science*. 273:797-801.

Cooper JA, Sefton MB, Hunter T. Diverse mitogenic agents induce the phosphorylation of two related 42,000-dalton proteins on tyrosine in quiescent chick cells. *Mol. Cell. Biol* 1984;4:30–37.

Cooper JA, Hunter T. Major substrate for growth factor-activated protein-tyrosine kinases is a lowabundance protein. *Mol Cell Biol* 1985;5:3304–3309.

Costa, M., M. Marchi, F. Cardarelli, A. Roy, F. Beltram, L. Maffei, and G.M. Ratto. 2006. Dynamic regulation of ERK2 nuclear translocation and mobility in living cells. *J Cell Sci*. 119:4952-63.

Cowley, S., H. Paterson, P. Kemp, and C.J. Marshall. 1994. Activation of MAP kinase kinase is necessary and sufficient for PC12 differentiation and for transformation of NIH 3T3 cells. *Cell*. 77:841-52.

Cuevas, B.D., A.N. Abell, J.A. Witowsky, T. Yujiri, N.L. Johnson, K. Kesavan, M. Ware, P.L. Jones, S.A. Weed, R.L. DeBiasi, Y. Oka, K.L. Tyler, and G.L. Johnson. 2003. MEKK1 regulates calpain-dependent proteolysis of focal adhesion proteins for rear-end detachment of migrating fibroblasts. *Embo J*. 22:3346-55.

Dalby, K.N., N. Morrice, F.B. Caudwell, J. Avruch, and P. Cohen. 1998. Identification of regulatory phosphorylation sites in mitogen-activated protein kinase (MAPK)-activated protein kinase-1a/p90rsk that are inducible by MAPK. *J Biol Chem*. 273:1496-505.

Davies, H., G.R. Bignell, C. Cox, P. Stephens, S. Edkins, S. Clegg, J. Teague, H. Woffendin, M.J. Garnett, W. Bottomley, N. Davis, E. Dicks, R. Ewing, Y. Floyd, K. Gray, S. Hall, R. Hawes, J. Hughes, V. Kosmidou, A. Menzies, C. Mould, A. Parker, C. Stevens, S. Watt, S. Hooper, R. Wilson, H. Jayatilake, B.A. Gusterson, C. Cooper, J. Shipley, D. Hargrave, K. Pritchard-Jones, N. Maitland, G. Chenevix-Trench, G.J. Riggins, D.D. Bigner, G. Palmieri, A. Cossu, A. Flanagan, A. Nicholson, J.W. Ho, S.Y. Leung, S.T. Yuen, B.L. Weber, H.F. Seigler, T.L. Darrow, H. Paterson, R. Marais, C.J. Marshall, R. Wooster, M.R. Stratton, and P.A. Futreal. 2002. Mutations of the BRAF gene in human cancer. *Nature*. 417:949-54.

Dayel, M.J., E.F. Hom, and A.S. Verkman. 1999. Diffusion of green fluorescent protein in the aqueous-phase lumen of endoplasmic reticulum. *Biophys J*. 76:2843-51.

Deak, M., A.D. Clifton, L.M. Lucocq, and D.R. Alessi. 1998. Mitogen- and stress-activated protein kinase-1 (MSK1) is directly activated by MAPK and SAPK2/p38, and may mediate activation of CREB. *Embo J*. 17:4426-41.

Di Fiore, P.P., and G.N. Gill. 1999. Endocytosis and mitogenic signaling. *Curr Opin Cell Biol*. 11:483-8.

Dickinson, R.J., and S.M. Keyse. 2006. Diverse physiological functions for dual-specificity MAP kinase phosphatases. *J Cell Sci*. 119:4607-15.

Dobrowolski, S., M. Harter, and D.W. Stacey. 1994. Cellular ras activity is required for passage through multiple points of the G0/G1 phase in BALB/c 3T3 cells. *Mol Cell Biol*. 14:5441-9.

Dougherty, M.K., J. Muller, D.A. Ritt, M. Zhou, X.Z. Zhou, T.D. Copeland, T.P. Conrads, T.D. Veenstra, K.P. Lu, and D.K. Morrison. 2005. Regulation of Raf-1 by direct feedback phosphorylation. *Mol Cell*. 17:215-24.

Dourdin, N., A.K. Bhatt, P. Dutt, P.A. Greer, J.S. Arthur, J.S. Elce, and A. Huttenlocher. 2001. Reduced cell migration and disruption of the actin cytoskeleton in calpain-deficient embryonic fibroblasts. *J Biol Chem*. 276:48382-8.

Douville, E., and J. Downward. 1997. EGF induced SOS phosphorylation in PC12 cells involves P90 RSK-2. *Oncogene*. 15:373-83.

Downward, J., Y. Yarden, E. Mayes, G. Scrace, N. Totty, P. Stockwell, A. Ullrich, J. Schlessinger, and M.D. Waterfield. 1984. Close similarity of epidermal growth factor receptor and v-erb-B oncogene protein sequences. *Nature*. 307:521-7.

Doye, V., and E. Hurt. 1997. From nucleoporins to nuclear pore complexes. *Curr Opin Cell Biol*. 9:401-11.

Eblen, S.T., A.D. Catling, M.C. Assanah, and M.J. Weber. 2001. Biochemical and biological functions of the N-terminal, noncatalytic domain of extracellular signal-regulated kinase 2. *Mol Cell Biol*. 21:249-59.

Eblen, S.T., J.K. Slack-Davis, A. Tarcsafalvi, J.T. Parsons, M.J. Weber, and A.D. Catling. 2004. Mitogen-activated protein kinase feedback phosphorylation regulates MEK1 complex formation and activation during cellular adhesion. *Mol Cell Biol*. 24:2308-17.

Edidin, M. 1992. Patches, posts and fences: proteins and plasma membrane domains. *Trends Cell Biol*. 2:376-80.

Edidin, M., M.C. Zuniga, and M.P. Sheetz. 1994. Truncation mutants define and locate cytoplasmic barriers to lateral mobility of membrane glycoproteins. *Proc Natl Acad Sci U S A*. 91:3378-82.

Ellenberg, J., E.D. Siggia, J.E. Moreira, C.L. Smith, J.F. Presley, H.J. Worman, and J. Lippincott-Schwartz. 1997. Nuclear membrane dynamics and reassembly in living cells: targeting of an inner nuclear membrane protein in interphase and mitosis. *J Cell Biol*. 138:1193-206.

Fagotto, F., U. Gluck, and B.M. Gumbiner. 1998. Nuclear localization signal-independent and importin/karyopherin-independent nuclear import of beta-catenin. *Curr Biol*. 8:181-90.

Favata, M.F., K.Y. Horiuchi, E.J. Manos, A.J. Daulerio, D.A. Stradley, W.S. Feeser, D.E. Van Dyk, W.J. Pitts, R.A. Earl, F. Hobbs, R.A. Copeland, R.L. Magolda, P.A. Scherle, and J.M. Trzaskos. 1998. Identification of a novel inhibitor of mitogen-activated protein kinase kinase. *J Biol Chem*. 273:18623-32.

Feder, T.J., I. Brust-Mascher, J.P. Slattery, B. Baird, and W.W. Webb. 1996. Constrained diffusion or immobile fraction on cell surfaces: a new interpretation. *Biophys J*. 70:2767-73.

Ferraro, E., D. Peluso, A. Via, G. Ausiello, and M. Helmer-Citterich. 2007. SH3-Hunter: discovery of SH3 domain interaction sites in proteins. *Nucleic Acids Res*. 35:W451-4.

Ferrell, J.E., Jr., and R.R. Bhatt. 1997. Mechanistic studies of the dual phosphorylation of mitogen-activated protein kinase. *J Biol Chem*. 272:19008-16.

Formstecher, E., J.W. Ramos, M. Fauquet, D.A. Calderwood, J.C. Hsieh, B. Canton, X.T. Nguyen, J.V. Barnier, J. Camonis, M.H. Ginsberg, and H. Chneiweiss. 2001. PEA-15 mediates cytoplasmic sequestration of ERK MAP kinase. *Dev Cell*. 1:239-50.

Fukuda, M., I. Gotoh, Y. Gotoh, and E. Nishida. 1996. Cytoplasmic localization of mitogen-activated protein kinase kinase directed by its NH2-terminal, leucine-rich short amino acid sequence, which acts as a nuclear export signal. *J Biol Chem*. 271:20024-8.

Fukuda M, Gotoh I, Adachi M, Gotoh Y, Nishida E. A novel regulatory mechanism in the mitogen-activated protein (MAP) kinase cascade. Role of nuclear export signal of MAP kinase kinase. *J Biol Chem.* 1997 Dec 19;272(51):32642-8.

Fukuda, M., Y. Gotoh, and E. Nishida. 1997. Interaction of MAP kinase with MAP kinase kinase: its possible role in the control of nucleocytoplasmic transport of MAP kinase. *Embo J*. 16:1901-8.

Gavin, A.C., and A.R. Nebreda. 1999. A MAP kinase docking site is required for phosphorylation and activation of p90(rsk)/MAPKAP kinase-1. *Curr Biol*. 9:281-4.

Gille, H., M. Kortenjann, T. Strahl, and P.E. Shaw. 1996. Phosphorylation-dependent formation of a quaternary complex at the c-fos SRE. *Mol Cell Biol*. 16:1094-102.

Gilmore T, Martin GS. Phorbol ester and diacylglycerol induces protein phosphorylation at tyrosine. *Nature* 1983;306:47–87.

Glading, A., R.J. Bodnar, I.J. Reynolds, H. Shiraha, L. Satish, D.A. Potter, H.C. Blair, and A. Wells. 2004. Epidermal growth factor activates m-calpain (calpain II), at least in part, by extracellular signal-regulated kinase-mediated phosphorylation. *Mol Cell Biol*. 24:2499-512.

Goold, R.G., and P.R. Gordon-Weeks. 2005. The MAP kinase pathway is upstream of the activation of GSK3beta that enables it to phosphorylate MAP1B and contributes to the stimulation of axon growth. *Mol Cell Neurosci*. 28:524-34.

Gotoh, Y., E. Nishida, T. Yamashita, M. Hoshi, M. Kawakami, and H. Sakai. 1990. Microtubule-associated-protein (MAP) kinase activated by nerve growth factor and epidermal growth factor in PC12 cells. Identity with the mitogen-activated MAP kinase of fibroblastic cells. *Eur J Biochem*. 193:661-9.

Grote, M., U. Kubitscheck, R. Reichelt, and R. Peters. 1995. Mapping of nucleoporins to the center of the nuclear pore complex by post-embedding immunogold electron microscopy. *J Cell Sci*. 108 (Pt 9):2963-72.

Halazonetis, T.D., K. Georgopoulos, M.E. Greenberg, and P. Leder. 1988. c-Jun dimerizes with itself and with c-Fos, forming complexes of different DNA binding affinities. *Cell*. 55:917-24.

Heim, R., D.C. Prasher, and R.Y. Tsien. 1994. Wavelength mutations and posttranslational autoxidation of green fluorescent protein. *Proc Natl Acad Sci U S A*. 91:12501-4.

Henrich, L.M., J.A. Smith, D. Kitt, T.M. Errington, B. Nguyen, A.M. Traish, and D.A. Lannigan. 2003. Extracellular signal-regulated kinase 7, a regulator of hormone-dependent estrogen receptor destruction. *Mol Cell Biol*. 23:5979-88.

Hill, C.S., and R. Treisman. 1995. Transcriptional regulation by extracellular signals: mechanisms and specificity. *Cell*. 80:199-211.

Hipskind, R.A., M. Baccarini, and A. Nordheim. 1994. Transient activation of RAF-1, MEK, and ERK2 coincides kinetically with ternary complex factor phosphorylation and immediate-early gene promoter activity in vivo. *Mol Cell Biol*. 14:6219-31.

Hoshino, R., Y. Chatani, T. Yamori, T. Tsuruo, H. Oka, O. Yoshida, Y. Shimada, S. Ari-i, H. Wada, J. Fujimoto, and M. Kohno. 1999. Constitutive activation of the 41-/43-kDa mitogen-activated protein kinase signaling pathway in human tumors. *Oncogene*. 18:813-22.

Huang, C.Y., and J.E. Ferrell, Jr. 1996. Ultrasensitivity in the mitogen-activated protein kinase cascade. *Proc Natl Acad Sci U S A*. 93:10078-83.

Huang, W., A. Alessandrini, C.M. Crews, and R.L. Erikson. 1993. Raf-1 forms a stable complex with Mek1 and activates Mek1 by serine phosphorylation. *Proc Natl Acad Sci U S A*. 90:10947-51.

Hughes, P.E., M.W. Renshaw, M. Pfaff, J. Forsyth, V.M. Keivens, M.A. Schwartz, and M.H. Ginsberg. 1997. Suppression of integrin activation: a novel function of a Ras/Raf-initiated MAP kinase pathway. *Cell*. 88:521-30.

Hunger-Glaser, I., E.P. Salazar, J. Sinnett-Smith, and E. Rozengurt. 2003. Bombesin, lysophosphatidic acid, and epidermal growth factor rapidly stimulate focal adhesion kinase phosphorylation at Ser-910: requirement for ERK activation. *J Biol Chem*. 278:22631-43.

Huttenlocher, A., M.H. Ginsberg, and A.F. Horwitz. 1996. Modulation of cell migration by integrin-mediated cytoskeletal linkages and ligand-binding affinity. *J Cell Biol*. 134:1551-62.

Huttenlocher, A., S.P. Palecek, Q. Lu, W. Zhang, R.L. Mellgren, D.A. Lauffenburger, M.H. Ginsberg, and A.F. Horwitz. 1997. Regulation of cell migration by the calcium-dependent protease calpain. *J Biol Chem*. 272:32719-22.

Ishibe, S., D. Joly, X. Zhu, and L.G. Cantley. 2003. Phosphorylation-dependent paxillin-ERK association mediates hepatocyte growth factor-stimulated epithelial morphogenesis. *Mol Cell*. 12:1275-85.

Jaaro H, Rubinfeld H, Hanoch T, Seger R. Nuclear translocation of mitogen-activated protein kinase kinase (MEK1) in response to mitogenic stimulation. *Proc Natl Acad Sci U S A.* 1997 Apr 15;94(8):3742-7.

Jacobs, D., D. Glossip, H. Xing, A.J. Muslin, and K. Kornfeld. 1999. Multiple docking sites on substrate proteins form a modular system that mediates recognition by ERK MAP kinase. *Genes Dev*. 13:163-75.

Jameson, L., and M. Caplow. 1981. Modification of microtubule steady-state dynamics by phosphorylation of the microtubule-associated proteins. *Proc Natl Acad Sci U S A*. 78:3413-7.

Jelinek, T., A.D. Catling, C.W. Reuter, S.A. Moodie, A. Wolfman, and M.J. Weber. 1994. RAS and RAF-1 form a signalling complex with MEK-1 but not MEK-2. *Mol Cell Biol*. 14:8212-8.

Jelinek, T., P. Dent, T.W. Sturgill, and M.J. Weber. 1996. Ras-induced activation of Raf-1 is dependent on tyrosine phosphorylation. *Mol Cell Biol*. 16:1027-34.

Kamakura, S., T. Moriguchi, and E. Nishida. 1999. Activation of the protein kinase ERK5/BMK1 by receptor tyrosine kinases. Identification and characterization of a signaling pathway to the nucleus. *J Biol Chem*. 274:26563-71.

Kant, S., S. Schumacher, M.K. Singh, A. Kispert, A. Kotlyarov, and M. Gaestel. 2006. Characterization of the atypical MAPK ERK4 and its activation of the MAPK-activated protein kinase MK5. *J Biol Chem*. 281:35511-9.

Karin, M. 1996. The regulation of AP-1 activity by mitogen-activated protein kinases. *Philos Trans R Soc Lond B Biol Sci*. 351:127-34.

Kasler, H.G., J. Victoria, O. Duramad, and A. Winoto. 2000. ERK5 is a novel type of mitogen-activated protein kinase containing a transcriptional activation domain. *Mol Cell Biol*. 20:8382-9.

Kato, Y., V.V. Kravchenko, R.I. Tapping, J. Han, R.J. Ulevitch, and J.D. Lee. 1997. BMK1/ERK5 regulates serum-induced early gene expression through transcription factor MEF2C. *Embo J*. 16:7054-66.

Keyse, S.M., and E.A. Emslie. 1992. Oxidative stress and heat shock induce a human gene encoding a protein-tyrosine phosphatase. *Nature*. 359:644-7.

Khokhlatchev, A.V., B. Canagarajah, J. Wilsbacher, M. Robinson, M. Atkinson, E. Goldsmith, and M.H. Cobb. 1998. Phosphorylation of the MAP kinase ERK2 promotes its homodimerization and nuclear translocation. *Cell*. 93:605-15.

Klemke, R.L., S. Cai, A.L. Giannini, P.J. Gallagher, P. de Lanerolle, and D.A. Cheresh. 1997. Regulation of cell motility by mitogen-activated protein kinase. *J Cell Biol*. 137:481-92.

Kolch, W. 2005. Coordinating ERK/MAPK signalling through scaffolds and inhibitors. *Nat Rev Mol Cell Biol*. 6:827-37.

Kondoh, K., and E. Nishida. 2007. Regulation of MAP kinases by MAP kinase phosphatases. *Biochim Biophys Acta*. 1773:1227-37.

Kondoh, K., K. Terasawa, H. Morimoto, and E. Nishida. 2006. Regulation of nuclear translocation of extracellular signal-regulated kinase 5 by active nuclear import and export mechanisms. *Mol Cell Biol*. 26:1679-90.

Kohno M. Diverse Mitogenic agents induce a rapid phosphorylation of a common set of cellular proteins at tyrosine in quiescent mammalian cells. *J. Biol. Chem* 1985;260:1771–1779.

Kopito, R.B., and M. Elbaum. 2007. Reversibility in nucleocytoplasmic transport. *Proc Natl Acad Sci U S A*. 104:12743-8.

Koster, M., T. Frahm, and H. Hauser. 2005. Nucleocytoplasmic shuttling revealed by FRAP and FLIP technologies. *Curr Opin Biotechnol*. 16:28-34.

Kouzarides, T., and E. Ziff. 1988. The role of the leucine zipper in the fos-jun interaction. *Nature*. 336:646-51.

Kruhlak, M.J., M.A. Lever, W. Fischle, E. Verdin, D.P. Bazett-Jones, and M.J. Hendzel. 2000. Reduced mobility of the alternate splicing factor (ASF) through the nucleoplasm and steady state speckle compartments. *J Cell Biol*. 150:41-51.

Kudo, N., N. Matsumori, H. Taoka, D. Fujiwara, E.P. Schreiner, B. Wolff, M. Yoshida, and S. Horinouchi. 1999. Leptomycin B inactivates CRM1/exportin 1 by covalent modification at a cysteine residue in the central conserved region. *Proc Natl Acad Sci U S A*. 96:9112-7.

Lao, D.H., P. Yusoff, S. Chandramouli, R.J. Philp, C.W. Fong, R.A. Jackson, T.Y. Saw, C.Y. Yu, and G.R. Guy. 2007. Direct binding of PP2A to Sprouty2 and phosphorylation changes are a prerequisite for ERK inhibition downstream of fibroblast growth factor receptor stimulation. *J Biol Chem*. 282:9117-26.

Lechner, C., M.A. Zahalka, J.F. Giot, N.P. Moller, and A. Ullrich. 1996. ERK6, a mitogen-activated protein kinase involved in C2C12 myoblast differentiation. *Proc Natl Acad Sci U S A*. 93:4355-9.

Lee, J.D., R.J. Ulevitch, and J. Han. 1995. Primary structure of BMK1: a new mammalian map kinase. *Biochem Biophys Res Commun*. 213:715-24.

Lenormand, P., C. Sardet, G. Pages, G. L'Allemain, A. Brunet, and J. Pouyssegur. 1993. Growth factors induce nuclear translocation of MAP kinases (p42mapk and p44mapk) but not of their activator MAP kinase kinase (p45mapkk) in fibroblasts. *J Cell Biol*. 122:1079-88.

Levkowitz, G., H. Waterman, S.A. Ettenberg, M. Katz, A.Y. Tsygankov, I. Alroy, S. Lavi, K. Iwai, Y. Reiss, A. Ciechanover, S. Lipkowitz, and Y. Yarden. 1999. Ubiquitin ligase activity and tyrosine phosphorylation underlie suppression of growth factor signaling by c-Cbl/Sli-1. *Mol Cell*. 4:1029-40.

Li, N., A. Batzer, R. Daly, V. Yajnik, E. Skolnik, P. Chardin, D. Bar-Sagi, B. Margolis, and J. Schlessinger. 1993. Guanine-nucleotide-releasing factor hSos1 binds to Grb2 and links receptor tyrosine kinases to Ras signalling. *Nature*. 363:85-8.

Lippincott-Schwartz, J., E. Snapp, and A. Kenworthy. 2001. Studying protein dynamics in living cells. *Nat Rev Mol Cell Biol*. 2:444-56.

Liu, Z.X., C.F. Yu, C. Nickel, S. Thomas, and L.G. Cantley. 2002. Hepatocyte growth factor induces ERK-dependent paxillin phosphorylation and regulates paxillin-focal adhesion kinase association. *J Biol Chem*. 277:10452-8.

Maccioni, R.B., and V. Cambiazo. 1995. Role of microtubule-associated proteins in the control of microtubule assembly. *Physiol Rev*. 75:835-64.

Mandl, M., D.N. Slack, and S.M. Keyse. 2005. Specific inactivation and nuclear anchoring of extracellular signal-regulated kinase 2 by the inducible dual-specificity protein phosphatase DUSP5. *Mol Cell Biol*. 25:1830-45.

Marais, R., Y. Light, H.F. Paterson, C.S. Mason, and C.J. Marshall. 1997. Differential regulation of Raf-1, A-Raf, and B-Raf by oncogenic ras and tyrosine kinases. *J Biol Chem*. 272:4378-83.

Marais, R., J. Wynne, and R. Treisman. 1993. The SRF accessory protein Elk-1 contains a growth factor-regulated transcriptional activation domain. *Cell*. 73:381-93.

Marchetti, S., C. Gimond, J.C. Chambard, T. Touboul, D. Roux, J. Pouyssegur, and G. Pages. 2005. Extracellular signal-regulated kinases phosphorylate mitogen-activated protein kinase phosphatase 3/DUSP6 at serines 159 and 197, two sites critical for its proteasomal degradation. *Mol Cell Biol*. 25:854-64.

Marchi M, D'Antoni A, Formentini I, Parra R, Brambilla R, Ratto GM, Costa M. The N-terminal domain of ERK1 accounts for the functional differences with ERK2. PLoS ONE. 2008;3(12):e3873. Epub 2008 Dec 4.

Marchi, M., A. Guarda, A. Bergo, N. Landsberger, C. Kilstrup-Nielsen, G.M. Ratto, and M. Costa. 2007. Spatio-temporal dynamics and localization of MeCP2 and pathological mutants in living cells. *Epigenetics*. 2:187-97.

Marshall, C.J. 1995. Specificity of receptor tyrosine kinase signaling: transient versus sustained extracellular signal-regulated kinase activation. *Cell*. 80:179-85.

Matsubayashi, Y., M. Fukuda, and E. Nishida. 2001. Evidence for existence of a nuclear pore complex-mediated, cytosol-independent pathway of nuclear translocation of ERK MAP kinase in permeabilized cells. *J Biol Chem*. 276:41755-60.

Mazzucchelli, C., C. Vantaggiato, A. Ciamei, S. Fasano, P. Pakhotin, W. Krezel, H. Welzl, D.P. Wolfer, G. Pages, O. Valverde, A. Marowsky, A. Porrazzo, P.C. Orban, R. Maldonado, M.U. Ehrengruber, V. Cestari, H.P. Lipp, P.F. Chapman, J. Pouyssegur, and R. Brambilla. 2002. Knockout of ERK1 MAP kinase enhances synaptic plasticity in the striatum and facilitates striatal-mediated learning and memory. *Neuron*. 34:807-20.

Metz, R., A.J. Bannister, J.A. Sutherland, C. Hagemeier, E.C. O'Rourke, A. Cook, R. Bravo, and T. Kouzarides. 1994. c-Fos-induced activation of a TATA-box-containing promoter involves direct contact with TATA-box-binding protein. *Mol Cell Biol*. 14:6021-9.

Mikula, M., M. Schreiber, Z. Husak, L. Kucerova, J. Ruth, R. Wieser, K. Zatloukal, H. Beug, E.F. Wagner, and M. Baccarini. 2001. Embryonic lethality and fetal liver apoptosis in mice lacking the c-raf-1 gene. *Embo J*. 20:1952-62.

Misteli, T., and D.L. Spector. 1997. Applications of the green fluorescent protein in cell biology and biotechnology. *Nat Biotechnol*. 15:961-4.

Monje, P., M.J. Marinissen, and J.S. Gutkind. 2003. Phosphorylation of the carboxyl-terminal transactivation domain of c-Fos by extracellular signal-regulated kinase mediates the transcriptional activation of AP-1 and cellular transformation induced by platelet-derived growth factor. *Mol Cell Biol*. 23:7030-43.

Moore, M.S. 1998. Ran and nuclear transport. *J Biol Chem*. 273:22857-60.

Muda, M., A. Theodosiou, C. Gillieron, A. Smith, C. Chabert, M. Camps, U. Boschert, N. Rodrigues, K. Davies, A. Ashworth, and S. Arkinstall. 1998. The mitogen-activated protein kinase phosphatase-3 N-terminal noncatalytic region is responsible for tight substrate binding and enzymatic specificity. *J Biol Chem*. 273:9323-9.

Murphy, L.O., J.P. MacKeigan, and J. Blenis. 2004. A network of immediate early gene products propagates subtle differences in mitogen-activated protein kinase signal amplitude and duration. *Mol Cell Biol*. 24:144-53.

Murphy, L.O., S. Smith, R.H. Chen, D.C. Fingar, and J. Blenis. 2002. Molecular interpretation of ERK signal duration by immediate early gene products. *Nat Cell Biol*. 4:556-64.

Nakabeppu, Y., K. Ryder, and D. Nathans. 1988. DNA binding activities of three murine Jun proteins: stimulation by Fos. *Cell*. 55:907-15.

Nakamura KD, Martinez R, Weber MJ. Tyrosine phosphorylation of specific proteins after mitogen stimulation of chicken embryo fibroblasts. *Mol Cell Biol* 1983;3:380–390.

Nguyen, A., W.R. Burack, J.L. Stock, R. Kortum, O.V. Chaika, M. Afkarian, W.J. Muller, K.M. Murphy, D.K. Morrison, R.E. Lewis, J. McNeish, and A.S. Shaw. 2002. Kinase suppressor of Ras (KSR) is a scaffold which facilitates mitogen-activated protein kinase activation in vivo. *Mol Cell Biol*. 22:3035-45.

Noguchi, T., R. Metz, L. Chen, M.G. Mattei, D. Carrasco, and R. Bravo. 1993. Structure, mapping, and expression of erp, a growth factor-inducible gene encoding a nontransmembrane protein tyrosine phosphatase, and effect of ERP on cell growth. *Mol Cell Biol*. 13:5195-205.

Pages, G., S. Guerin, D. Grall, F. Bonino, A. Smith, F. Anjuere, P. Auberger, and J. Pouyssegur. 1999. Defective thymocyte maturation in p44 MAP kinase (Erk 1) knockout mice. *Science*. 286:1374-7.

Palecek, S.P., J.C. Loftus, M.H. Ginsberg, D.A. Lauffenburger, and A.F. Horwitz. 1997. Integrin-ligand binding properties govern cell migration speed through cell-substratum adhesiveness. *Nature*. 385:537-40.

Papas, T.S., R.J. Fisher, N. Bhat, S. Fujiwara, D.K. Watson, J. Lautenberger, A. Seth, Z.Q. Chen, L. Burdett, L. Pribyl, and et al. 1989. The ets family of genes: molecular biology and functional implications. *Curr Top Microbiol Immunol*. 149:143-7.

Partikian, A., B. Olveczky, R. Swaminathan, Y. Li, and A.S. Verkman. 1998. Rapid diffusion of green fluorescent protein in the mitochondrial matrix. *J Cell Biol*. 140:821-9.

Patel, S.S., B.J. Belmont, J.M. Sante, and M.F. Rexach. 2007. Natively unfolded nucleoporins gate protein diffusion across the nuclear pore complex. *Cell*. 129:83-96.

Pelicci, G., L. Lanfrancone, F. Grignani, J. McGlade, F. Cavallo, G. Forni, I. Nicoletti, F. Grignani, T. Pawson, and P.G. Pelicci. 1992. A novel transforming protein (SHC) with an SH2 domain is implicated in mitogenic signal transduction. *Cell*. 70:93-104.

Peters, R. 2005. Translocation through the nuclear pore complex: selectivity and speed by reduction-of-dimensionality. *Traffic*. 6:421-7.

Phair, R.D., and T. Misteli. 2000. High mobility of proteins in the mammalian cell nucleus. *Nature*. 404:604-9.

Pierrat, B., J.S. Correia, J.L. Mary, M. Tomas-Zuber, and W. Lesslauer. 1998. RSK-B, a novel ribosomal S6 kinase family member, is a CREB kinase under dominant control of p38alpha mitogen-activated protein kinase (p38alphaMAPK). *J Biol Chem*. 273:29661-71.

Prendergast, F.G. 1999. Biophysics of the green fluorescent protein. *Methods Cell Biol*. 58:1-18.

Price, M.A., A.E. Rogers, and R. Treisman. 1995. Comparative analysis of the ternary complex factors Elk-1, SAP-1a and SAP-2 (ERP/NET). *Embo J*. 14:2589-601.

Pulido, R., A. Zuniga, and A. Ullrich. 1998. PTP-SL and STEP protein tyrosine phosphatases regulate the activation of the extracellular signal-regulated kinases ERK1 and ERK2 by association through a kinase interaction motif. *Embo J*. 17:7337-50.

Ranganathan, A., M.N. Yazicioglu, and M.H. Cobb. 2006. The nuclear localization of ERK2 occurs by mechanisms both independent of and dependent on energy. *J Biol Chem*. 281:15645-52.

Rapp, U.R., M.D. Goldsborough, G.E. Mark, T.I. Bonner, J. Groffen, F.H. Reynolds, Jr., and J.R. Stephenson. 1983. Structure and biological activity of v-raf, a unique oncogene transduced by a retrovirus. *Proc Natl Acad Sci U S A*. 80:4218-22.

Raviv, Z., E. Kalie, and R. Seger. 2004. MEK5 and ERK5 are localized in the nuclei of resting as well as stimulated cells, while MEKK2 translocates from the cytosol to the nucleus upon stimulation. *J Cell Sci*. 117:1773-84.

Ray, L.B., and T.W. Sturgill. 1987. Rapid stimulation by insulin of a serine/threonine kinase in 3T3-L1 adipocytes that phosphorylates microtubule-associated protein 2 in vitro. *Proc Natl Acad Sci U S A*. 84:1502-6.

Reszka, A.A., R. Seger, C.D. Diltz, E.G. Krebs, and E.H. Fischer. 1995. Association of mitogen-activated protein kinase with the microtubule cytoskeleton. *Proc Natl Acad Sci U S A*. 92:8881-5.

Robinson, F.L., A.W. Whitehurst, M. Raman, and M.H. Cobb. 2002. Identification of novel point mutations in ERK2 that selectively disrupt binding to MEK1. *J Biol Chem*. 277:14844-52.

Robinson, M.J., and M.H. Cobb. 1997. Mitogen-activated protein kinase pathways. *Curr Opin Cell Biol*. 9:180-6.

Robinson, M.J., S.A. Stippec, E. Goldsmith, M.A. White, and M.H. Cobb. 1998. A constitutively active and nuclear form of the MAP kinase ERK2 is sufficient for neurite outgrowth and cell transformation. *Curr Biol*. 8:1141-50.

Rohan, P.J., P. Davis, C.A. Moskaluk, M. Kearns, H. Krutzsch, U. Siebenlist, and K. Kelly. 1993. PAC-1: a mitogen-induced nuclear protein tyrosine phosphatase. *Science*. 259:1763-6.

Rojas, M., S. Yao, and Y.Z. Lin. 1996. Controlling epidermal growth factor (EGF)-stimulated Ras activation in intact cells by a cell-permeable peptide mimicking phosphorylated EGF receptor. *J Biol Chem*. 271:27456-61.

Rout, M.P., J.D. Aitchison, A. Suprapto, K. Hjertaas, Y. Zhao, and B.T. Chait. 2000. The yeast nuclear pore complex: composition, architecture, and transport mechanism. *J Cell Biol*. 148:635-51.

Rout, M.P., and S.R. Wente. 1994. Pores for thought: nuclear pore complex proteins. *Trends Cell Biol*. 4:357-65.

Rubinfeld, H., T. Hanoch, and R. Seger. 1999. Identification of a cytoplasmic-retention sequence in ERK2. *J Biol Chem*. 274:30349-52.

Ryan, K.J., and S.R. Wente. 2000. The nuclear pore complex: a protein machine bridging the nucleus and cytoplasm. *Curr Opin Cell Biol*. 12:361-71.

Sasagawa, S., Y. Ozaki, K. Fujita, and S. Kuroda. 2005. Prediction and validation of the distinct dynamics of transient and sustained ERK activation. *Nat Cell Biol*. 7:365-73.

Sassone-Corsi, P., J.C. Sisson, and I.M. Verma. 1988. Transcriptional autoregulation of the proto-oncogene fos. *Nature*. 334:314-9.

Schaeffer, H.J., A.D. Catling, S.T. Eblen, L.S. Collier, A. Krauss, and M.J. Weber. 1998. MP1: a MEK binding partner that enhances enzymatic activation of the MAP kinase cascade. *Science*. 281:1668-71.

Schaeffer, H.J., and M.J. Weber. 1999. Mitogen-activated protein kinases: specific messages from ubiquitous messengers. *Mol Cell Biol*. 19:2435-44.

Schaller, M.D. 2001. Biochemical signals and biological responses elicited by the focal adhesion kinase. *Biochim Biophys Acta*. 1540:1-21.

Schlessinger, J. 2000a. Cell signaling by receptor tyrosine kinases. *Cell*. 103:211-25.

Schlessinger, J. 2000b. New roles for Src kinases in control of cell survival and angiogenesis. *Cell*. 100:293-6.

Schlessinger, J. 2002. Ligand-induced, receptor-mediated dimerization and activation of EGF receptor. *Cell*. 110:669-72.

Schumacher, S., K. Laass, S. Kant, Y. Shi, A. Visel, A.D. Gruber, A. Kotlyarov, and M. Gaestel. 2004. Scaffolding by ERK3 regulates MK5 in development. *Embo J*. 23:4770-9.

Sciaky, N., J. Presley, C. Smith, K.J. Zaal, N. Cole, J.E. Moreira, M. Terasaki, E. Siggia, and J. Lippincott-Schwartz. 1997. Golgi tubule traffic and the effects of brefeldin A visualized in living cells. *J Cell Biol*. 139:1137-55.

Seger, R., and E.G. Krebs. 1995. The MAPK signaling cascade. *Faseb J*. 9:726-35.

Sgambato, V., P. Vanhoutte, C. Pages, M. Rogard, R. Hipskind, M.J. Besson, and J. Caboche. 1998. In vivo expression and regulation of Elk-1, a target of the extracellular-regulated kinase signaling pathway, in the adult rat brain. *J Neurosci*. 18:214-26.

Sharma, P., Veeranna, M. Sharma, N.D. Amin, R.K. Sihag, P. Grant, N. Ahn, A.B. Kulkarni, and H.C. Pant. 2002. Phosphorylation of MEK1 by cdk5/p35 down-regulates the mitogen-activated protein kinase pathway. *J Biol Chem*. 277:528-34.

Shaul, Y.D., and R. Seger. 2006. ERK1c regulates Golgi fragmentation during mitosis. *J Cell Biol*. 172:885-97.

Slack-Davis, J.K., S.T. Eblen, M. Zecevic, S.A. Boerner, A. Tarcsafalvi, H.B. Diaz, M.S. Marshall, M.J. Weber, J.T. Parsons, and A.D. Catling. 2003. PAK1 phosphorylation of MEK1 regulates fibronectin-stimulated MAPK activation. *J Cell Biol*. 162:281-91.

Smith, C.L., R. Afroz, G.J. Bassell, H.M. Furneaux, N.I. Perrone-Bizzozero, and R.W. Burry. 2004. GAP-43 mRNA in growth cones is associated with HuD and ribosomes. *J Neurobiol*. 61:222-35.

Soloaga, A., S. Thomson, G.R. Wiggin, N. Rampersaud, M.H. Dyson, C.A. Hazzalin, L.C. Mahadevan, and J.S. Arthur. 2003. MSK2 and MSK1

mediate the mitogen- and stress-induced phosphorylation of histone H3 and HMG-14. *Embo J*. 22:2788-97.
Sorokin, A.V., E.R. Kim, and L.P. Ovchinnikov. 2007. Nucleocytoplasmic transport of proteins. *Biochemistry (Mosc)*. 72:1439-57.
Stork, P.J., and J.M. Schmitt. 2002. Crosstalk between cAMP and MAP kinase signaling in the regulation of cell proliferation. *Trends Cell Biol*. 12:258-66.
Subauste, M.C., O. Pertz, E.D. Adamson, C.E. Turner, S. Junger, and K.M. Hahn. 2004. Vinculin modulation of paxillin-FAK interactions regulates ERK to control survival and motility. *J Cell Biol*. 165:371-81.
Sundberg-Smith, L.J., J.T. Doherty, C.P. Mack, and J.M. Taylor. 2005. Adhesion stimulates direct PAK1/ERK2 association and leads to ERK-dependent PAK1 Thr212 phosphorylation. *J Biol Chem*. 280:2055-64.
Swaminathan, R., C.P. Hoang, and A.S. Verkman. 1997. Photobleaching recovery and anisotropy decay of green fluorescent protein GFP-S65T in solution and cells: cytoplasmic viscosity probed by green fluorescent protein translational and rotational diffusion. *Biophys J*. 72:1900-7.
Tan, P.B., and S.K. Kim. 1999. Signaling specificity: the RTK/RAS/MAP kinase pathway in metazoans. *Trends Genet*. 15:145-9.
Tanoue, T., M. Adachi, T. Moriguchi, and E. Nishida. 2000. A conserved docking motif in MAP kinases common to substrates, activators and regulators. *Nat Cell Biol*. 2:110-6.
Tanoue, T., and E. Nishida. 2002. Docking interactions in the mitogen-activated protein kinase cascades. *Pharmacol Ther*. 93:193-202.
Teis, D., W. Wunderlich, and L.A. Huber. 2002. Localization of the MP1-MAPK scaffold complex to endosomes is mediated by p14 and required for signal transduction. *Dev Cell*. 3:803-14.
Terasawa, K., K. Okazaki, and E. Nishida. 2003. Regulation of c-Fos and Fra-1 by the MEK5-ERK5 pathway. *Genes Cells*. 8:263-73.
Tolwinski NS, Shapiro PS, Goueli S, Ahn NG. Nuclear localization of mitogen-activated protein kinase kinase 1 (MKK1) is promoted by serum stimulation and G2-M progression. Requirement for phosphorylation at the activation lip and signaling downstream of MKK. *J Biol Chem.* 1999 Mar 5;274(10):6168-74.
Tortorella, L.L., C.B. Lin, and P.F. Pilch. 2003. ERK6 is expressed in a developmentally regulated manner in rodent skeletal muscle. *Biochem Biophys Res Commun*. 306:163-8.
Traverse, S., K. Seedorf, H. Paterson, C.J. Marshall, P. Cohen, and A. Ullrich. 1994. EGF triggers neuronal differentiation of PC12 cells that overexpress the EGF receptor. *Curr Biol*. 4:694-701.
Treisman, R. 1994. Ternary complex factors: growth factor regulated transcriptional activators. *Curr Opin Genet Dev*. 4:96-101.
Tsien, R.Y. 1998. The green fluorescent protein. *Annu Rev Biochem*. 67:509-44.
Ussar, S., and T. Voss. 2004. MEK1 and MEK2, different regulators of the G1/S transition. *J Biol Chem*. 279:43861-9.
Vantaggiato, C., I. Formentini, A. Bondanza, C. Bonini, L. Naldini, and R. Brambilla. 2006. ERK1 and ERK2 mitogen-activated protein kinases affect Ras-dependent cell signaling differentially. *J Biol*. 5:14.
Volmat, V., M. Camps, S. Arkinstall, J. Pouyssegur, and P. Lenormand. 2001. The nucleus, a site for signal termination by sequestration and inactivation of p42/p44 MAP kinases. *J Cell Sci*. 114:3433-43.
Wasylyk, B., J. Hagman, and A. Gutierrez-Hartmann. 1998. Ets transcription factors: nuclear effectors of the Ras-MAP-kinase signaling pathway. *Trends Biochem Sci*. 23:213-6.

Wasylyk, C., A.P. Bradford, A. Gutierrez-Hartmann, and B. Wasylyk. 1997. Conserved mechanisms of Ras regulation of evolutionary related transcription factors, Ets1 and Pointed P2. *Oncogene*. 14:899-913.

Waters, S.B., D. Chen, A.W. Kao, S. Okada, K.H. Holt, and J.E. Pessin. 1996. Insulin and epidermal growth factor receptors regulate distinct pools of Grb2-SOS in the control of Ras activation. *J Biol Chem*. 271:18224-30.

Weber, J.D., D.M. Raben, P.J. Phillips, and J.J. Baldassare. 1997. Sustained activation of extracellular-signal-regulated kinase 1 (ERK1) is required for the continued expression of cyclin D1 in G1 phase. *Biochem J*. 326 (Pt 1):61-8.

Weingarten, M.D., A.H. Lockwood, S.Y. Hwo, and M.W. Kirschner. 1975. A protein factor essential for microtubule assembly. *Proc Natl Acad Sci U S A*. 72:1858-62.

Wente, S.R. 2000. Gatekeepers of the nucleus. *Science*. 288:1374-7.

Werner, M.H., M. Clore, C.L. Fisher, R.J. Fisher, L. Trinh, J. Shiloach, and A.M. Gronenborn. 1995. The solution structure of the human ETS1-DNA complex reveals a novel mode of binding and true side chain intercalation. *Cell*. 83:761-71.

Whitehurst, A., M.H. Cobb, and M.A. White. 2004. Stimulus-coupled spatial restriction of extracellular signal-regulated kinase 1/2 activity contributes to the specificity of signal-response pathways. *Mol Cell Biol*. 24:10145-50.

Whitehurst, A.W., J.L. Wilsbacher, Y. You, K. Luby-Phelps, M.S. Moore, and M.H. Cobb. 2002. ERK2 enters the nucleus by a carrier-independent mechanism. *Proc Natl Acad Sci U S A*. 99:7496-501.

Whitmarsh, A.J., P. Shore, A.D. Sharrocks, and R.J. Davis. 1995. Integration of MAP kinase signal transduction pathways at the serum response element. *Science*. 269:403-7.

Wiedlocha, A., and V. Sorensen. 2004. Signaling, internalization, and intracellular activity of fibroblast growth factor. *Curr Top Microbiol Immunol*. 286:45-79.

Willis, D., K.W. Li, J.Q. Zheng, J.H. Chang, A. Smit, T. Kelly, T.T. Merianda, J. Sylvester, J. van Minnen, and J.L. Twiss. 2005. Differential transport and local translation of cytoskeletal, injury-response, and neurodegeneration protein mRNAs in axons. *J Neurosci*. 25:778-91.

Wojnowski, L., A.M. Zimmer, T.W. Beck, H. Hahn, R. Bernal, U.R. Rapp, and A. Zimmer. 1997. Endothelial apoptosis in Braf-deficient mice. *Nat Genet*. 16:293-7.

Xing, J., D.D. Ginty, and M.E. Greenberg. 1996. Coupling of the RAS-MAPK pathway to gene activation by RSK2, a growth factor-regulated CREB kinase. *Science*. 273:959-63.

Xu, H., and M. Goldfarb. 2001. Multiple effector domains within SNT1 coordinate ERK activation and neuronal differentiation of PC12 cells. *J Biol Chem*. 276:13049-56.

Xu, L., C. Alarcon, S. Col, and J. Massague. 2003. Distinct domain utilization by Smad3 and Smad4 for nucleoporin interaction and nuclear import. *J Biol Chem*. 278:42569-77.

Xu, L., Y.G. Chen, and J. Massague. 2000. The nuclear import function of Smad2 is masked by SARA and unmasked by TGFbeta-dependent phosphorylation. *Nat Cell Biol*. 2:559-62.

Xu, L., and J. Massague. 2004. Nucleocytoplasmic shuttling of signal transducers. *Nat Rev Mol Cell Biol*. 5:209-19.

Yan, C., H. Luo, J.D. Lee, J. Abe, and B.C. Berk. 2001. Molecular cloning of mouse ERK5/BMK1 splice variants and characterization of ERK5 functional domains. *J Biol Chem*. 276:10870-8.

Yan, J., S. Roy, A. Apolloni, A. Lane, and J.F. Hancock. 1998. Ras isoforms vary in their ability to activate Raf-1 and phosphoinositide 3-kinase. *J Biol Chem*. 273:24052-6.

Yang, F., L.G. Moss, and G.N. Phillips, Jr. 1996. The molecular structure of green fluorescent protein. *Nat Biotechnol*. 14:1246-51.

Yang, S.H., P.R. Yates, A.J. Whitmarsh, R.J. Davis, and A.D. Sharrocks. 1998. The Elk-1 ETS-domain transcription factor contains a mitogen-activated protein kinase targeting motif. *Mol Cell Biol*. 18:710-20.

Yao, Z., I. Flash, Z. Raviv, Y. Yung, Y. Asscher, S. Pleban, and R. Seger. 2001. Non-regulated and stimulated mechanisms cooperate in the nuclear accumulation of MEK1. *Oncogene*. 20:7588-96.

Yazicioglu, M.N., D.L. Goad, A. Ranganathan, A.W. Whitehurst, E.J. Goldsmith, and M.H. Cobb. 2007. Mutations in ERK2 binding sites affect nuclear entry. *J Biol Chem*. 282:28759-67.

Yin, Y., Y.X. Liu, Y.J. Jin, E.J. Hall, and J.C. Barrett. 2003. PAC1 phosphatase is a transcription target of p53 in signalling apoptosis and growth suppression. *Nature*. 422:527-31.

York, R.D., H. Yao, T. Dillon, C.L. Ellig, S.P. Eckert, E.W. McCleskey, and P.J. Stork. 1998. Rap1 mediates sustained MAP kinase activation induced by nerve growth factor. *Nature*. 392:622-6.

Yung, Y., Z. Yao, T. Hanoch, and R. Seger. 2000. ERK1b, a 46-kDa ERK isoform that is differentially regulated by MEK. *J Biol Chem*. 275:15799-808.

Zhang, F., A. Strand, D. Robbins, M.H. Cobb, and E.J. Goldsmith. 1994. Atomic structure of the MAP kinase ERK2 at 2.3 A resolution. *Nature*. 367:704-11.

Zheng, C.F., and K.L. Guan. 1993. Properties of MEKs, the kinases that phosphorylate and activate the extracellular signal-regulated kinases. *J Biol Chem*. 268:23933-9.

Zhou, B., Z.X. Wang, Y. Zhao, D.L. Brautigan, and Z.Y. Zhang. 2002. The specificity of extracellular signal-regulated kinase 2 dephosphorylation by protein phosphatases. *J Biol Chem*. 277:31818-25.

Zhou, G., Z.Q. Bao, and J.E. Dixon. 1995. Components of a new human protein kinase signal transduction pathway. *J Biol Chem*. 270:12665-9.

Zhu, A.X., Y. Zhao, D.E. Moller, and J.S. Flier. 1994. Cloning and characterization of p97MAPK, a novel human homolog of rat ERK-3. *Mol Cell Biol*. 14:8202-11.

ACKNOWLEDGEMENTS

First of all I would like to express my sincere gratitude to Dr. Gian Michele Ratto, senior scientist at the National Enterprise for nanoScience and nanotechnology of Pisa, who has been my supervisor since the beginning of my graduate study. He provided me with valuable assistance in the laboratory experience and he gave me many important advices during the course of this work.
I shared with him the genuine delight of every experimental success, every time both amazed in front of the marvelous perfection of the nature.
I'm also very grateful to him for patiently reviewing my manuscript.
I wish to express my warmest thanks to Dr. Mario Costa, researcher at the Neuroscience Institute, CNR of Pisa, who gave me many precious advises and help me to solve many technical difficulties during my laboratory experience and not only.
Special thanks are due to Prof. Fabio Beltram, director of the National Enterprise for nanoScience and nanotechnology of Pisa, who directed me in molecular biophysical studies and provided valuable suggestions that improved the quality of this study.
Special gratitude goes to Prof. Lamberto Maffei, director of the Neuroscience Institute CNR of Pisa, for providing wise advises and for giving me the opportunity to work in his laboratory.
My sincere thanks are due to the official referees, Professor Rony Seger, Department of Biological Regulation at the Weizmann Institute of Science, Israel, and Professor Riccardo Brambilla, Department of Molecular Biology and Functional Genomics, Fondazione San Raffaele, Milano, for their detailed review, constructive criticism and excellent advice during the preparation of this thesis.
I wish to extend my hearties thanks to everybody who has helped me with my work and to all the people of the Neuroscience Institute for their kindness and affection.
A special thank goes to the other PhD students who share with me the same room at the Neuroscience Institute of Pisa. They always gave me a solid support and had a lot of patience especially during my difficult moments.

My warmest appreciation goes to my boyfriend Rudy and my parents. I thank them for their love, their support, and their confidence throughout these years. My parents have always put education as a first priority in my life, and raised me to set high goals for myself. They taught me to value honesty, courage, and humility above all other virtues.
I dedicate this work to them, to honour their love, patience, and support during these years.

This reseach project has been carried out within a PhD program
sponsored by Scuola Normale Superiore and Italian Institute of Technology